FIRE SPREAD ON EXTERIOR WALLS

By

Felix Nyuk Poh Bong

Supervised by

Colleen Wade

Building Research Association of New Zealand

A report submitted in partial fulfilment of the
requirements for the degree of
Master of Engineering
in Fire Engineering

in the

Department of Civil Engineering
University of Canterbury
Private Bag 4800
Christchurch, New Zealand

February 2000

ABSTRACT

This report describes methods of predicting heat flux exposure to external walls due to the impingement of flame issuing through a window opening. A heat transfer model was set up for the purpose of predicting the geometry of the emerging flame and the resultant heat flux exposure to the wall surface.

An existing flame spread model implemented in the *BRANZFIRE* model was selected for characterising the flame spread on exterior wall cladding materials, as a function of the heat flux exposure (from the projecting flame to the wall) and the material flammability properties of the wall material. Modifications were made to the flame spread model. The result was a prediction of rate and extent of the upward flame spread as a function of time and the heat release rate of the burning cladding material.

It is concluded that the flame spread model has the potential to determine the flame spread characteristics associated with four different cladding materials. The flame spread model gave conservative prediction for three of the tested cladding materials.

Overall, the heat transfer model seems to predict the total heat flux density received by the exposing wall with reasonable accuracy. Further validation of the heat transfer model is needed before it can be successfully integrated into the flame spread model to provide a useful tool for characterising flame spread and estimating the heat flux exposure conditions.

ACKNOWLEDGEMENTS

I wish to acknowledge my deepest appreciation for the generous help and encouragement given to me by the following people and organisations, without whose involvement this research project could not have been completed.

- The Building Research Association of New Zealand (BRANZ), in Judgeford, Porirua where this research was undertaken. Being able to view interesting fire tests was invaluable, as was the high level of support afforded to me by their staff.

- Colleen Wade, my research supervisor at BRANZ, for her conscientious and enthusiastic supervision of this project. Without her invaluable contribution, this research would not have been possible.

- Dr Charley Fleischmann, for his dedicated work in the Fire Engineering program and his organisation of my research at BRANZ. His help in organising the financial support for my research at BRANZ is most appreciated.

- Associate Professor Andy Buchanan, for giving me the opportunity to participate in the Fire Engineering program at the University of Canterbury. All his help and guidance during the Fire Engineering programme is greatly appreciated.

- Joop de Ruiter and Ed Soja, for their help in conducting the cone calorimeter tests.

- Thanks are also due to Ron Stevens and Celia Tatham for proofreading and commenting on this report.

- My 1999/2000 ME (Fire) classmates for their friendly help and advice.

- I thank my family and my girlfriend, Pui Yan, for their endless support. I would not be here without it.

TABLE OF CONTENTS

LIST OF FIGURES

LIST OF TABLES

NOMENCLATURE

A_f	=	total surface area of triangular shaped flame (m^2)
A_p	=	pyrolysis area (m^2)
A_T	=	total enclosing surface areas of fire compartment (excluding the window) (m^2)
A_v	=	upper area of the vent (m^2)
A_w	=	window area (m^2)
d	=	characteristics dimensions (m)
D	=	depth of fire compartment (m)
E	=	cellulosic fuel energy yield (MJ/kg)
g	=	acceleration due to gravity (9.807 m/s^2)
h	=	height of window/vent (m)
h_{ig}	=	total heat transfer coefficient from surface at ignition (W/m^2K)
h_w	=	height above the top of window (m)
H	=	height of fire compartment (m)
I_z	=	radiative heat flux (kW/m^2)
k	=	thermal conductivity (W/m K)
k_o	=	Oleszkiewicz's emprical factor
$k\rho c$	=	thermal inertia (W^2s/m^4K^2)
K	=	flame area constant (m^2/kW)
l	=	distance along flame centre line from window (m)
l_w	=	distance along flame centre line from window to the top of window (m)
L	=	total mass of fire load (kg)
$\dot{m}$	=	burning rate (kg/s)
$\dot{m}_f$	=	fuel-controlled burning rate (kg/s)
$\dot{m}_o$	=	mass flow rate of hot gases out through the vent (kg/s)
$\dot{m}_v$	=	ventilation-controlled burning rate (kg/s)
n	=	flame length power
Nu	=	Nusselt number
Pr	=	Prandtl number

$\dot{q}''_c$	=	convective heat flux (kW/m^2)
$\dot{q}''_{crit}$	=	critical heat flux for ignition (kW/m^2)
$\dot{q}''_e$	=	external heat flux incident on a surface (kW/m^2)
$\dot{q}''_f$	=	incident heat flux from the flame (kW/m^2)
$\dot{q}''_{int}$	=	incident heat flux to a surface due to heated gas layers and other surfaces (kW/m^2)
$\dot{q}''_{net}$	=	net heat flux to the wall cladding (kW/m^2)
$\dot{q}''_r$	=	radiative heat flux from the burning of excess fuel (kW/m^2)
$\dot{Q}_{ef}$	=	heat release rate of excess fuel burning outside the fire compartment (kW)
$\dot{Q}'_f$	=	energy release rate for the emerging flame equivalent to a line source (kW/m)
$\dot{Q}''_p$	=	peak rate of heat release measured in cone calorimeter test (kW/m^2)
$\dot{Q}(t)$	=	heat release at time t (kW)
$\dot{Q}''(t)$	=	heat release rate per unit area at time t (kW/m^2)
Re	=	Reynolds number
t_{ig}	=	time to ignition in cone calorimeter (sec)
T_c	=	fire temperature in the compartment (K)
T_F	=	flame temperature at certain height above window (K)
T_{ig}	=	surface temperature for ignition (K)
T_o	=	flame temperature at window or temperature of ouflowing hot gases (K)
T_w	=	surface temperature of wall cladding (K)
T_α	=	reference temperature of ambient air (K)
u	=	velocity of wind (m/s)
u_o	=	velocity of outflowing gases (m/s)
w	=	width of window (m)
w_x	=	maximum flame width in forced draft condition (m)
W	=	width of compartment (m)
x	=	horizontal distance of flame tip from window (m)
$x_{p,o}$	=	initial pyrolysis front in lateral direction (m)
X	=	centre line distance of flame tip from window (m)
y	=	distance between neutral plane and top of window (m)

y_f = flame length in upward direction (m)

y_p = pyrolysis front in upward direction (m)

$y_{p,o}$ = initial pyrolysis front in upward direction (m)

z = vertical distance of flame tip above top of window (m)

α = convective heat transfer coefficient (kJ/kg K)

σ = Stefan-Boltzmann constant (5.67×10^{-8} W/m^{2}K^4)

ρ = density (kg/m^3)

ρ_a = density of ambient air (kg/m^3)

ρ_o = density of outflowing gases at window (kg/m^3)

ε_f = emmisivity of flame

ε_w = emmisivity of wall cladding

θ_c = fire temperature rise in the compartment (K)

λ = flame thickness (m)

ΔA_p = incremental change in pyrolysis area (m^2)

υ = kinematic viscosity of gases (m^2/s)

λ_r = radiative fraction of energy loss by radiation from the flame

η = $\dfrac{A_T}{A_w h^{1/2}}$ (m$^{-1/2}$)

ψ = $\dfrac{L}{(A_w A_T)^{1/2}}$ (kg/m^2)

μ = dynamic viscosity of gases (kg/m s)

τ = fire duration (min)

CHAPTER 1

1 INTRODUCTION

The research work that is presented in this report is a partial fulfilment of the requirements of the Master of Engineering in Fire Engineering degree at the University of Canterbury, Christchurch, New Zealand. The research was conducted at The Building Research Association of New Zealand (BRANZ) under the supervision of Colleen Wade.

1.1 An Introduction to Fire Spread on Exterior Walls

There are relatively few reported cases involving exterior upward fire spread on combustible claddings. There are even fewer cases where fire spread on combustible claddings is likely to have compromised life safety. This may be due to the historical use of noncombustible materials on facades as is required by many building codes around the world. In addition, an exterior wall fire usually results from an intense fire within the building and the building fire usually masks the exterior wall fire. Thus, it sometimes can be very difficult to distinguish between the contribution made by the building fire and that made by an exterior wall fire involving combustible cladding material.

A small number of such incidents does not necessarily mean that fire spread on exterior claddings does not present significant risk to both property protection and life safety. This is because:

1. As more and more high-rise buildings are built in New Zealand and overseas and with the increasing use of combustible exterior claddings, exterior fire spread problems become increasingly more important as rapid fire spread from

floor to floor can happen via combustible exterior claddings in some buildings and create a hazardous situation for building occupants.

2. In the case of very tall buildings, an exterior wall fire may create a problem for firefighters, as the fire may not be reached by fire-fighting appliances.
3. Fire spread on combustible cladding systems can also be life-threatening in some buildings such as health-care units and detention centers as the occupants in these buildings may not be able to escape to a safe place without assistance.
4. Considerable property losses may arise by damage to the wall as a result of an exterior wall fire.
5. Fire spread on combustible cladding systems could also compromise sprinkler systems if the fire were to spread into several floors setting sprinkler heads off at each level, and creating a greater demand for water than can be supplied.

Fire spread over combustible cladding is starting to attract the attention of researchers in recent years. Changes to building codes have also been initiated in countries such as New Zealand, in order to provide better alternative classification schemes for the fire safety performance of exterior cladding systems.

1.2 Performance-based Codes – The New Zealand Experience

The traditional point of view is that facades should be made of noncombustible materials. However, this point of view is seen as out of date, since it not based on a performance measure. This aspect was recognised with the introduction of the performance-based New Zealand Building Code (NZBC) [1] in 1992. The NZBC aims to prevent fire spread from the floor of origin to the floors above and below in order to provide life safety and protection to neighbouring property. The relevant clause of the NZBC, dealing with the fire performance of external walls, is given in Clause 3.3.5, which states:

> *External walls and roofs shall have resistance to the spread of fire, appropriate to the fire load within the building and to the proximity of other household units and other property.*

The Building Industry Authority (BIA) in New Zealand has published "The Approved Documents" [2], which include the Acceptable Solution method. The Acceptable Solution provides one approved means of complying with the NZBC. Section C3/AS1 of the Acceptable Solution provides some specific requirements in meeting the fire performance of external walls given in Clause 3.3.5 of the NZBC. The necessary protection in meeting this specific requirement can be achieved by one or a combination of:

- Building separation in relation to permissible areas of openings in the external wall
- An adequate fire resistance rating for primary and secondary elements of the building, depending on the nature of the building and the presence or otherwise of other fire-protection systems
- Providing parapets, spandrels or aprons
- Restricted use of combustible surface finishes

A further requirement of C3/AS1 seeks to reduce the likelihood of upward flame spread through exterior wall claddings as a result of flames projecting through lower window openings in the same building and igniting the facade above, or as a result of direct flame impingement from an adjacent building on fire. The surface finishes of exterior wall claddings are regulated in the Acceptable Solutions to control the ignitibility or the contribution of the exterior wall claddings to fire development (i.e. combustibility). Table 1.1 shows the requirement on exterior surface finishes of external walls from the Acceptable Solutions, depending on the type of occupancy, building height, and distance of wall from relevant boundary. The existing requirements given by Table 1.1 seek to inhibit fire spread on exterior wall claddings by controlling the ignitability or combustibility of the exterior wall cladding.

Table 1.1: Exterior surface finishes of external walls [2]

Building Height (m)	Purpose groups SC SD SA SR	All other purpose groups	
		Distance from relevant boundary	
		Less than 1.0 m	1.0 m or more
Up to 7	Ig = 0	Ig = 0	N/R
Up to 16	Non-combustible (Note 1)	Ig = 0	N/R
Up to 25	Non-combustible (Note 1)	Ig = 0	Ig = 0 (Note 2)
Over 25	Non-combustible	Non-combustible	Non-combustible (Note 2)

Key : Ig = 0 represents ignitability index of zero
N/R = no restriction

Purpose groups: SC Sleeping Care, hospitals, rest homes etc.
SD Sleeping Detention, prisons, psychiatric hospitals etc.
SA Sleeping accommodation, hotels, motels etc.
SR Sleeping Residential, apartments etc.

NOTES:
1. For purpose groups SA and SR Ig = 0 may be used.
2. No requirement if distance to relevant boundary is greater than 7.0 m.

NZBC [1] requires the ignitability of the exterior wall cladding materials to be tested in accordance with AS 1530.3 [3], whereas AS 1530.1 [4] is used for determining combustibility of the exterior wall cladding materials. Wade [5] identified the shortcomings of the specified test methods in assessing the performance of exterior cladding materials. The ignitability test method does not represent the more severe actual thermal exposure resulting from a window fire plume. The combustibility test was developed only for solid homogeneous materials. However, the combustibility test method is a very restricted test. For example, cellulose fibre-cement boards are not permitted in some buildings because they are a combustible cladding material. However, cellulose fibre-cement boards do not contribute significantly to fire development.

BRANZ has undertaken research to improve the existing shortfall of the requirements in the NZBC. An alternative classification scheme for exterior wall cladding materials

has been proposed based on the rate of heat release or 'degree of combustibility'. The classification of cladding materials based on heat release rate data will be further discussed in Section 2.4.2.

1.3 Research Purpose

The rate of upward flame spread will be indirectly influenced by the combustibility and ignitibility of the exterior wall cladding. The specified test methods (AS 1530.1 and AS 1530.3) aim to evaluate the ignitability or the contribution of the cladding to fire development (i.e. combustibility), rather than evaluating flame spread directly. Wade [5] suggested that further research was needed in areas such as the conditions leading to self-propagation of fire on wall cladding materials and further measurement of heat fluxes resulting from window fire plumes. This led to BRANZ carrying out research into the flame-spread characteristics that are necessary for a cladding material to be able to propagate fire [7]. An existing analytical vertical flame spread model was developed to determine the likelihood of combustible cladding materials being able to propagate flame spread on a building facade under exposure of window fire plumes, based on parameters derived from cone calorimeter tests. However, this analytical method is a crude engineering attempt to model a physically very complex reality. To improve the modelling of fire spread on combustible cladding materials, a detailed numerical solution is feasible. The advantage of a numerical solution over an analytical solution is that the actual heat release rates of cladding materials from cone calorimeter tests at various heat fluxes can be integrated into the model.

The purpose of this study is to develop improved information for a numerical model of flame spread on exterior wall claddings. Generally, the fire spread research presented in this report can be divided into two individual parts, namely:

1. The investigation of heat flux exposure condition to external walls due to impingement by external flame through a window opening.
2. An existing procedure/model is selected for predicting upward flame spread as a function of heat flux exposure and material flammability properties.

The first part of this study looks at the methods of predicting the incident heat flux to wall results from a window fire plume, based on the geometry and temperature distribution of the external flame issuing through a window opening developed from empirically derived correlations. The predicted results were compared with the experimental data available from literature.

The second part of this study includes the prediction of upward flame spread over the surface of a wall from an existing flame spread model The model will take cone calorimeter data for a specified cladding system as input, correlating the data to obtain modelling parameters such as ignition temperature and thermal inertia. However, the flame spread model is applicable only to cladding materials which are mechanically stable under the fire conditions to which they are exposed (i.e. it is assumed that the cladding system remains in place and fire spread is due to the surface burning and spreading flame). Some cladding materials may fail by lack of adequate fixing or adhesion of the surface layer, which can then fall off, exposing more combustible materials beneath.

A series of large-scale flame spread experiments on four generic wall cladding systems were carried out at BRANZ. This was intended to provide some full-scale flame spread data for exterior claddings and some indication of the mechanical performance characteristics of cladding materials in fire. To ensure that the upward flame spread model produced useful results, the calculated values were compared with the experimental data from the full-scale tests. The necessary inputs for the flame spread model are the incident heat flux and the flame height, which are specified according to the experimental exposure conditions.

It is considered that the heat flux exposure prediction method could be used in conjunction with the upward flame spread model to assess the rate and extent of flame spread. The proposed outcome aimed to provide an improved method of predicting fire spread and the potential hazards associated with exterior cladding materials.

1.4 Overview of this Report

The content of this report is outlined below.

Chapter 2 reviews the current knowledge of fire spread on exterior wall claddings by means of a literature review of the mechanisms of vertical fire spread, the contributing factors to fire spread on combustible cladding materials, past incidents involving combustible cladding systems, and a research review.

Chapter 3 provides background information on the behaviour of flames projecting through a window opening. This includes the geometry of the projecting flame and the variation of flame temperatures with height above the window opening.

Chapter 4 describes the methods used to predict heat flux exposure conditions to the exterior wall due to the impingement of external flame through a window opening. An EXCEL spreadsheet was set up to describe the heat flux exposure condition to the external wall, based on the window size and geometry and the fire compartment and fuel characteristics. The prediction of total heat flux density received by the exposing wall was compared with the experimental data available from literature. From the comparison made, the appropriateness and/or deficiencies of these methods were highlighted.

Chapter 5 is a description of the selected flame spread model for describing the rate and extent of flame spread. Appropriate modifications to the flame spread model were made. A characterisation of the flame issuing from a vent and the resultant thermal exposure to the wall is also included.

Chapter 6 introduces the experimental techniques used to obtain full-scale fire and material properties. This is divided into two main parts, the bench-scale testing using the cone calorimeter and the full-scale fire testing. Sensitivity analysis of the ignition data was conducted on one of the cladding materials to determine the effect of ignition data on the material's flammability properties. The material flammability properties for each of the cladding materials are also presented.

Chapter 7 discusses the qualitative assessments made by comparing the experimental data with the outputs from the heat transfer and with flame spread models.

Chapter 8 outlines the conclusions and recommendations made in this study. This chapter also highlights the limitations associated with each of the models.

CHAPTER 2

2 LITERATURE REVIEW

This background chapter reviews the current knowledge of fire spread on exterior wall claddings. It summaries the mechanisms on vertical fire spread, contributing factors to fire spread on combustible cladding materials, the effectiveness of protection in reducing thermal exposure to building facade and upper floors, past incidents involving combustible and non-combustible cladding systems and research on exterior cladding systems.

2.1 Mechanisms of Vertical Fire Spread

Fire can spread from one storey to another via various paths [8], including:

- Combustible cladding materials - Fire can spread vertically up a building via combustible cladding materials. Ignition of the combustible cladding materials may occur as a result of exposure to flame projecting from a window or radiant heat received from fire in an adjacent building or exposure to an external fire near the wall.

- Exterior windows - The possibility of external fire spread from storey to storey as a result of flames emerging from the windows is of some concern, especially for high rise buildings. The window-to-window "leap-frogging" mechanism involves the ignition of combustible materials inside an upper window, as a result of intense heat from flames projected from a lower window. Furthermore the projecting flames through window openings may ignite the facade of adjacent properties.

- Failure at the junction of a floor and exterior wall - Cracks formed between the edge of the floor slab and the building facade allow flames and hot gases to pass through.

- Failure of floor/ceiling fire separation - Fire spread occurs as the floor/ceiling fire separations do not provide sufficient fire resistance to prevent the fire spreading from floor to floor.

- Services penetrations and gaps - Inadequate stopping of service penetrations and gaps can promote fire spread.

- Melting of metals and alloys - This happens as the intense heat from fires exceeds the melting points of alloys or metals and causes them to melt or distort.

- Service ducts and shafts - Service ducts and shafts can be found in multi-storey buildings for transporting people and services. Fire spread is possible through walls around the duct and openings within the duct.

- Stairways - Stairways are open shafts and they act as chimneys for hot gases and flames to migrate.

2.2 Fire Spread on Exterior Wall

The first three mechanisms have been identified as the fire spread mechanisms involved in exterior-wall fires [9]. Fire spread through combustible cladding materials is of interest to this research. The second mechanism tends to be very spectacular and can be life threatening. The risk resulting from "leap-frogging" mechanism can be minimised with appropriate protections. Failure at the junction of a floor and exterior wall can be eliminated with the application of appropriate requirements from the building code.

2.2.1 Effect of Combustible Exterior Wall Claddings

A window fire plume usually results from an intense fire within a building. The generated convective and radiant heat fluxes to the wall are high enough to create a fire hazard to combustible exterior wall cladding systems. There are many factors which affect the rate of flame spread vertically on the combustible exterior wall cladding systems. These are illustrated schematically in Figure 2.1.

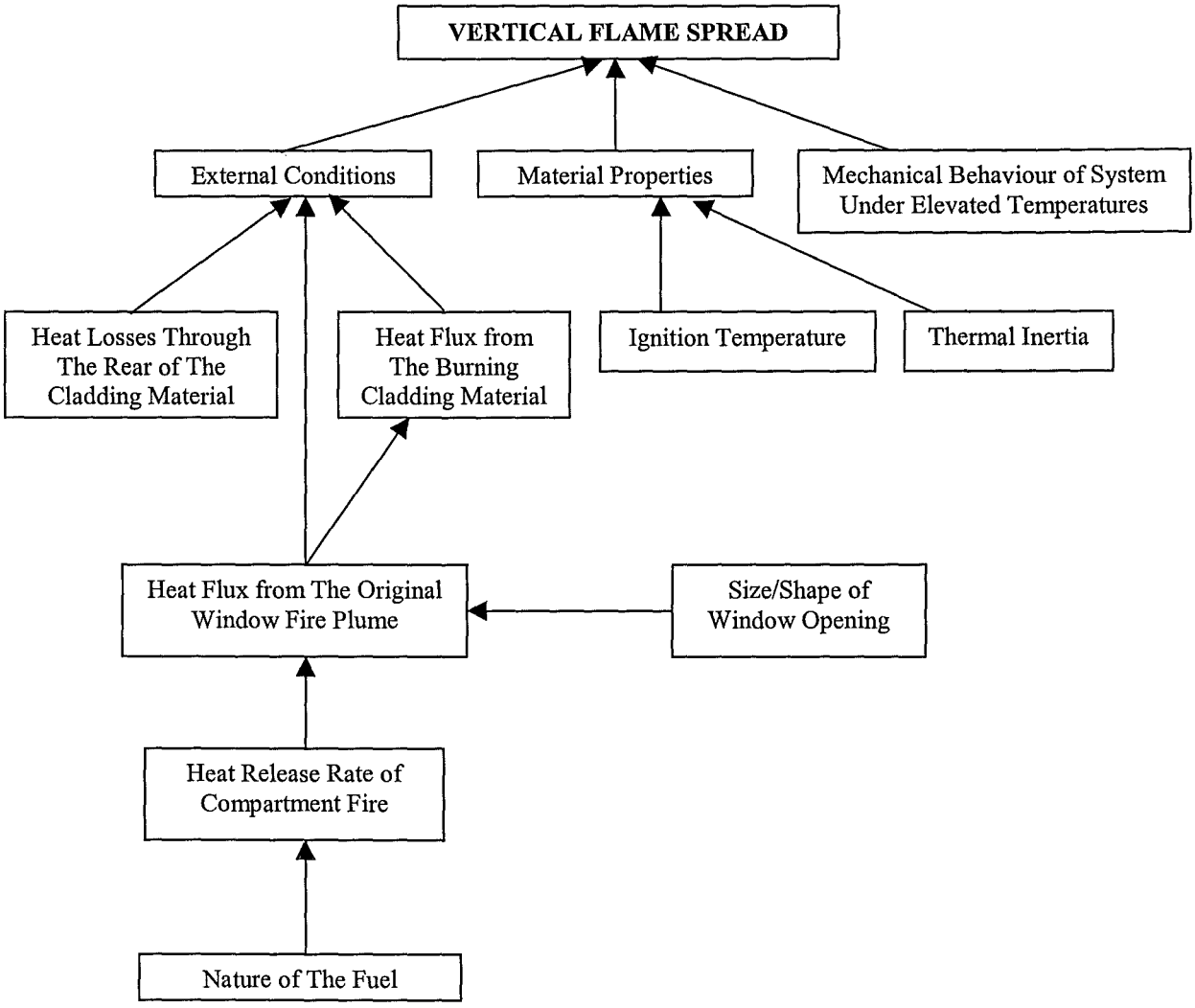

Figure 2.1: Factors affecting the rate of vertical fire spread on exterior wall cladding material [5]

Flame spread and growth of a material are determined by the thermal response of the material of the material to an imposed heat flux distribution. Thermal response of a material comprises the preheating of material up to a pyrolysis or ignition temperature

as well as the rate of mass pyrolysis and the burning properties of the pyrolysing gases. The incident total heat flux to exterior wall cladding systems is made up of the heat flux from burning cladding material and the window fire plume.

Other contributing factors to vertical flame spread are the material properties of cladding system and the mechanical behaviour of the cladding system under elevated temperatures.

Not all combustible exterior claddings can sustain vertical flame spread. Combustible cladding materials such as cellulose fibre cement sheets do not significantly contribute to fire development. As for composite materials, the propensity of the vertical flame spread is influenced by the outer protective layer applied to the core material and the preservation of integrity when exposed to fire. Provided that adequate outer-layer protection is applied to the core, combustibility of the core material presents less danger and can be safely used in a facade assembly under some circumstances.

2.2.2 Effect of Facade Geometry

In order to minimise the risk of secondary fire at the level above the fire compartment, exterior architecture designs are used as protection to minimise the fire exposure. Generally, there are two types of projections, namely vertical and horizontal projections used as external protection to reduce the fire exposure to floors and facade above the fire compartment, as a result of window fire plume. The horizontal projections can be a canopy or a balcony, which is applied to the wall immediately above the window opening. The vertical projections simulate a spandrel wall, which is a noncombustible wall with no openings. The horizontal and vertical projections are shown in Figure 2.2.

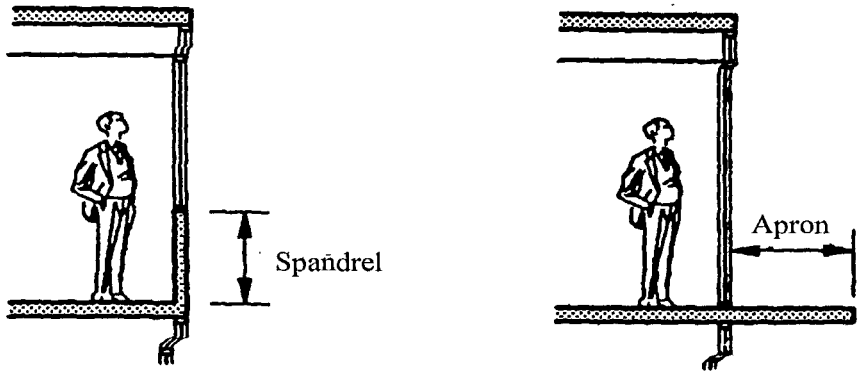

a) Vertical projection **b) Horizontal projection**

Figure 2.2: Horizontal and vertical projections [2]

The horizontal projection installed above an exposing window acts as a flame deflector to the flame projecting from a window opening (Figure 2.3). This type of projection offers substantial protection to the wall above the window and protects the storeys above from the intense heat given off by a window fire plume.

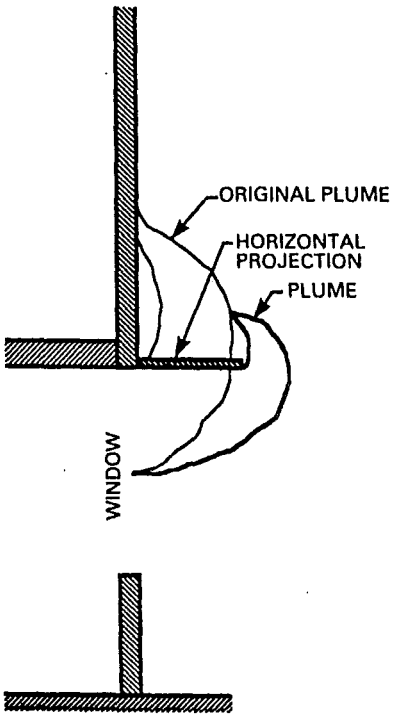

Figure 2.3: Effect of horizontal projection on fire plume [9]

Figure 2.4 shows relative exposure collected in the series of experiments by Oleszkiewicz [10] for various depths of projection. The relative exposure was taken by normalising the average time heat flux density with the average reading at 1 m above the opening. It can be seen from Figure 2.4 that the protection afforded to the wall above the window opening increases with the depth of the projection. The heat exposure decreases considerably even with a 0.3 m deep projection. In this particular test, a 1 m deep projection was found to be very effective in reducing the heat exposure. The exposure was reduced to as much as 85% below the readings taken without any protection.

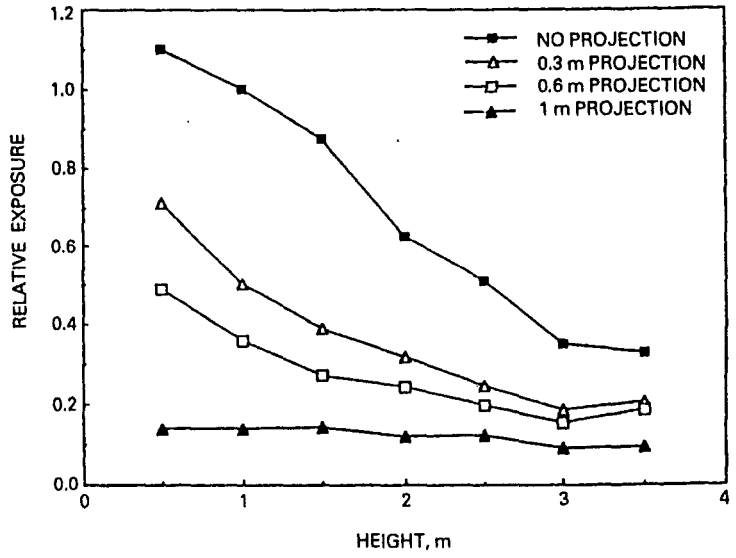

Figure 2.4: Heat flow data for various depths of projection [10]

The vertical projection or spandrel wall, however, was found to be not as practical as the horizontal projection in reducing the exposure resulting from a window fire plume. For example, a 2.5 m high spandrel wall will be required to achieve a 50% decrease in exposure to the wall above the window opening.

Another type of projection, a pair of vertical panels, was included in the study by Yung and Oleszkiewicz [9]. Such panels act as typical building projections, such as sunshades, and are applied perpendicularly to the wall on both sides of the window. Figure 2.5 shows the deflection of the fire plume due to the presence of this projection. Clearly, vertical panels increase the fire exposure to the wall above. The increase in heat transfer to the wall above is caused by the vertical extension of the combustion

zone within the plume, as a result of restricted lateral air entrainment to the plume in the presence of the vertical panels.

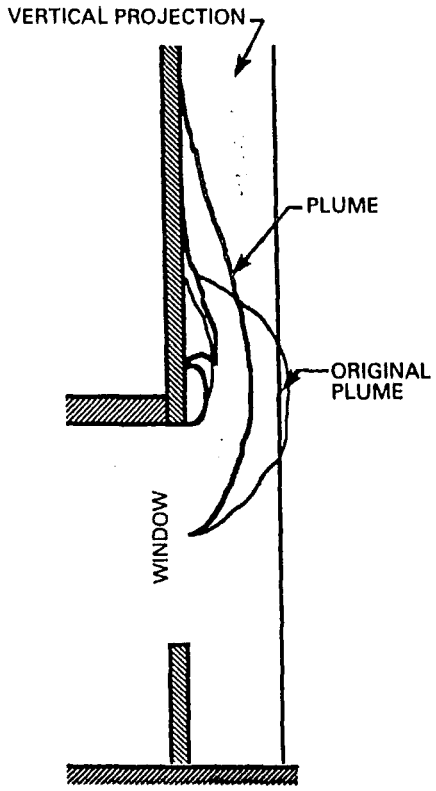

Figure 2.5: Effect of vertical panels on fire plume [9]

2.3 Historical Fire Record Involving Vertical Fire Spread

Few overseas incidents involving fire spread through combustible claddings have been available in the literature. The following examples are extracted from the study report by Wade and Clampett [11] to give readers a general idea of fire spread through exterior walls. Although there are relatively few documented cases involving fire spread through combustible claddings and such spread does not generally directly threaten the building occupants, there are other serious vertical fire spread incidents where combustible cladding has not been involved. This type of facade fires may endanger the occupants of the building. For example, the secondary fires involving the ignition of the combustible materials in the upper floors as a result of the intense thermal exposure from the window fire plume can threaten the building occupants.

2.3.1 Fires Involving Combustible Claddings

2.3.1.2 Apartment Building, Munich (1996)

This was a five-storey apartment building in Munich. The building facade was made of a composite thermal insulation (about 100 mm thick) comprising polystyrene and foam plastics slabs and a reinforced covering layer. The fire originated in a nearby rubbish container and ignited the cladding and caused extensive damage to the building facade (Figure 2.6). Flames spread into rooms at upper floors through broken windows.

2.3.1.3 Te Papa (Museum of New Zealand), Wellington (1997)

This is a newly-built multi-level national museum located in Wellington. The exterior cladding used comprised a thin aluminium-faced panel with a polyethylene core, mounted over extruded foam polystyrene insulation board and building paper. During the construction of this building, a fire occurred on the exterior facade as a result of burning building paper, which was ignited by a worker when heat welding a roof membrane (Figure 2.7).

2.3.1.4 Knowsley Heights, Liverpool (1991)

An eleven-storey apartment building. Fire was started deliberately in the rubbish compound outside the building. The fire spread up rapidly through a 90 mm gap between the tower's rubberized paint-covered concrete outer wall and a recently installed rain screen cladding (with limited combustibility). The fire spread all the way to the highest floor and seriously damaged the outer walls and windows of all the upper floors (Figure 2.8). This rapid fire spread was believed to be caused by the lack of fire barriers in the cavity gap passing all eleven floors and providing a flue for hot gases to rise.

2.3.1.5 Winnipeg, Manitoba (1990)

This fire involved an eight-storey unsprinklered apartment building with an open-air parking garage located in the ground floor. The building's exterior walls were covered with a combustible Exterior Insulation and Finish System (EIFS). Fire initially started

in the garage and quickly involved all 25 cars that were parked there. Flames issuing from the garage exposed and eventually ignited the EIFS on the exterior walls. The fire then spread to the top of the fourth storey.

Figure 2.6: Apartment Building, Munich

Figure 2.7: Te Papa, Wellington

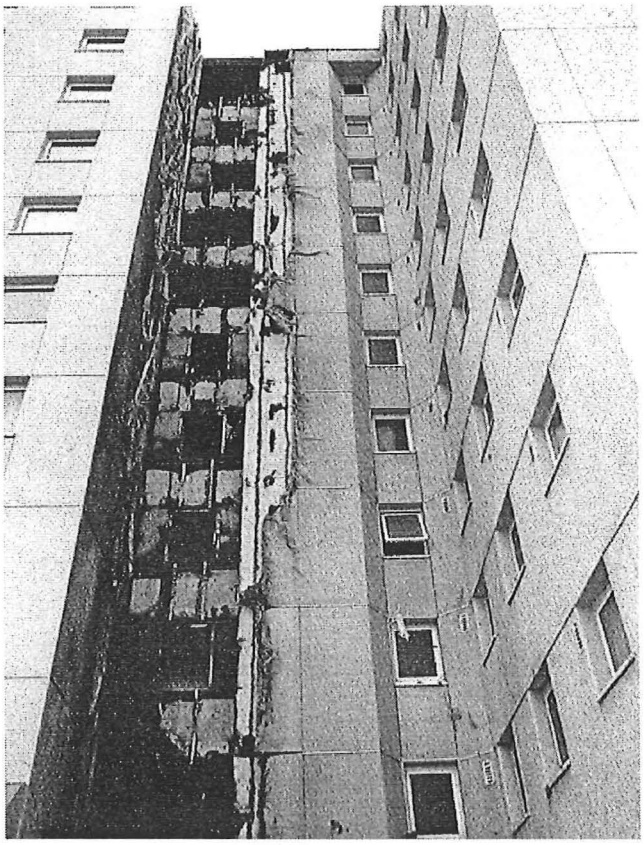

Figure 2.8: Knowsley Heights Fire

The combustion of gaseous hydrocarbons released by the decomposing organic components in an EIFS resulted in the thermal destruction of EIFS. A portion of the heat created by this combustion was fed back to the EIFS and caused further damage. The heat feedback from the burning wall was sufficient for destruction to continue, without any external heat exposure. This could become a very hazardous scenario, as the fire could spread to the top of the wall, regardless of the height of the wall.

2.3.2 Fires Involving Non-Combustible Claddings

Despite the low number of the reported exterior wall fires, there are other serious vertical fire spread incidents involving non-combustible cladding. For example, The First Interstate Bank fire, Los Angeles [12], where flames and hot gases were allowed to pass through to the floor above due to inadequate fire stopping of the gap between the edge of the floor slab and the exterior wall. Another example is the Andraus Building fire, Brazil [13], which involved a 31-storey department store and office building. The fire broke through the windows of the department store and then spread externally up to the upper 24 floors. The intense radiant heat from the external fire front ignited combustible ceiling tiles and wood partitions on each floor. Therefore vertical fire spread in multi-storey buildings can happen in several ways without involving a combustible cladding system, and it can often lead to very serious consequences in terms of building damage and life safety.

2.4 Research Review of Fire Spread on Claddings

Research on combustible wall claddings has been conducted in New Zealand and overseas to evaluate the fire safety performance of exterior cladding materials and the applicability of various test methods in the assessment of flame spread potential. Wade and Clampett [11 & 14] give an excellent review of international research on the fire safety performance of exterior cladding materials, fire test methods, relevant building regulations and real fire experiences concerning fire spread via exterior walls.

2.4.1 Canadian Research

The international research presented in this report is based on the research carried out by the National Research Council of Canada (NRCC) [15], which includes the full-scale experimental studies of fire exposure to exterior walls, fire hazards associated with the use of combustible claddings, and the development of new test methods for assessing the flammability of combustible claddings.

2.4.1.1 Full-Scale Fire Tests

The full-scale tests involved a three-storey burn facility (Figure 2.9) with a single-room opening, through which flames issued as from a window of a flashed-over room. The fuel for the experimental fire was propane gas. A flat facade specimen of 5 m wide by about 10.3 m high was used in the test. The duration of fire exposure was 25 minutes.

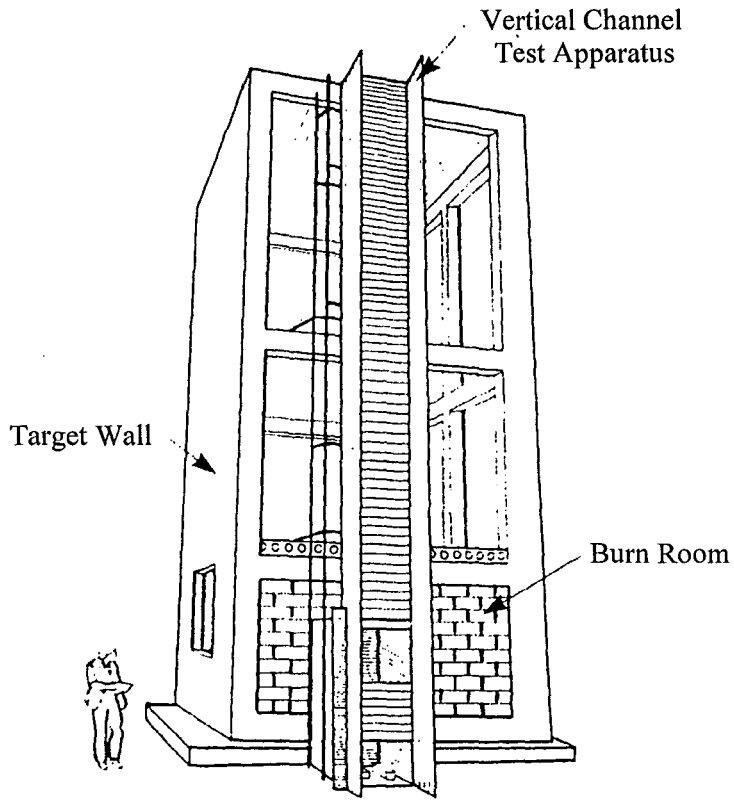

Figure 2.9: Three-storey burn facility used for full-scale tests [15]

Measurements were made with several thermocouples and heat flux transducers. The primary variables used for assessing fire safety performance of combustible claddings

were visual flame spread distance and maximum heat flux density recorded at 3.5 m and 5.5 m above the top of the window opening on the centre line of the wall. The results for non-combustible (marinite) walls were used to assess fire exposure of other combustible cladding materials in terms of maximum heat flux densities and vertical flame spread distance (Table 2.1).

Table 2.1: Vertical flame spread distance and maximum heat flux densities recorded in full-scale experiments [15]

Assembly	Flame dist. (m)	Heat flux density, kW/m² @ 3.5 m	@ 5.5 m
1–Marinite over concrete block wall	2.0[a]	16	10
2–Gypsum sheathing on glass fiber insulated wood frame wall	3.0	15	10
3.1–Vinyl siding on gypsum sheathing on glass fiber insulated wood frame wall	3.0	23	17
3.2–Aluminum siding on wood chip board on glass fiber insulated wood frame wall	4.5	70	20
3.3–12.7 mm flame retardant treated plywood on untreated wood studs, with phenolic foam insulation in cavities	3.0	29	20
3.4–Aluminum sheet (0.75mm) on flame retardant treated wood studs, with phenolic foam insulation in cavities	3.2	20	12
3.5–76mm expanded polystyrene insulation, glass fiber mesh, 7mm synthetic plaster, on gypsum sheathing, glass fiber insulated steel stud wall	4.5	31	8
3.6–Composite panels (6mm FRP membranes, 127mm polyurethane foam core) attached to concrete block wall	4.0	24	10
3.7–102mm expanded polystyrene insulation bonded to gypsum sheathing, covered with glass fiber mesh embedded in 4mm synthetic plaster	4.5	48	37
3.8–76mm expanded polystyrene insulation bonded to gypsum sheathing, covered with glass fiber mesh embedded in 4mm synthetic plaster	2.0	27	11
4.1–8mm wood chip board on glass fiber insulated wood frame wall	7.5	61	79
4.2–Vinyl siding on 8mm wood chip board on glass fiber insulated wood frame wall	7.5	82	111
4.3–Aluminum siding on 25mm strapping, 25mm expanded polystyrene, 19mm plywood, glass fiber insulated wood frame wall	7.5	30	31

[a]height of exposing flame

The performance of each assembly indicated in Table 2.1 was then catagorised according to the maximum flame spread distance, as shown in Figure 2.10. The maximum flame spread distance was defined as the distance between the top of window opening and the highest observable instance of flaming along the wall.

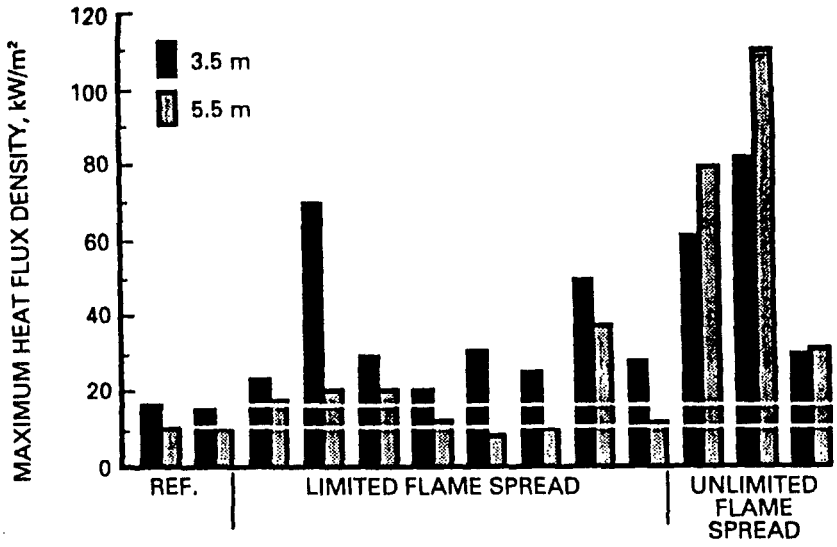

Figure 2.10: Maximum one-minute averaged heat flux density at 3.5 m and 5.5 m above window for thirteen specimens given in Table 2.1 [15]

It can be seen from Figure 2.10 that the performance of each assembly was categorised into three groups, namely:

1. **No flame spread**: Specimens that did not support the spread of flame beyond the extent of the external flame.
2. **Limited flame spread**: The recorded flame spread distance on the specimen stopped or receded before the end of the test.
3. **Unlimited flame spread**: The recorded flame spread extended to the top of the wall.

It was found that higher heat flux density was recorded at the lower level of the specimen (closer to window opening) than that recorded at the higher level (further away from the window opening) for specimens that did not support the flame spread to the top of the wall. However, the reverse condition was observed for the specimens that supported flame spread to the top of the wall. The significant heat output from the

burning portion of the wall may have contributed to the higher heat flux density at the higher level of the specimen.

2.4.1.2 Reduced- Scale Fire Tests

Reduced-scale fire tests are desirable in order to assess the fire safety performance of exterior cladding materials, as they are less expensive to run and more suitable for most testing organisations to carry out. The tests must be able to discriminate the good and bad performing exterior cladding materials in terms of their flame spread propensity in real fire situations. An interesting find in the NRCC tests [15] is the suitability of a reduced-scale test in assessing the flame spread propensity of combustible claddings. The reduced-scale test methods investigated by NRCC include the Vertical Channel Tests, IMO Surface Flammability Tests, Modified Roof Deck Tests and Steiner Tunnel Tests.

The Vertical Channel Tests resemble the heat exposure of the full-scale tests but with a much narrower (0.85 m wide) and slightly shorter (7.3 m high) specimen. Figure 2.9 shows the vertical channel tests attached to the full-scale test facility.

The Vertical Channel tests gave indications of flame spread characteristics similar to those obtained in full-scale tests. This method is able to discriminate between the good and bad performances of cladding materials as well as the full-scale tests. This suggests that the Vertical Channel test can be a feasible method of evaluating the performance of external cladding systems, since it is less costly to run and a less complex testing method than the full-scale tests.

However, IMO Surface Flammability Tests, Modified Roof Deck Tests and Steiner Tunnel Tests are not suitable for assessing the fire safety performance of the cladding materials. The reasons are:

- IMO Surface Flammability Tests: The small size of this apparatus does not accommodate the full thickness of a representative wall assembly and the typical elements and features of the wall assembly.

- Modified Roof Deck Tests: Inadequate heating of the specimens due to insufficient heat exposure resulted in this test method. The wall assembly produced falling debris on to the burners and obstructed them.

- Steiner Tunnel Tests: This method was able to differentiate between some of the specimens based on their flame spread propensities but it gave poor prediction of performance of the wall assemblies which are made of multiple-layer composite materials.

2.4.2 Research in New Zealand

Test methods such as AS 1530.1 [4] and AS 1530.3 [3] are used to classify the fire performance of exterior cladding materials based on stringent pass/fail criteria. The disadvantages of these test methods, especially for those newly developed combustible systems (which are claimed to have many economic and aesthetic advantages and not to propagate fire on the exterior of buildings) have been recognised by regulatory authorities in New Zealand. An improved classification scheme based on the concept of total heat release and rate of heat release was proposed by Wade [5] and it is included in the following table.

Table 2.2: Suggested performance criteria for exterior wall claddings based on peak rate of heat release and total heat release [5]

Category	Peak Rate of Heat Release* (kW/m^2)	Total Heat Release* (MJ/m^2)
A	≤ 100	≤ 25
B	≤ 150	≤ 50
C	≤ 350	≤ 125

*Obtained from cone calorimeter tests at $50kW/m^2$ and duration of 15 mins

Generally, category A is intended to apply to products which will not propagate vertical flame spread, such as fibre-cement board, paper-faced gypsum plasterboard and metal sheet. Cladding materials, which present limited flame spread, but may have

local damage can be classified as category B. Category C applies to cladding materials which result in vertical flame spread, but exclude materials significantly worse than wood claddings.

In addition to the classification scheme based on the concept of rate of heat release, the flame spread characteristics of exterior wall claddings have been analysed by applying an analytical method for concurrent flow flame spread on a vertical surface [7]. This analytical method is used to observe flame acceleration and deceleration characteristics for the range of cladding materials tested in a cone calorimeter (Figure 2.11). The analytical method, in conjunction with material flammability parameters (thermal inertia and surface ignition temperature), is used to derive scientifically based performance criteria based on flame spread propensities of cladding materials.

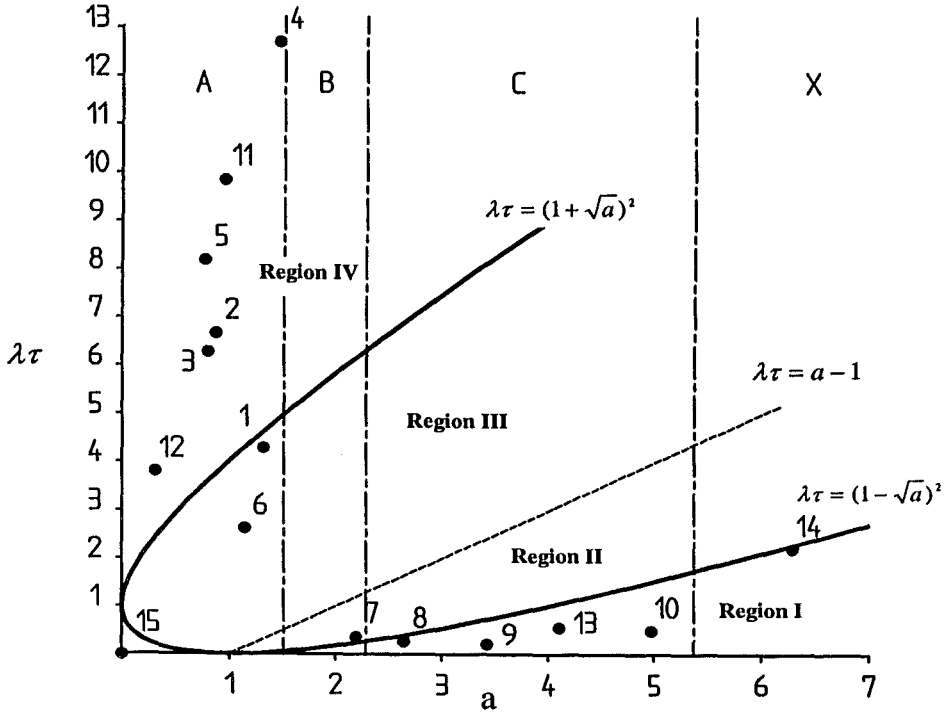

Region I: Exponentially accelerating flame spread

Region 2: Initial acceleration, but decelerates and stops at a finite time

Region 3: Initial deceleration. There was no acceleration until the velocity has been negative for some time

Region 4: Decelerate all the time

A, B, C & X are the classifications based in the Flame Spread Performance Criteria (Table 2.2)

Numbers **1-15** represents a series of products tested at BRANZ (see Table 2.3)

Figure 2.11: Regions of flame front acceleration and deceleration [7]

Table 2.3 shows the products tested at BRANZ and they are classified in accordance with the rate of heat release and the analytical method for flame spread. It can be seen from Table 2.3 that the classification scheme for exterior wall claddings proposed by the analytical method seems to agree well with the classification scheme based on peak rate of heat release and total heat release. It indicates that the method can be used to rank combustible cladding materials according to their flame spread propensities. However, this classification scheme is only applicable to those cladding systems which maintain mechanical integrity and exhibit idealised heat release behaviour (i.e. exponential decay phase after the peak rate of heat release).

Table 2.3: Flame spread performance of selected exterior wall claddings [7]

ID	Generic Description	Peak HRR kW/m^2	Total HR MJ/m^2	Category	Region at 50	Region at 75
15	Metal sheet	0	0	A	IV	
2	Fibre-cement board	58	2	A	IV	III
5	Plaster	51	3	A	IV	
1	EIFS	88	3	A	III	III
4	Metal sheet	98	3	A	IV	
12	Fibre-cement board	21	5	A	IV	
11	Fibre-cement board	64	6	A	IV	
6	Plaster	76	6	A	III	III
3	Fibre-cement board	53	6	A	IV	
7	PVC	182	39	C	II	I
9	Timber	229	67	C	I	I
13	Timber	273	77	C	I	
10	Hardboard WB	332	96	C	I	I
8	Timber	177	106	C	I	
14	Hardboard WB	419	106	X	I	

The similarity of the classification methods based on the rate of heat release and flame spread propensities is summarised in Table 2.4.

Table 2.4: Performance criteria based on degree of combustibility or analytical solution

PERFORMANCE CRITERIA		
Peak Rate of Heat Release and Total Heat Release (Category)	**Analytical Solution (Regions)**	**Flame Spread Characteristic on Exterior Cladding System**
A	III & IV	No vertical flame spread
B	II & III	Limited vertical flame spread
C	I & II	Possible vertical flame spread*

*Exclude materials significantly worse than wood claddings.

CHAPTER 3

3 FLAME ISSUING THROUGH A WINDOW OPENING

3.1 Introduction

To study the flame spread on exterior claddings, the behaviour of internal fire and flames projected through window openings must be understood. Law [16] has reviewed the early works on correlating external flame length and flame temperature based on given fire compartment dimensions, window dimensions, quantity of combustibles and the ventilation condition in her study to understand external flame behaviour. This chapter summaries Law's equations of the flame behaviour, and these equations are ultilised in developing the heat transfer model. A sample of the developed spreadsheet for the heat transfer model is given at the end of this chapter. The input and outputs of the spreadsheet are also included in this chapter.

3.2 Internal Fire Behaviour

A fire in the building, without the intervention of fire brigade and sprinklers, can be considered to go through three phases: growth, full development and decay once the fuel is exhausted [8]. Once the fire reaches the fully developed stage, the room condition reaches flashover condition. Drysdale [17] uses three basic measures to gauge flashover. This can be the temperature of 600 °C under the ceiling, a radiation heat flux of 20 kW/m^2, or the emerging of flames from window openings. The external venting flame poses a risk to exterior wall cladding, as the venting flame may ignite the combustible cladding materials. The size, temperature and duration of the external venting flames from a window opening are affected by the fire loads, the size of fire compartment, the size of window opening, and ventilation conditions. Each of these factors is discussed as follows.

3.2.1 Fire Compartment

The compartment in its simplest form is illustrated in Figure 3.1. In practice, there could be several window configurations on a fire compartment but they were not included in Law's study.

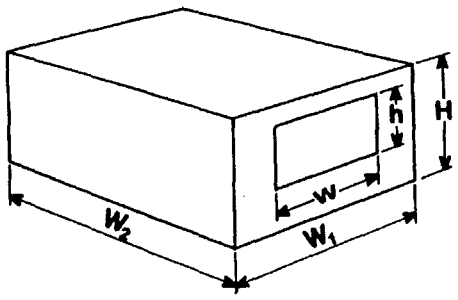

Figure 3.1: Simple fire compartment [16]

3.2.2 Fire Loads

In both large-scale and model-scale experiments, wood cribs and some furniture have usually been used as experimental fires as it is an easily reproducible fuel. Heat given off from different burning materials is converted into equivalent amounts of wood, which will give approximately the same amount of heat when burnt. It is assumed by Law that the information derived from fires involving mainly wood fuel may give reasonable correlation with domestic, office, and similiar types of fire load.

The fire load density is expressed in the amount of wood (kg) per unit area (m^2). The fire load per unit area varies with the type of occupancy for the particular building under consideration.

3.2.3 Draft Conditions

Most of the correlations which were derived from experiments were conducted in still air or a light wind condition. This may be termed as "natural draft" condition, in which the air flow has been controlled by the fire behaviour and compartment size. In

contrast, the "forced draft" condition represents an extra air supply into the fire compartment. The extra air supply can come from openings on the opposite sides of a fire compartment. Different amounts of available air in these two draft conditions will have an influence on the behaviour of the fire.

3.2.4 Rate of Burning

It is necessary to work out the rate of burning, as it will affect the size and duration of external venting flames. There exist two burning conditions: ventilation-controlled fires or fuel-controlled fires. Thus, it is very important to be able to distinguish between these two regimes.

(a) Fuel-Controlled Fires

Law has found that the rate of weight loss is approximately steady over the fully developed period when the weight falls from 80% to 30% of its initial value. This rate of weight loss is defined as the average rate of burning. This burning rate represents the rate of burning of total mass of the fire load over the effective fire duration, τ. For any given type of fuel, the fuel-controlled burning rate $(\dot{m}_f)$ is directly proportional to the total mass of the fire load (L), and is given by:

$$\dot{m}_f = \frac{L}{\tau} \qquad \ldots (3.1)$$

In free burning conditions, τ is represented by τ_f, and it is determined by the characteristics of the fire load. For instance, thick fuels with small surface areas give larger values of τ_f, and thus smaller burning rates.

The free burning fire duration, τ_f, is assumed by Law to be 20 minutes, which is common for most types of furniture found in buildings. Thus, the burning rate is given by:

$$\dot{m}_f = \frac{L}{1200} \qquad \text{... (3.2)}$$

(b) Ventilation-Controlled Fires

In ventilation-controlled fires, there is an upper limit to the fuel that could be burnt in the fire compartment.

Thomas and Heselden [18] analysed a set of data of 400 experiments conducted under the auspices of the Council Internationale du Batiment (CIB), using wood cribs as the fuel, and varying the compartment size and shape, the ventilation parameter $(A_w h^{1/2})$ and the fire load density. The ventilation-controlled burning rate $(\dot{m}_v)$ was developed from the analysis of these data, and it is given by:

$$\dot{m}_v = 0.18 \frac{\left(1 - e^{-0.036\eta}\right) A_w h^{1/2}}{(D/W)^{1/2}} \qquad \text{... (3.3)}$$

where η is given by:

$$\eta = \frac{A_t}{A_w h^{1/2}} \qquad \text{... (3.4)}$$

The important parameters which affect the rate of burning in ventilation-controlled conditions, by considering air flow and a heat balance, have been identified as the height of the window (h), the area of window opening (A_w), the ratio of the depth to width to the compartment (D/W), and the total area of the enclosing surface (excluding window) through which the heat is lost (A_t). The effects of compartment size and window opening are included in variable "η".

The burning rate given by Eq. (3.3) can be said to be the theoretical maximum rate of fuel that can be combusted within the fire compartment. This implies that if the rate of production of fuel volatiles due to the thermal decomposition in the fire room exceeds this value, excess fuel will be ejected out the window to produce external burning.

The burning rate $(\dot{m})$ should be calculated from Eqs (3.2) and (3.3) for particular fire load and compartment size. Whichever gives the lower value ($\dot{m}_f$ or $\dot{m}_v$) is the burning condition as this is governed by the lower burning rate.

3.2.5 Fire Temperature in the Compartment

There is an upper limit to the temperature attained within the fire compartment. This maximum temperature depends on the available fire load and the fire compartment and window dimensions. Law proposed Eq. (3.5) to estimate the maximum fire temperature rise in the fire compartment, $\theta_{c(\max)}$, over the fully developed fire period, as a function of η. The effects of fire compartment and window dimensions are included in variable "η".

$$\theta_{c(\max)} = \frac{6000\left(1-e^{-0.1\eta}\right)}{\eta^{1/2}} \qquad \ldots (3.5)$$

As shown in Figure 3.2, the results of large-scale tests with low fire load densities, fall well below maximum temperatures given by Eq. (3.5).

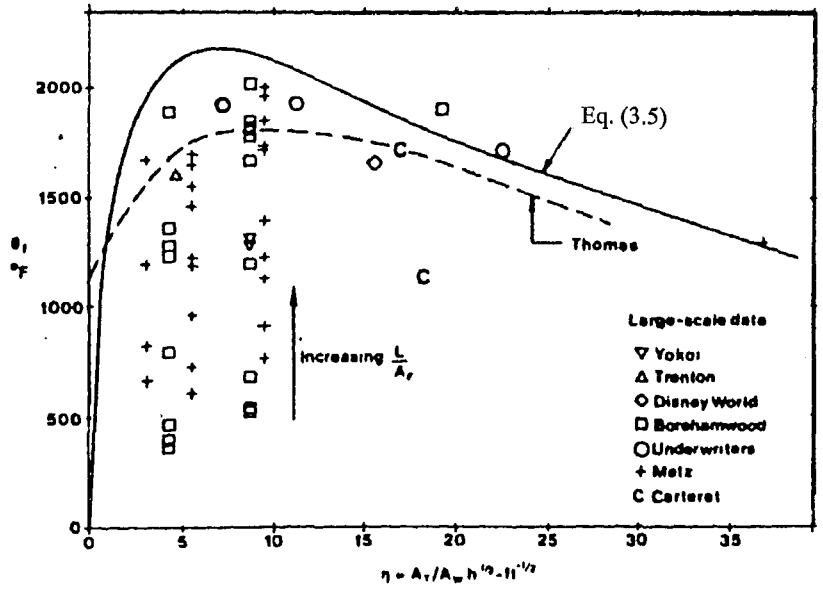

Figure 3.2: Variation of average fire temperature rise (θ_c) with compartment size and window area in natural draft condition [16]

The fire temperature attained for low fire loads depends not only on the fire load density, but also on the fire load in relation to ventilation and compartment size. Another important parameter, "ψ", is introduced to relate the fire load to ventilation and compartment size. It has been used to modify Eq. (3.5) for the upper limit, as follows:

$$\frac{\theta_c}{\theta_{c(\max)}} = 1 - e^{-0.054\psi} \qquad \ldots (3.6)$$

where ψ is given by:

$$\psi = \frac{L}{(A_w A_T)^{1/2}} \qquad \ldots (3.7)$$

By combining Eqs. (3.5) and (3.6), an estimation of fire temperature attained within the compartment, T_c ,can be estimated by:

$$T_c = T_\infty + \frac{6000\left(1-e^{-0.1\eta}\right)}{\eta^{\frac{1}{2}}}\left(1-e^{-0.054\psi}\right) \quad \ldots (3.8)$$

where T_∞ is the ambient temperature (K).

It has been shown that the fire temperature in the compartment for forced draft condition shows no significant variation of temperature with η or air supply. The estimated fire temperature attained within the compartment for forced draft can be related to ψ and is given by the following expression.

$$T_c = T_\infty + 1200\left(1-e^{-0.04\psi}\right) \quad \ldots (3.9)$$

It will be expected that the T_c would decrease with increasing air supply. Eq. (3.9) may overestimate the fire temperature where there is a strong wind.

3.3 Behaviour of the Flame Issuing Through A Window Opening

In order to be able to calculate the amount of heat transfer from the projecting flame to the exterior wall cladding, it is necessary to be able to determine the shape and size of the flames issuing from the window opening and the temperature distribution within the flame.

The first comprehensive study of flame projection from windows was made by Yokoi [19]. He derived correlations for the plume rising from various size and shape windows in a 0.4x0.4x0.2 m high model room containing alcohol fires. He has demonstrated that a flame projecting out of a window will vary on the basis of a

number of factors, including the effect of a wall above the window, the shape of the window, the effects of horizontal projections or balconies. These factors will have an effect on the temperature distribution and trajectory of the external venting flames. Yokoi defined a geometric parameter, *n*, which was the ratio of twice the width of the opening, *2w*, to the height of the opening, *h*. He used this defined aspect ratio as the parameter to investigate the trajectory of the plume formed at the window. He has demonstrated that the width to height ratio has an important effect on the flame trajectory: with wide windows the flame does not project far from the facade, but clings to the wall above, whilst with narrow windows it tends not to.

Figures 3.3 and 3.4 illustrates the main features of interest for flames projected through a window opening for both natural draft and forced draft conditions. The position of the tip of the flame is generally defined as the point along the axis at which the flame temperature has dropped to 540 °C [20]. At this point, the flame loses its luminous character.

The geometrical model of the flame projection is kept simple to facilate calculations.

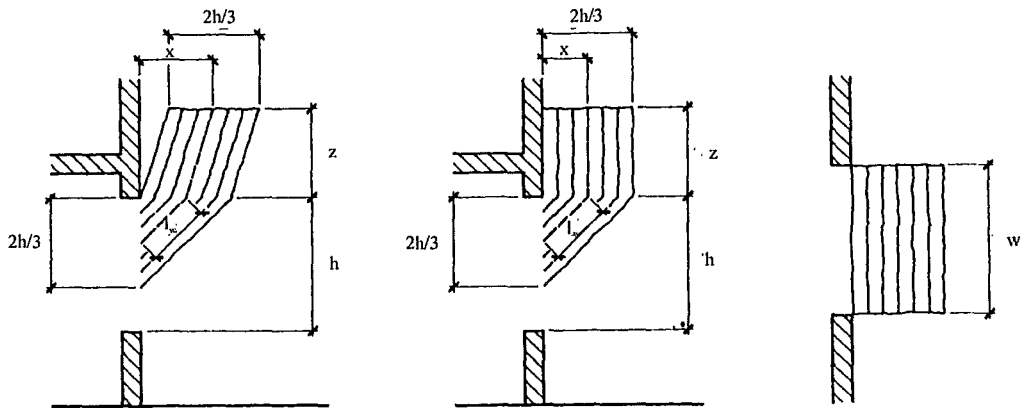

a) h>1.25w or no wall above b) h<1.25w, wall above

Figure 3.3: Assumed trajectory of emerging flame (natural draft) [16]

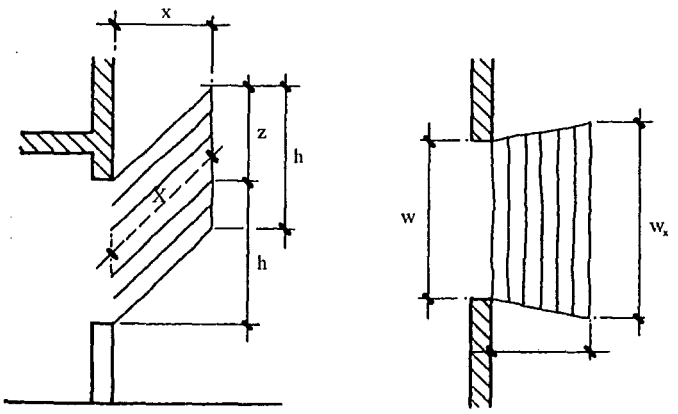

Figure 3.4: Assumed trajectory of emerging flame (forced draft) [16]

3.3.1 Flame Depth

In natural draft condition, Law assumed that the flame emerges above the neutral plane from the upper two-thirds of a window (i.e. 2/3h). Flame tends to emerge from the upper two-thirds of a window, with cold air being drawn in below the neutral plane.

With force draft, the flame can emerge from the whole window, as shown in Figure 3.4.

3.3.2 Flame Height

(a) Natural Draft

Thomas and Law [21] analysed the data by Yokoi [19], Wester et al. and Seigel [20] and proposed the following correlation for flame height, which applies to wood crib fires in enclosures in the absence of wind:

$$z = 16\left(\frac{\dot{m}h}{A_w\rho(g)^{1/2}}\right)^{2/3} - h \qquad \text{... (3.10)}$$

Eq. (3.10) can be simplified by assuming the density of gases, ρ, is 0.45 kg/m^3 at 540 °C and g = 9.81 m/s^2, into the following equation:

$$z = 12.8\left(\frac{\dot{m}}{w}\right)^{2/3} - h \qquad \text{... (3.11)}$$

(b) Forced Draft

In the case of forced draft conditions, the buoyancy and turbulent mixing effects are less significant and the flame has more of the character of a jet [20]. The wind may affect the flame size and direction for a given rate of burning. Law modified the correlation given by Seigel and proposed the following correlation for the height of the flame tip above the top of the window opening, which includes the effect of wind.

$$z = 23.9\left(\frac{1}{u}\right)^{0.43}\left(\frac{\dot{m}}{A_w^{1/2}}\right) - h \qquad \text{... (3.12)}$$

where u is the velocity of wind (m/s).

3.3.3 Horizontal Projection

(a) Natural Draft

The following correlations have been devised by Law for the horizontal distance of the flame tip from the window:

Presence of wall above window opening

For h<1.25w:

$$x = \frac{1}{3}h \qquad \text{... (3.13)}$$

For h>1.25w, and distance to any other window exceeding four times the width of individual window, w:

$$x = 0.3h\left(\frac{h}{w}\right)^{0.54} \quad \text{... (3.14)}$$

No wall above window opening

$$x = 0.6h\left(\frac{z}{h}\right)^{\frac{1}{3}} \quad \text{... (3.15)}$$

The overall horizontal projection of the flame is defined as $x + h/3$. For wide windows in relation to its height (h<1.25w), the flame will tend to lean back against the wall and the outward projection of the flame is approximately two thirds the window height. As for a narrow window, it is expected that the flame will be projected further away and it can be calculated by Eq. (3.14).

(b) Forced Draft

The correlation between the horizontal projection with the flame height and window speed is given by Law as:

$$x = 0.61\left(\frac{u^2}{h}\right)^{0.22}(z+h) \quad \text{... (3.16)}$$

where u is the velocity of the wind (m/s).

Eq. (3.16) can be used for both a wall and no wall above the window opening in forced draft conditions.

3.3.4 Flame Width

(a) Natural Draft

Observations of flame behaviour at windows suggest that the maximum width of the emerging flame will be little different from the window width. Therefore it is reasonable to assume that the effective width of the flame remains the same size as the width of the window.

It is also assumed that the flame temperature remains constant across the full width of the flame axis. This is likely to be a conservative assumption, and, will compensate for any slight widening of the flame under some conditions.

(b) Forced Draft

In the forced draft condition, the flame width usually exceeds the window width. This happens when the hot gases move away from the window opening and results in slight widening of the projecting flame. The average widening angle made by the emerging flame is about 11°. Thus, the maximum flame width, w_x, of the projecting flame in forced draft condition is given by Law as:

$$w_x = w + 0.4x \qquad \text{... (3.17)}$$

The flame width increases with horizontal projection distance. Therefore, it is proposed that the width of the projecting flame near the window should be the same as the width of the window, increasing to (w+0.4x) at the flame tip, as shown in Figure 3.4.

3.3.5 Flame Length along Axis

(a) Natural Draft

Law has proposed the following formulae to calculate the length of the flame axis (or the centre line distance), X, from the window plane to the flame tip in the presence of a wall or no wall above a window opening.

Presence of wall above window opening and $h < 1.25w$

$$X = z + l_w \qquad \text{... (3.18)}$$

No wall above window opening or $h > 1.25w$

$$X = \sqrt{z^2 + \left(x - \frac{h}{3}\right)^2} + l_w \qquad \text{... (3.19)}$$

For Eqs. (3.18) and (3.19), the distance along the flame centre line from window to the top of the window, l_w, is given by:

$$l_w = \sqrt{x^2 + \left(\frac{h}{3}\right)^2} \qquad \text{... (3.20)}$$

(b) Forced Draft

The distance along the flame axis, X, from the window plane to the flame tip may be calculated from simple flame geometry (Figure 3.4). It is given by:

$$X = \left(z^2 + x^2\right)^{1/2} \quad \text{... (3.21)}$$

3.3.6 Temperature at Flame Axis

(a) Natural Draft

Law has given the following correlations for the flame temperature along the centre line axis of the flame.

The flame temperature at a certain height above window (T_F) is represented by:

$$T_F = T_\infty + \left(T_o - T_\infty\right)\left(1 - \frac{0.027lw}{\dot{m}}\right) \quad \text{... (3.22)}$$

where l is the distance along the flame centerline from the window (m).

The calculated flame temperature by Eq. (3.22) is conservative, and consistently gives higher calculated values than the measured temperatures in the experiments conducted by Turan et al [22].

Assuming that the ambient temperature (T_∞) is 293 K and temperature at the flame tip is 813 K [20] for $l = X$, Eq. (3.22) is rearranged to give the flame temperature at the window (T_o) as:

$$T_o = T_\infty + \frac{520}{\left(1 - \frac{0.027Xw}{\dot{m}}\right)} \quad \text{... (3.23)}$$

A substantial amount of unburnt gas can be emitted from the fire compartment in ventilation-controlled fires. This leads to extra burning taking place outside the fire compartment. Therefore, it is expected that the window temperature (T_o) may be greater than the fire temperature in the compartment (T_c).

It is assumed that the flame temperature varies linearly with the distance across the flame axis, and remains constant across the width and through the thickness of the flame. The full-scale flashover fire experiments [22] have shown that only the first assumption is valid. However, this simplified assumption shall err on the conservative side.

(b) Forced Draft

In forced draft condition, the emerging flame is treated as a jet flame [20]. Unlike natural draft condition, the flame temperatures at the window or at a certain height above the window are dependent on the area of window opening rather than the width of window opening.

Law has improved the correlations given by Seigel [20] on the temperature distribution in flame for the forced draft condition and come up with the following correlations.

For the flame temperature at any point along the flame axis:

$$T_F = T_\infty + (T_o - T_\infty)\left(1 - \frac{0.019 l \sqrt{A_w}}{\dot{m}}\right) \quad \text{... (3.24)}$$

For the flame temperature at window:

$$T_o = T_\infty + \frac{520}{\left(1 - \frac{0.019 X \sqrt{A_w}}{\dot{m}}\right)} \quad \text{... (3.25)}$$

In contrast to natural draft condition, the flame temperature at the window in forced draft condition may be less than the fire temperature in the compartment (T_c).

CHAPTER 4

4 HEAT TRANSFER TO EXTERIOR WALL CLADDINGS

4.1 Introduction

Flame emerging from a window opening will expose the wall above the window. It is essential to analyse the external heat transfer to exterior wall claddings. There are two components of fire exposure on the exterior wall from the flame issuing from a window. First, the venting flame plume itself acts as a radiator. As the venting flame plume washes up and over the faces of the exterior wall above the opening, it also imposes a convective heat component. The total heat flux received by the exterior wall is defined as the sum of intensity of both convective and radiant components to the exposed wall.

The model of heat transfer to exterior walls is based on the behaviour of flame issuing through a window opening discussed in Chapter 3. The heat transfer model is capable of predicting the total heat flux impinging on exterior walls. Methods of calculating external heat flux by Law [16] and Oleszkiewicz [23] are reviewed in the following section. The methods of predicting external heat flux were also derived from first principle methods. These three methods are included in the model of heat transfer for predicting the heat flux impinging on the exposed wall. The heat flux predictions from these three methods were compared with the experimental data to see the appropriateness and deficiencies of each method.

4.2 Convection

The projecting flame will transfer heat to the cooler surrounding facade by convection heat transfer, $\dot{q}''_c$. Convection heat transfer can be expressed as:

$$\dot{q}''_c = \alpha(T_F - T_w) \quad \text{... (4.1)}$$

where α is the convection heat transfer coefficient (W/m^2.K), T_F is the flame temperature varies with the position above the window (K) and T_w is the surface temperature of the wall cladding (K).

In order to determine the convective heat transfer, an appropriate α value must be determined for the wall cladding being heated by the projecting flame. Below are the methods derived by Law [16], Oleszkiewicz [23] and from first principle methods to calculate the convective heat transfer coefficient, α.

4.2.1 Law's Method

The convective heat transfer coefficient, α, depends on the mass flow per unit area, $u_o\rho$, of the hot gases and the size and orientation of the receiving surface.

Law derived the convective heat transfer coefficient for natural draft conditions based on the relationship between the Nusselt number, *Nu*, and the Reynolds number, *Re*, where:

$$Nu = \frac{\alpha d}{k} \quad \text{... (4.2)}$$

$$\mathrm{Re} = \frac{u_o \rho d}{\mu} \quad \text{... (4.3)}$$

The thermal properties of the gases, thermal conductivity (k) and dynamics viscosity (μ) are taken at the "film" temperature, that is the mean of the temperature of the hot gases and the wall surface.

For the parallel flow of the emerging flame across the exterior wall, the relationship between Nusselt number and Reynolds number is given by Law as:

$$Nu = 0.12\,\mathrm{Re}^{0.6} \qquad \text{... (4.4)}$$

The mass flow of gases leaving the window depends on the process by which air is drawn into the fire. Law assumed that the mass flow rate leaving the window for ventilation controlled fire is about $6.4\dot{m}$. The flames and hot gases are assumed to leave the compartment at about $2h/3$ below the top of the window. The mass flow per unit area of the hot gases and flame is estimated to be:

$$u_o \rho \approx \frac{9.6\dot{m}}{A_w} \qquad \text{... (4.5)}$$

By substituting Eq. (4.5) into Eq. (4.3), the Reynolds number becomes:

$$\mathrm{Re} = \frac{9.6\dot{m}d}{A_w \mu} \qquad \text{... (4.6)}$$

By substituting Eq. (4.6) into Eq. (4.4), the Nusselt number then becomes:

$$Nu = 0.47\left(\frac{\dot{m}d}{A_w \mu}\right)^{0.6} \qquad \text{... (4.7)}$$

Combining Eqs. (4.7) and (4.2) yields:

$$\alpha = 0.47 k_z \left(\frac{\dot{m}}{A_w \mu} \right)^{0.6} \left(\frac{1}{d} \right)^{0.4} \quad \text{... (4.8)}$$

Law has found that the convective heat transfer coefficient is not very sensitive to film temperature and a representative temperature of 732 °C is adopted. Thus, Eq. (4.8) becomes:

$$\alpha = 0.0132 \left(\frac{\dot{m}}{A_w} \right)^{0.6} \left(\frac{1}{d} \right)^{0.4} \quad \text{... (4.9)}$$

The convective heat transfer coefficient given by Eq. (4.9) is overestimated for a free-burning fire but it still gives a slightly conservative solution (i.e. gives higher convective heat transfer rate to the exposing wall).

4.2.2 Oleszkiewicz's Method

The original convective heat transfer coefficient by Law (Eq. 4.9) includes the shape of the receivers (beams or columns). Oleszkiewicz [23] eliminated the dependence of the procedure on the shape of the receivers, and formulated with the following expression for the convective heat transfer coefficient.

$$\alpha = k_o \left(\frac{\dot{m}}{A_w} \right)^{0.6} \quad \text{... (4.10)}$$

Eq. (4.10) is based on the assumption that the mass velocity within the window plume is proportional to the ratio of burning rate to the window area. The empirical factor, k_o, was determined by correlating the calculated convective heat flux density with the

experimental measurement[+]. The numerical value of k was found to be 0.013. Eq. (4.10) then becomes:

$$\alpha = 0.013\left(\frac{\dot{m}}{A_w}\right)^{0.6} \quad \text{... (4.11)}$$

4.2.3 First Principle Methods

In a room fire, the gases can flow out through two processes [24]. Firstly, the heating of air in a room causes the air to expand. The expanded air will be pushed out through all available vents and hence throughout the entire building. Secondly, the products of combustion and smoke together with the hot gases will rise in a plume to the ceiling. The build-up of this will eventually fall below the top of a vent. As the fire grows larger, hot gases flow buoyantly out of the place of origin. At this moment, the buoyant flow out will exceed the expansion of gases by the fire. At this stage of the process, the smoke and perhaps flames are issued out of the top of a window opening, while cold gas flows in below (Figure 4.1). The emerging flame from the window opening is treated as vent flow.

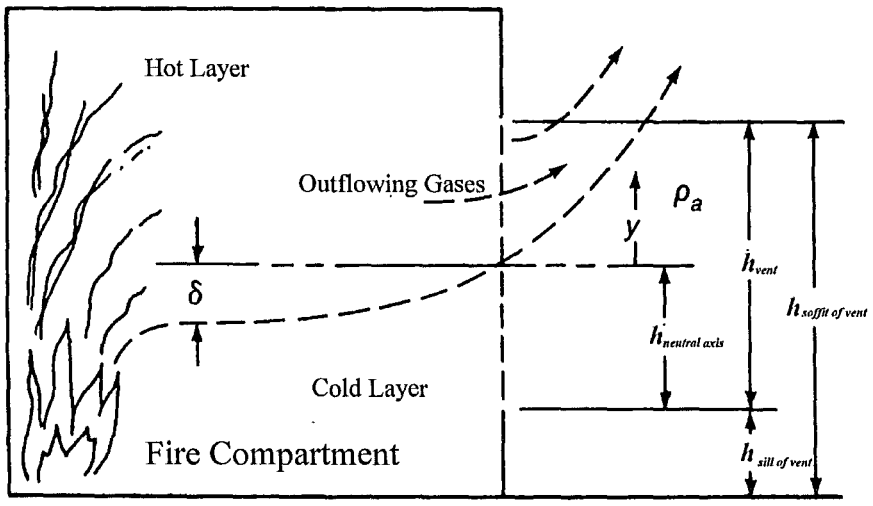

Figure 4.1: Buoyant flow out of the window of a fire compartment [24]

[+] Wood cribs fires conducted in a 2.4 m wide by 3.6 m deep by 2.4 m high burn room with the front wall extended to 6.1 m in height and 3.6 m in width.

The appropriate flow formula for hot gases flow through the window opening is given as [24]:

$$u_o = \left[2gy\left(\frac{\rho_\infty - \rho_o}{\rho_o} \right) \right]^{1/2} \quad \text{... (4.12)}$$

where ρ_o is the density of the hot gases and ρ_∞ is the density of the ambient air.

Rearranging Eq. (4.12) using ideal gas law, $\rho_o T_o = \rho_\infty T_\infty$, it then becomes:

$$u_o = \left[2gy\left(\frac{T_o}{T_\infty} + 1 \right) \right]^{1/2} \quad \text{... (4.13)}$$

where T_∞ is the ambient temperature (K), T_o is the temperature of outflowing hot gases (K) and y is given as:

$$y = \frac{2}{3}h \quad \text{... (4.14)}$$

The velocity of the emerging flame from the window opening can be worked out by Eq. (4.12), provided that the flame temperature at the window is estimated from Eq. (3.23) or Eq. (3.25). The velocity of the emerging flame is substituted back into Eq. (4.3) to work out the Reynolds number. Due to the boundary layer effects, the density and dynamics viscosity of gases are taken at the "film" temperature. The characteristic dimension, *d*, is taken as the sum of distance above the window opening and the height of outflowing flame through the window opening, which is two-thirds the height of the window.

The emerging flame can be treated as an applied flow across the surface of the wall cladding, therefore the wall will undergo forced convection. Small disturbances may be

amplified downstream for forced convective flows. This leads to transition from laminar to turbulent flow conditions [25]. For sufficiently large Reynolds numbers (Re > 5 x 10^5) for flow over a flat plate, a transition to turbulence occurs.

In order to accurately calculate the convective heat transfer, the temperature-dependent expression for a convective heat transfer coefficient, α is given as follows:

$$\alpha = \frac{Nuk}{d} \qquad \text{... (4.15)}$$

The Nusselt number for forced convection can be expressed as [25]:

For laminar flow (Re < 5 x 10^5)

$$Nu = 0.332\,\mathrm{Re}^{\frac{1}{2}}\,\mathrm{Pr}^{\frac{1}{3}} \qquad \text{... (4.16)}$$

For turbulent flow (5 x 10^5 < Re < 10^8)

$$Nu = 0.0296\,\mathrm{Re}^{\frac{4}{5}}\,\mathrm{Pr}^{\frac{1}{3}} \qquad \text{... (4.17)}$$

where Pr is the Prandtl number.

By using the convective heat transfer coefficient calculated with Eq. (4.15) the convection heat transfer from the projecting flame to the wall cladding can be precisely calculated from Eq. (4.1).

4.3 Radiation

4.3.1 Law's Method

The radiant heat from the window fire plume is a function of the geometry, temperature and emmisivity of the flame. The expression for the net rate of heat transfer by radiation from the flame, z, is given by:

$$I = \varepsilon_f \varepsilon_w \sigma \left(T_F^{\ 4} - T_w^{\ 4} \right) \quad \text{... (4.18)}$$

where ε_f is the emmisivity of the flame, ε_w is the emmisivity of the wall, σ is the Stefan-Boltzmann constant ($5.67x10^{-11}$ kW/m^2.K^4).

As the facade is engulfed in flame, it is reasonable to assume that the effective radiating temperature for the point on the surface receiving the maximum rate of heating would be given by Eq. (3.22).

The emmisivity of the exterior wall, ε_w, will depend on the applied coating to the exterior wall claddings. The flame emmisivity, ε_f, will depend on the flame thickness, λ, and is given by Law as:

$$\varepsilon_f = 1 - e^{-0.3\lambda} \quad \text{... (4.19)}$$

4.3.2 Oleszkiewicz's Method

A constant flame thickness was assumed in the Law's original radiant heat transfer. This simple and conservative assumption, however, is unrealistic for the calculation of heat transfer in the area near the top of the flame.

Oleszkiewicz [23] modified the flame shape and assumed a triangular shaped flame, as shown in Figure 4.2. The flame thickness near the top of the window is assumed to be two-thirds the height of the window.

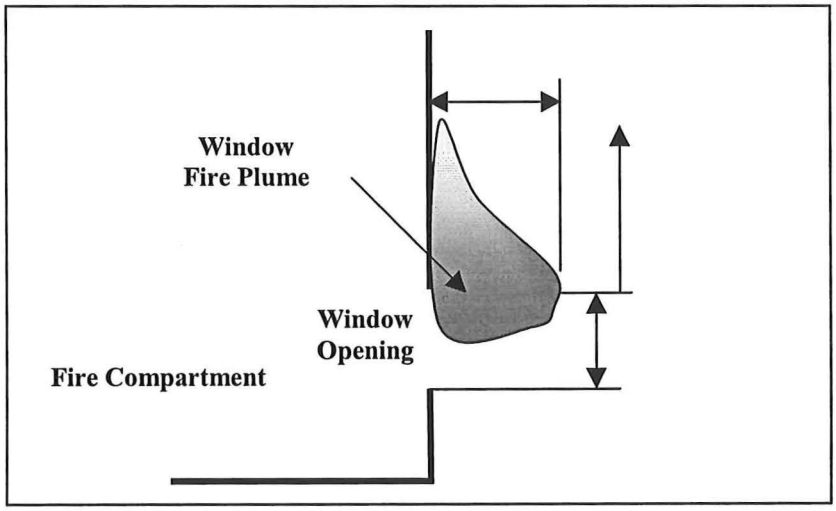

Figure 4.2: Assumed shape of emerging flame [23]

Local emmisivity of the flame was calculated using Eq. (4.19), but with a variable flame thickness at a certain height above the window. The variable flame thickness above the window is given by:

$$\lambda = \frac{2}{3} h \left(\frac{z - h_w}{z} \right) \qquad \ldots (4.20)$$

As before, the radiant heat flux density is calculated using Eq. (4.18). The same radiant heat flux density is added to the convective heat flux density calculated from the first principle methods for working out the total heat flux density.

4.4 Model of Heat Transfer to Wall Surface

The heat transfer model is capable of predicting the burning rate, trajectory and temperature of an emerging flame based on Law's procedure, and subsequently the estimated heat flux impinging on the exterior cladding. While Law [16] developed a method to describe the flame trajectory and temperature distribution for both the natural and forced draft conditions, only the natural draft condition is implemented in this model. The reason for this was that appropriate comparison can then be made between the calculated results and the full-scale experimental data [23] which were conducted in natural draft condition (or still air condition) and with a single window opening.

It will be important to take into account the heat release due to the combustion of excess fuels outside the window opening because it can have a significant effect on the opening flames and plume. In order to assess the heat release of excess fuels, it is necessary to predict the rate of excess fuel ejecting out from the fire compartment. This is considered as the difference between the rate of generation of combustible fuels by thermal decomposition ($\dot{m}_f$) and the rate of consumption of the fuels by the combustion within the compartment ($\dot{m}_v$). The heat release rate of excess fuel, $\dot{Q}_{ef}$, is simply the difference between the maximum heat release of fuel and the ventilation-controlled heat release in the fire compartment, and can be predicted by:

$$\dot{Q}_{ef} = E\left(\dot{m}_f - \dot{m}_v\right) \qquad \text{... (4.21)}$$

where E is the cellulosic fuel energy yield (MJ/kg).

The intensity of radiation and convection received by the exterior wall cladding varies with the position of the cladding in relation to the window. The heat flux exposure is expected to decrease with an increase in vertical distance above the window. This is because the flame temperature decreases along its vertical length (Figure 4.3).

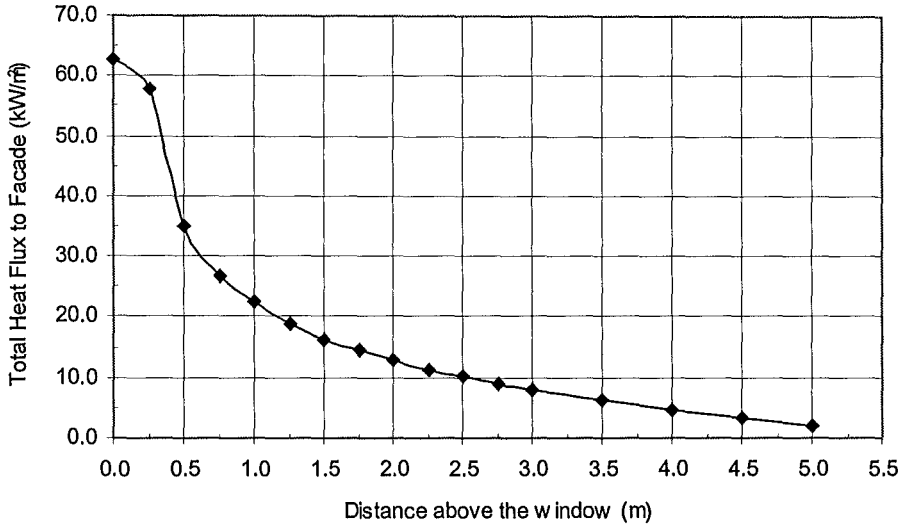

Figure 4.3: Thermal exposure of exterior cladding above window (using first principle methods)

The total radiative heat flux from the burning of excess fuel (kW/m^2) is then given by:

$$\dot{q}''_r = \frac{\lambda_r \dot{Q}_{ef}}{A_f} \qquad \text{... (4.22)}$$

where λ_r is radiative fraction of energy loss by radiation from the flame and the total surface area of the triangular shaped flame (A_f) can be determined from:

$$A_f = wz + 2\left(\frac{zh}{3}\right) + \left(\frac{2wh}{3}\right) + w\sqrt{\left(\frac{2}{3}h\right)^2 + z^2} \qquad \text{... (4.23)}$$

The model assumed cellulosic fuel as the combustible burning on the fire compartment. The required inputs into the model are the dimensions of the fire compartment and window opening, the fire load per unit floor area, cellulosic fuel energy yield, the duration of burning and the ambient temperature. A sample printout of heat transfer model created in Excel spreadsheets is depicted Figure 4.4.

Heat Transfer Model

INPUT

D=	4.4	m	Room Depth
W=	5.95	m	Room Width
H=	2	m	Room Height
w=	2	m	Window Opening Width
h=	2	m	Window Opening Height
h/w=	1.00		Aspect ratio
E=	15	MJ/kg	Cellulosic fuel energy yield
FLED=	26.3	kg/m²	Fire Load per unit Floor Area
t=	20	min	Free Burning Fire Duration (=20 min for most types of furniture)
T_o=	293	K	Ambient Temperature

OUTPUT

L=	689	kg	Total Fire Load in Room
At=	90	m²	Total Area of Floor, Ceiling and Walls less Window Area
Aw=	4	m²	Window Area
η=	15.87	m^-½	
ψ=	36.34	kg/m²	
Tf=	1296	K	Fire Temperature in the Compartment
ε_f=	0.95		Emissivity of the fire
Q_o=	152.1	kW/m²	Radiation emitted from the opening
R1=	0.57	kg/sec	Fuel Controlled Burning Rate
R2=	0.52	kg/sec	Ventilation Controlled Burning Rate
Q=	7.7	MW	estimated heat release in room
Q_w=	0.9	MW	estimated heat release at window (in ventilation-controlled conditions)
Q_t=	8.6	MW	total HRR
z+h=	5.6	m	Height of Flame Tip Above the Window Sill
z=	3.6	m	Height of the Flame Tip Above the Window Head
n=	2.00		Yokoi's window shape factor
x=	0.62	m	Horizontal Projection of the Centre of the Flame Tip
l=	0.913	m	Distance along Flame Centre Line from Window
X=	1.54	m	Centre Line Distance of flame tip from wimdow
T_o=	913	K	Flame Temperature at the Window
u=	7.44	m/sec	Maximum velocity of gases through opening
ε_e=	0.33		Emissivity of the Emerging Flame
A_e=	35.7	m_2	Total Area of the Emerging Flame
Q_e/A_e	24.6	kW/m²	Heat flux density due to extra burning

Properties of Air

Temp (K)	kinematic visc (m²/s)	conductivity (w/mK)	Pr
250	1.14E-05	0.0223	0.720
300	1.59E-05	0.0263	0.707
350	2.09E-05	3.00E-02	0.700
400	2.64E-05	3.38E-02	0.690
450	3.24E-05	3.78E-02	0.686
500	3.88E-05	4.07E-02	0.684
550	4.56E-05	4.39E-02	0.683
600	5.27E-05	4.69E-02	0.685
650	6.02E-05	4.97E-02	0.690
700	6.81E-05	5.24E-02	0.695
750	7.64E-05	5.49E-02	0.702
800	8.49E-05	5.73E-02	0.709
850	9.38E-05	5.96E-02	0.716
900	1.03E-04	6.20E-02	0.720
950	1.12E-04	6.43E-02	0.723
1000	1.22E-04	6.67E-02	0.726
1100	1.42E-04	7.15E-02	0.728
1200	1.63E-04	7.63E-02	0.728
1300	1.85E-04	8.20E-02	0.719
1400	2.13E-04	9.10E-02	0.703
1500	2.40E-04	1.00E-01	0.685

HEAT FLUX CALCULATION

height above the window head (m)	Flame Thickness (m) λ (m)	Emmisivity of Flame ε	Flame Temperature T_f (K)	Re	Nu	Convective H.T Coefficient (α) First W/m²K	Convective H.T Coefficient (α) Law W/m²K	Convective H.T Coefficient (α) Olesz W/m²K	I_r (Extra Burning) (kW/m²)	I_r (Total) kW/m²	Convective Heat Flux (I_c) First kW/m²	Convective Heat Flux (I_c) Law kW/m²	Convective Heat Flux (I_c) Olesz kW/m²	Total Heat Flux (I_o) First kW/m²	Total Heat Flux (I_o) Law kW/m²	Total Heat Flux (I_o) Olesz kW/m²
0.00	1.33	0.33	854	188512	440	90.1	9.7	44.3	2.4	12.2	50.6	5.4	24.9	62.7	17.7	37.1
0.25	1.24	0.31	837	244462	541	86.1	6.7	44.3	2.3	10.8	46.9	3.7	24.1	57.7	14.5	35.0
0.50	1.15	0.29	821	283062	608	48.4	5.1	44.3	2.1	9.5	25.6	2.7	23.4	35.1	12.2	32.9
0.75	1.05	0.27	805	321661	674	35.8	4.3	44.3	2.0	8.3	18.3	2.2	22.7	26.6	10.5	31.0
1.00	0.96	0.25	789	395380	793	30.6	3.9	44.3	1.8	7.2	15.2	1.9	22.0	22.4	9.1	29.2
1.25	0.87	0.23	772	437742	861	26.6	3.5	44.3	1.7	6.2	12.7	1.7	21.3	19.0	7.9	27.5
1.50	0.77	0.21	756	480104	927	23.8	3.3	44.3	1.5	5.3	11.0	1.5	20.5	16.3	6.8	25.8
1.75	0.68	0.18	740	576789	1072	22.9	3.1	44.3	1.4	4.4	10.2	1.4	19.8	14.6	5.8	24.2
2.00	0.59	0.16	724	623555	1141	21.3	2.9	44.3	1.2	3.6	9.2	1.3	19.1	12.8	4.9	22.7
2.25	0.49	0.14	707	670322	1208	20.1	2.8	44.3	1.0	2.9	8.3	1.2	18.4	11.2	4.1	21.3
2.50	0.40	0.11	691	796053	1385	19.9	2.7	44.3	0.8	2.2	7.9	1.1	17.7	10.2	3.3	19.9
2.75	0.31	0.09	675	847970	1457	19.1	2.6	44.3	0.6	1.6	7.3	1.0	16.9	8.9	2.6	18.6
3.00	0.21	0.06	659	899886	1528	18.3	2.5	44.3	0.5	1.1	6.7	0.9	16.2	7.8	2.0	17.3
3.50	0.03	0.01	626	1121417	1820	18.0	2.3	44.3	0.1	0.1	6.0	0.8	14.8	6.1	0.9	14.9
.	.	.	.	.	.	.	.	.	.	.	.	.	.	.	.	.
.	.	.	.	.	.	.	.	.	.	.	.	.	.	.	.	.
Continued																

Figure 4.4: Heat transfer model constructed using Excel spreadsheets

4.5 Practical Application of the Heat Transfer Model

To evaluate the prediction of heat flux by the heat transfer model, the model outputs were compared with the experimental data obtained from full-scale testing conducted at the National Research Council of Canada [23]. The comparison included the heat flux prediction by three described methods in the model, namely First Principle methods, Law's method and Oleszkiewicz's method.

4.5.1 Full-Scale Experiment

The National Research Council of Canada (NRCC) full-scale experiments were conducted in a three-storey high burn facility (Figure 2.9). The facility was made of a three-storey high (10.3 m) reinforced concrete frame. A burn room (8.95 m wide by 4.4m deep by 2.75 m high) was located on the ground floor and a concrete block front wall was covered with 13 mm thick non-combustible board. The burn room consisted of a reinforced concrete floor, concrete walls, and a precast concrete panel ceiling. The wall and ceiling were covered on the room side with 25 mm thick ceramic fibre insulation. A window opening was provided in the front wall of the burn room. This was the only opening in the room boundaries and different sizes of window were used to study the effect of window geometry on flame projecting from a window opening. The total heat flux received by the exterior wall was recorded at four locations at 1.0 m intervals, starting at 0.5 m above the window.

Propane gas was used as the experimental fire. The model assumes cellulosic fuel, such as wood cribs, as the compartment fire, with net calorific value of 16 MJ/kg. In order to match the heat release rate of propane gas, the fuel load per unit floor area was adjusted until it achieved the heat release rate of propane gas.

Table 4.1 shows the variation of time-averaged total heat flux density with heat release rate, height above window, and window dimensions. The total heat flux calculated by three described methods is also included in Table 4.1.

Window	Height Above Window (m)	Heat Flux Density (kW/m^2)															
		5.5 MW				6.9 MW				8.6 MW				10.3 MW			
		Measured	Calculated			Measured	Calculated			Measured	Calculated			Measured	Calculated		
			1st Principle	Law	Igor		1st Principle	Law	Igor		1st Principle	Law	Igor		1st Principle	Law	Igor
Window 1 (0.94 m wide by 2 m high)	0.5	43.9	34.1	11.6	38.8	58.6	35.1	13.3	42.9	75.5	38.9	17.2	46.8	-	-	-	-
	1.5	12.4	17.0	7.3	33.6	17.7	18.6	9.2	38.1	25.9	22.3	12.8	41.7	-	-	-	-
	2.5	7.7	11.7	4.6	29.0	9.9	13.1	6.5	33.7	15.9	16.4	9.8	37.0	-	-	-	-
	3.5	3.9	8.2	2.7	24.9	5.1	9.9	4.4	29.8	8.1	12.8	7.3	32.7	-	-	-	-
Window 2 (0.94 m wide by 2.7 m high)	0.5	18.2	49.0	14.9	39.0	34.8	46.9	14.9	41.8	53.2	49.2	16.8	45.6	68.3	52.9	20.5	49.3
	1.5	6.3	23.1	9.1	32.2	10.4	23.4	10.0	36.4	15.9	25.2	12.2	40.8	23.2	28.7	15.8	44.3
	2.5	3.5	14.9	5.1	26.5	6.0	16.2	6.7	31.7	9.8	18.4	9.1	36.4	13.7	21.7	12.4	39.7
	3.5	1.7	10.1	2.3	21.7	3.0	11.9	4.1	27.5	4.8	13.8	6.5	32.3	6.7	16.9	9.5	35.4
Window 3 (2.6 m wide by 1.37 m high)	0.5	24.5	21.6	6.3	23.3	53.2	21.9	7.0	26.7	104.3	23.6	8.9	30.3	208.7	26.5	11.9	33.3
	1.5	22.9	8.3	1.9	15.5	33.1	9.2	2.9	19.8	58.6	10.9	4.5	23.4	122.4	13.3	7.0	25.8
	2.5	13.2	-	-	-	17.2	5.3	1.0	14.3	51.2	6.6	2.1	17.7	103.9	8.3	3.8	19.4
	3.5	11.5	-	-	-	15.6	-	-	-	28.3	-	-	-	56.5	4.7	1.4	13.5
Window 4 (2.6 m wide by 2 m high)	0.5	10.5	32.7	7.7	22.0	17.4	32.5	8.6	25.0	29.5	32.3	9.3	28.0	43.4	34.8	12.0	31.5
	1.5	5.2	-	-	-	9.4	12.3	2.6	16.4	14.8	13.9	4.0	20.7	20.8	16.2	6.3	24.0
	2.5	4.5	-	-	-	7.4	-	-	-	12.6	7.7	1.2	15.2	16.3	9.4	2.7	17.8
	3.5	2.9	-	-	-	7.4	-	-	-	8.2	-	-	-	9.6	-	-	-
Window 5 (2.6 m wide by 2.7 m high)	0.5	6.5	47.4	7.3	20.5	11.4	47.0	10.5	25.2	17.4	47.3	11.5	28.0	29.1	47.6	13.0	30.8
	1.5	2.9	-	-	-	5.3	-	-	-	8.1	17.1	3.4	17.9	12.8	19.3	5.7	21.9
	2.5	2.0	-	-	-	4.2	-	-	-	5.7	-	-	-	9.1	10.5	2.0	15.0
	3.5	1.4	-	-	-	2.9	-	-	-	3.6	-	-	-	5.6	-	-	-

"-": No calculated heat flux as the flame height does not reach this level

Shaded regions represent burning of excess fuel outside the fire compartment.

Table 4.1: Variation of total heat flux density

Using a propane gas burner with 10.3 MW fire output, a heat flux in excess of 200 kW/m^2 was recorded 0.5 m above Window 3. Most typically, the total heat flux impinging on the exterior wall does not exceed 60 kW/m^2 at 0.5 m above the window opening for fires up to about 7 MW.

4.5.1.1 Effect of Heat Release Rate on Heat Transfer to Exterior Wall

Figure 4.5 shows the variation of total heat flux density with height above the window for one window (2.6 m wide by 2 m high) and for different heat release rates.

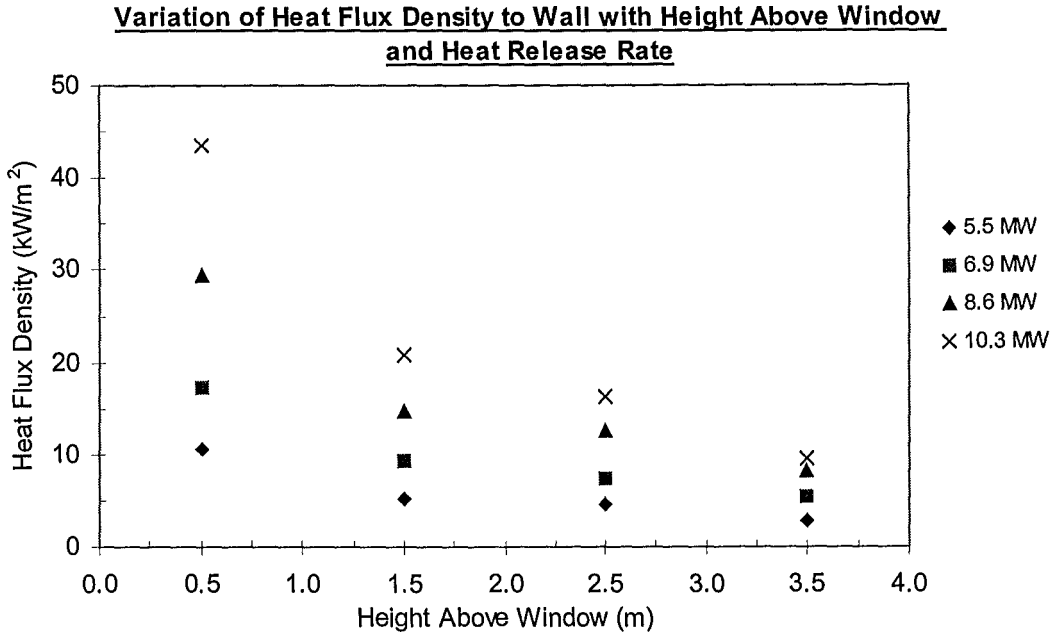

Figure 4.5: Variation of total heat flux density with height above the window and heat release rates for 2.6 m wide and 2 m high window*

The intensity of radiation and convection received from window fire plume (outflowing flame and hot gases) varies with the heat release rate and the position of the exterior wall in relation to the window. As expected, the heat flux exposure increases for higher heat release rates and decreases with an increase in height above the window.

---

* Data used in Figure 4.5 is obtained from the NRCC full-scale experiments [23].

4.5.1.2 Effect of Window Dimensions on Heat Transfer to Exterior Wall

Figure 4.6 shows the total heat flux density measured at 0.5 m above the top of the window opening versus the heat release rate in the fire for five different window dimensions.

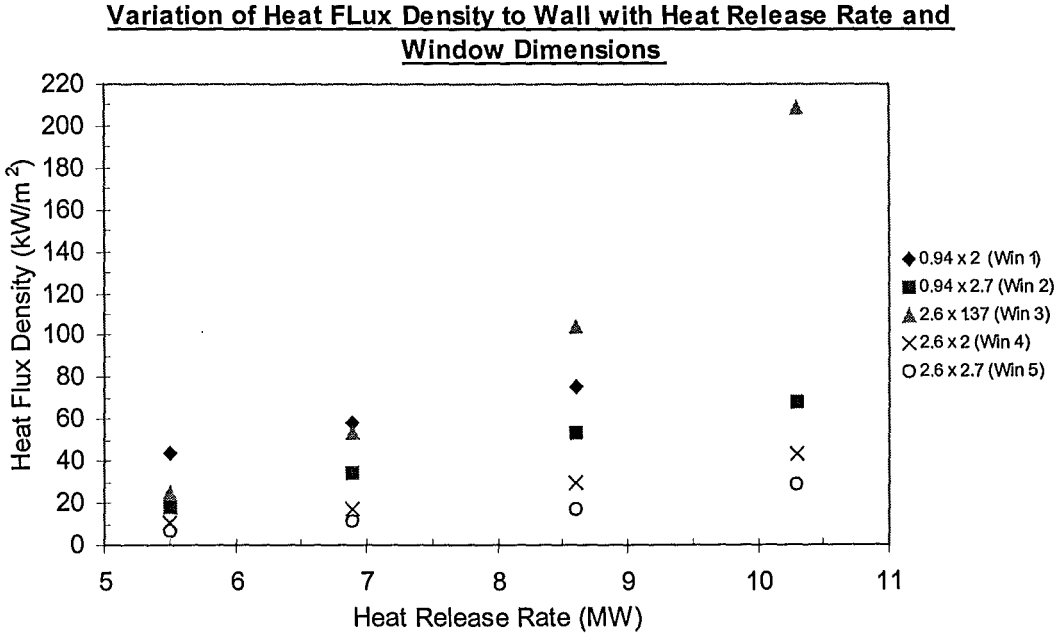

Figure 4.6: Variation of total heat flux density with height above window for different heat release rates*

The exposure increases with increasing heat release rate and decreasing window size. It can be seen in Figure 4.6 that the smallest window (Window 1) has significant high heat flux impinging on the exterior wall compared to other window geometries except Window 3. The total heat flux drops from 43.9 kW/m^2 to 6.5 kW/m^2 at 0.5 m above the window when the window area is increase from 1.88 m^2 (Window 1) to 7.02 m^2 (Window 5).

The total heat flux impinging on the exterior wall tends to increase faster with window dimensions than the heat release rate of burning fuel because an increasing portion of

---

* Data used in Figure 4.6 is obtained from the NRCC full-scale experiments [23].

excess fuel burns outside the fire compartment when the compartment becomes ventilation-controlled.

4.5.2 Comparison of Calculated Results and Experimental Data

4.5.2.1 First Principle's Method

Window 1 (0.94 m wide by 2 m high)

Figure 4.7 compares the calculated and measured total heat flux density for window 1 (0.94 m wide by 2 m high).

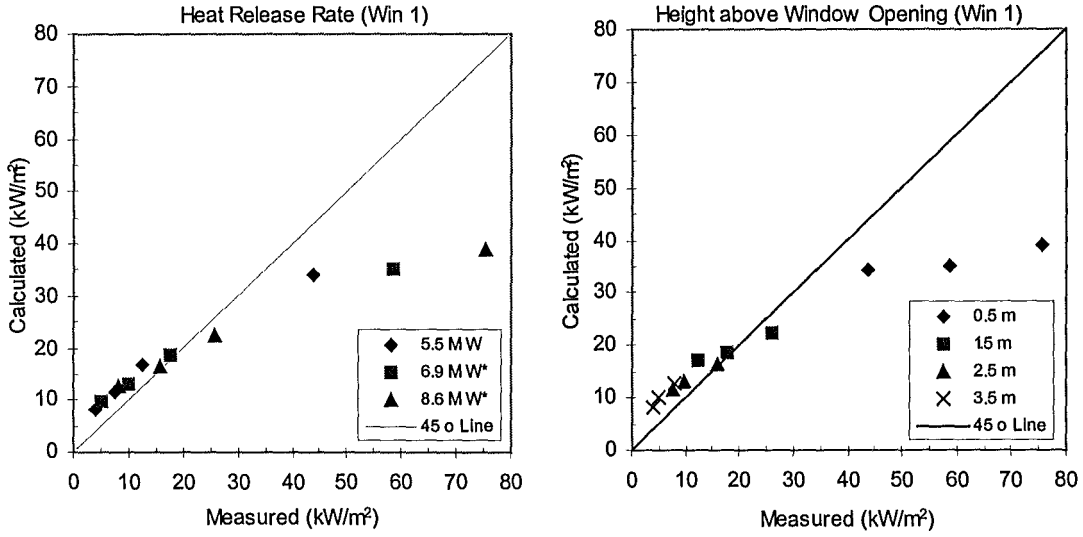

"*": Burning of excess fuel outside the fire compartment

Figure 4.7: Calculated and measured total heat flux density for Window 1

Generally First Principle gives conservative results for Window 1. However, it underestimates the heat flux density at 0.5 m above the window opening. It is suspected that the flaming region becomes turbulent near the window as some extra burning takes place outside the window. The radiative heat flux to exterior wall from extra burning has been included in the total heat flux received by the exterior wall. This radiative heat flux does not have a significant effect on the total heat flux received by the exterior wall because there is a significant fraction of energy loss by radiation from the flame. The margin between the measured and calculated heat flux density becomes larger with an increasing heat release rate. For example, the calculated heat

flux is 38.9 kW/m^2 at 0.5 m above the window for a heat release rate of 8.6 MW, which is 50% lower than the actual measurement of 75.5 kW/m^2.

Window 2 (0.94 m wide by 2.7 m high)

Figure 4.8 compares the calculated and measured total heat flux density for Window 2 (0.94 m wide by 2.7 m high).

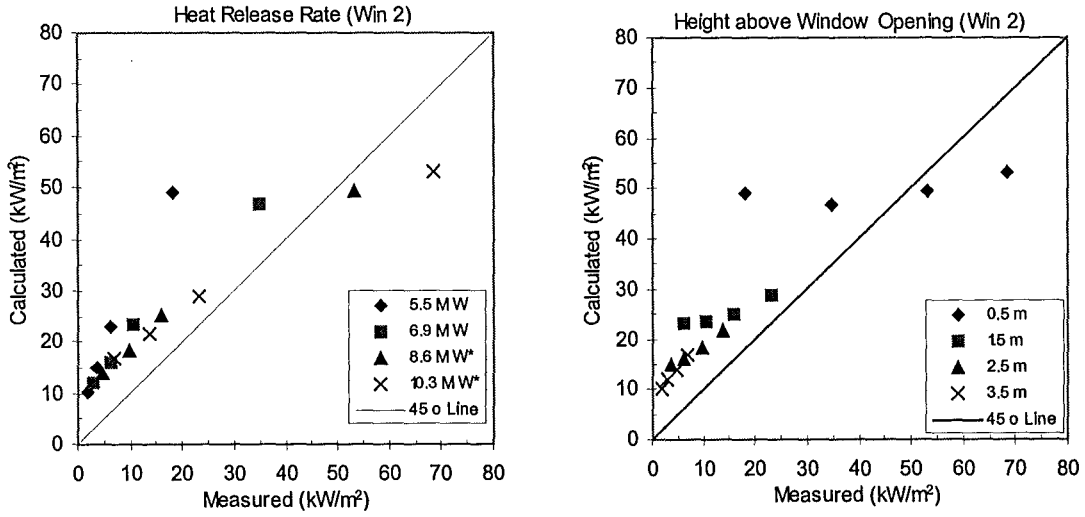

"*": Burning of excess fuel outside the fire compartment

Figure 4.8: Calculated and measured total heat flux density for Window 2

Window 2 has the same width as Window 1 but has greater height. The model yields conservative results for heat flux density. Again, the model slightly underestimates the heat flux density at the position closer to the window for heat release rates of 8.6 MW and 10.3 MW. This may be caused by the turbulent region near the window as a result of extra burning of fuel occurring outside the window.

It can be seen from Table 4.1 that the actual heat flux impinging on the exterior wall for Window 2 is lower than the heat flux recorded for the previous window (Window 1). As the vertical height of the window increases, the emerging flame will be projected further away from the exterior wall. This will help to reduce the heat flux impinging on the exterior wall.

Window 3 (2.6 m wide by 1.37 m high)

Figure 4.9 compares the calculated and measured total heat flux density for Window 3 (2.6 m wide by 2.7 m high).

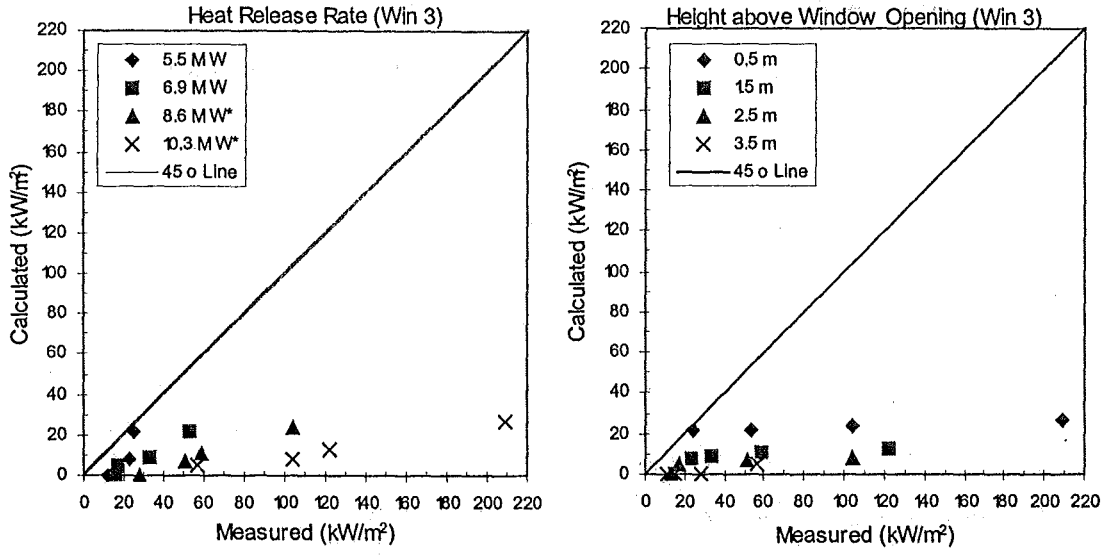

"*": Burning of excess fuel outside the fire compartment

Figure 4.9: Calculated and measured total heat flux density for Window 3

First principle methods severely underestimate the heat flux for this window. All the calculated heat flux densities are 60% to 80% lower than the actual measurements.

The width of the window is twice the vertical height of the window. This wide and short window causes the emerging flame to "hug" the exterior window. The hugging effect may be caused by the velocity in which the hot gases leave the fire compartment [23]. The gases are buoyancy-driven, and the buoyancy effect increases with the height of the window opening. Thus the low velocity flames emerging from a low window opening remained better attached to the facade above the window. On the other hand, the "narrow" flames issuing from a taller window will be projected further away from the window.

As the heat release rate grows to 8.6 MW or 10.3 MW, an increasing portion of combustion takes place outside the fire compartment. The effects of "hugging" and burning of excess fuel outside the fire compartment contribute much to the higher heat flux received by the wall.

Window 4 (2.6 m wide by 2 m high)

Figure 4.10 compares the calculated and measured total heat flux density for Window 4 (2.6 m wide by 2 m high).

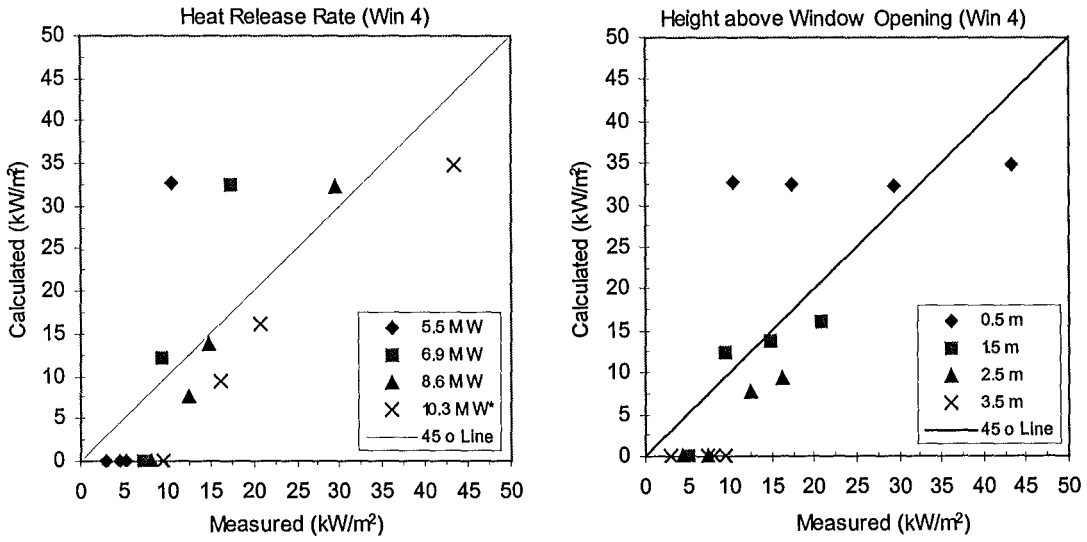

"*": Burning of excess fuel outside the fire compartment

Figure 4.10: Calculated and measured total heat flux density for Window 4

The model gives conservative results for all fires except 10.3 MW experimental fire. The compartment becomes ventilation-controlled for 10.3 MW experimental fire. The model produces slightly lower heat flux density for this fire, as extra burning takes place outside the window.

The model overestimates the heat flux density for both 5.5 MW and 6.9 MW experimental fires. For these two cases, the flame height is estimated to be less than 2 m. Thus there is not calculated heat flux beyond the height of the flame.

The actual heat flux density for the positions higher than 1.5 m above the window for these fires is less than 10 kW/m^2. The approximate heat flux required to ignite easily ignitable items such as thin curtains varies from 10-20 kW/m^2 [26]. Hence ignition of exterior wall claddings is not expected under the exposure of the low heat flux.

Window 5 (2.6 m wide by 2.7 m high)

Figure 4.11 compares the calculated and measured total heat flux density for Window 5 (2.6 m wide by 2.7 m high).

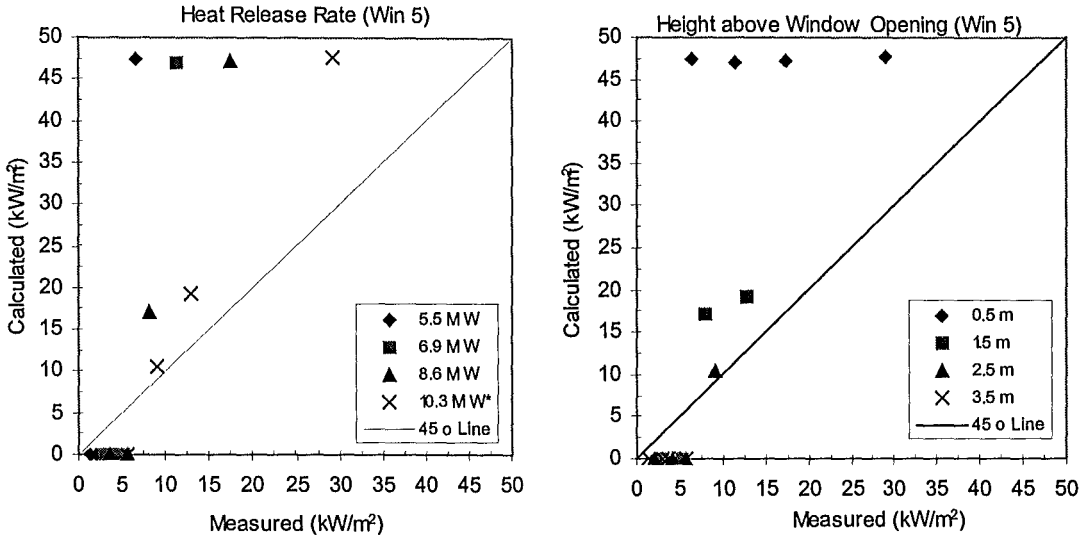

"*": Burning of excess fuel outside the fire compartment

Figure 4.11: Calculated and measured total heat flux density for Window 5

All the heat flux density calculations from the model are conservative. The thermal exposure of this window is the lowest of all, as this is the biggest window used in this particular experiment. Large windows allow more fuel to be burned inside the fire compartment than the small window, thus decreasing the fire plume intensity. For instance, the flame height for the 5.5 MW experimental fire decreases from 4.83 m to 0.77 m for Window 1 and Window 5 respectively.

4.5.2.2 Law's Method

Figure 4.12 compares the calculated and measured total heat flux density for all windows.

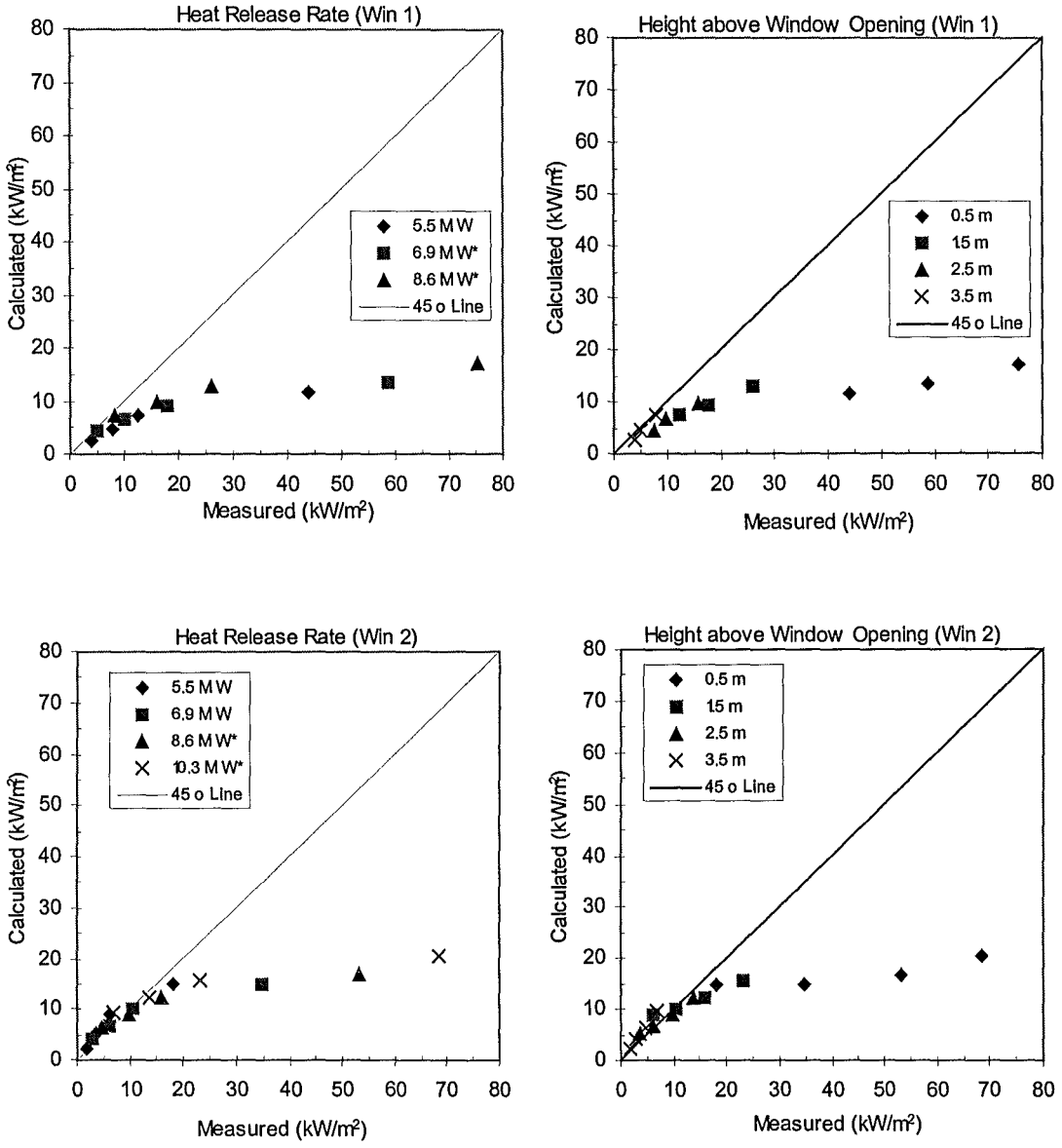

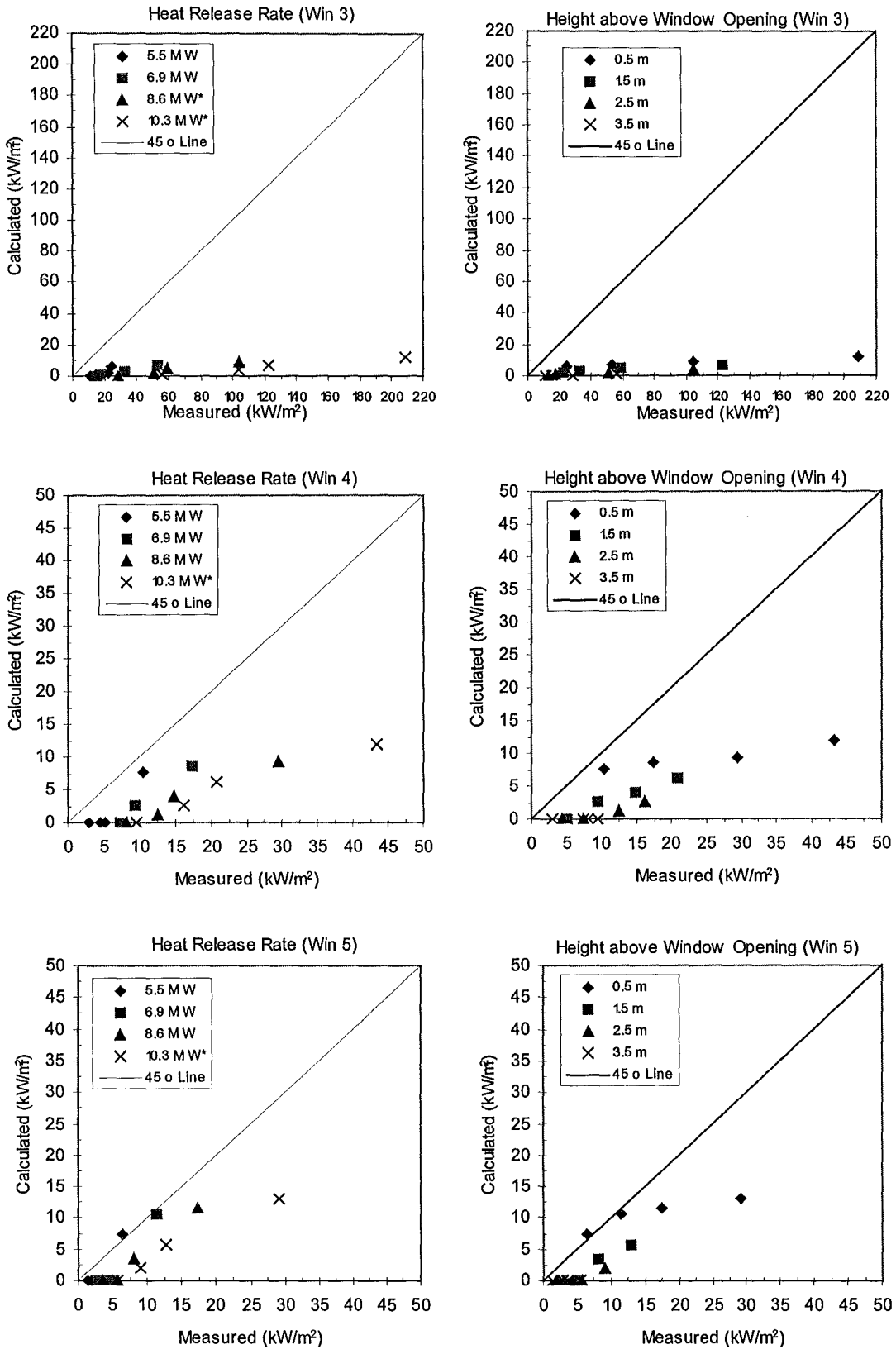

"*": Burning of excess fuel outside the fire compartment

Figure 4.12: Calculated and measured total heat flux density for all windows

Windows 1 to 5

Law's model underestimates the heat flux density, especially near the top of the window. The model only works well for Window 2 except at 0.5 m above the top of the window. High heat flux is received near the top of the window due to the extra burning in ventilation-controlled fires.

4.5.2.3 Oleszkiewicz's Method

Figure 4.13 compares the calculated and measured total heat flux density for all windows.

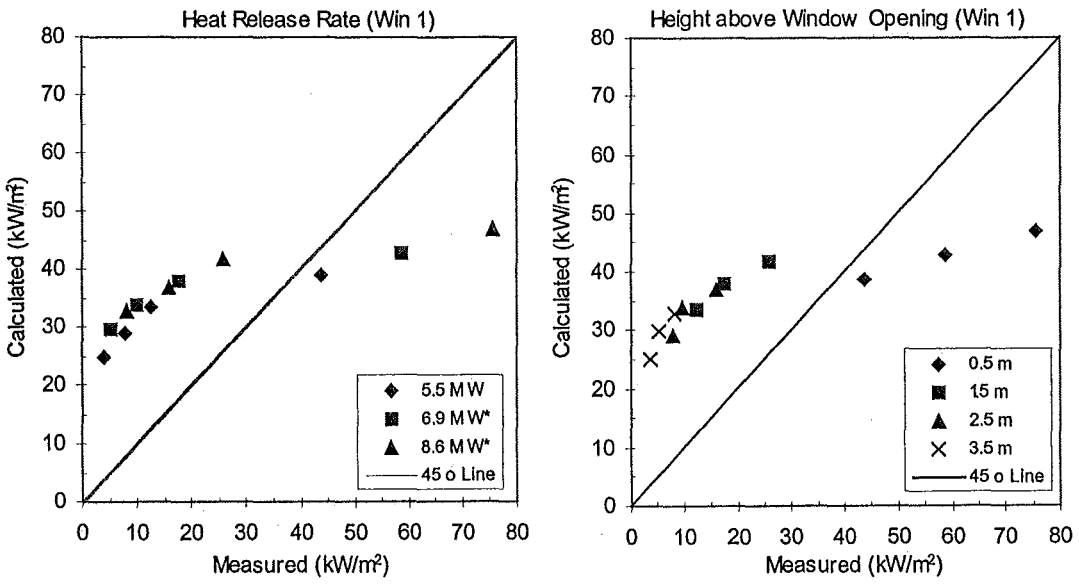

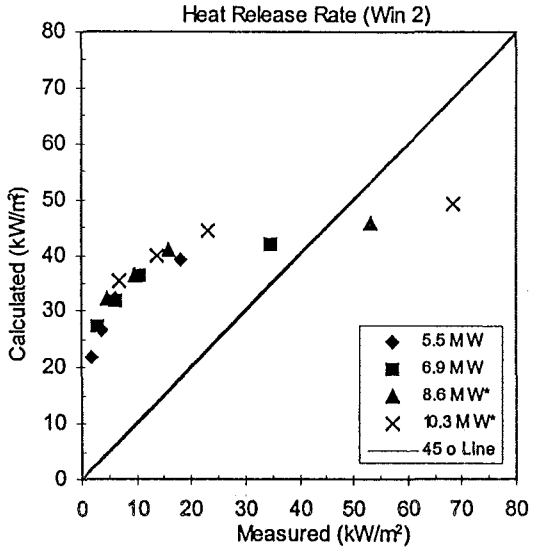
Heat Release Rate (Win 2)
Calculated (kW/m²)
Measured (kW/m²)
5.5 MW
6.9 MW
8.6 MW*
10.3 MW*
45 o Line

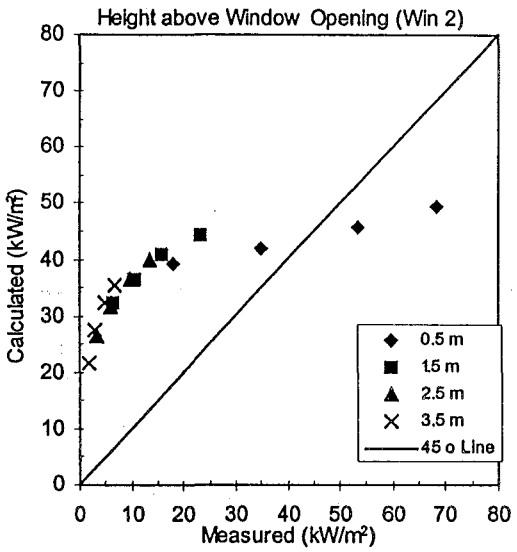
Height above Window Opening (Win 2)
Calculated (kW/m²)
Measured (kW/m²)
0.5 m
1.5 m
2.5 m
3.5 m
45 o Line

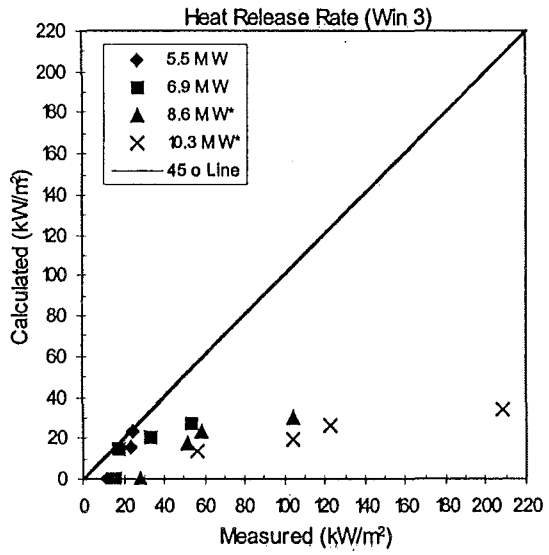
Heat Release Rate (Win 3)
Calculated (kW/m²)
Measured (kW/m²)
5.5 MW
6.9 MW
8.6 MW*
10.3 MW*
45 o Line

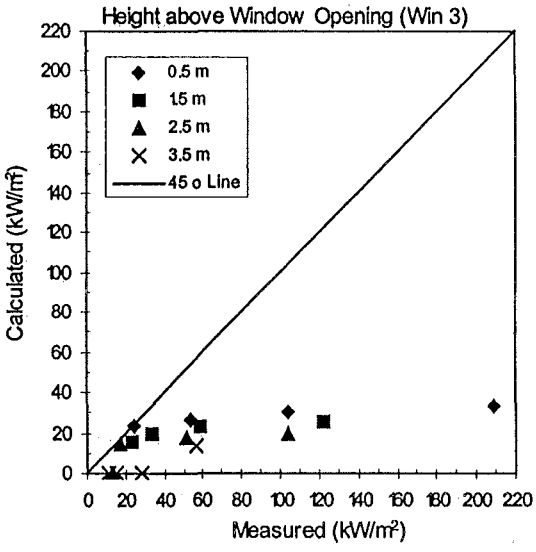
Height above Window Opening (Win 3)
Calculated (kW/m²)
Measured (kW/m²)
0.5 m
1.5 m
2.5 m
3.5 m
45 o Line

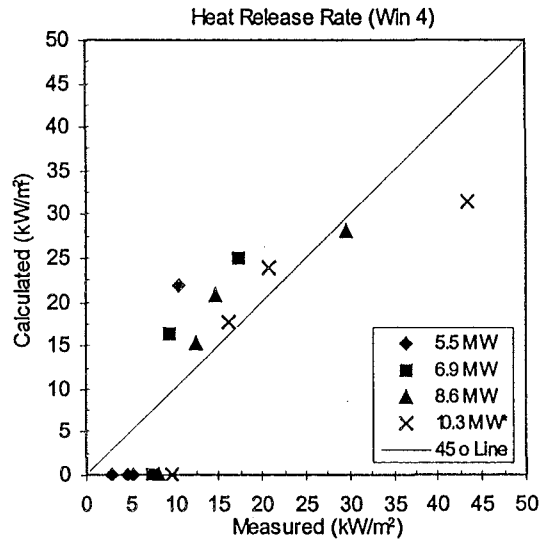
Heat Release Rate (Win 4)
Calculated (kW/m²)
Measured (kW/m²)
5.5 MW
6.9 MW
8.6 MW
10.3 MW*
45 o Line

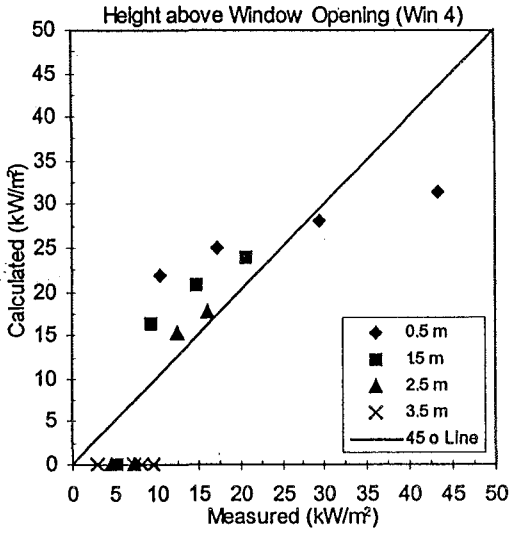
Height above Window Opening (Win 4)
Calculated (kW/m²)
Measured (kW/m²)
0.5 m
1.5 m
2.5 m
3.5 m
45 o Line

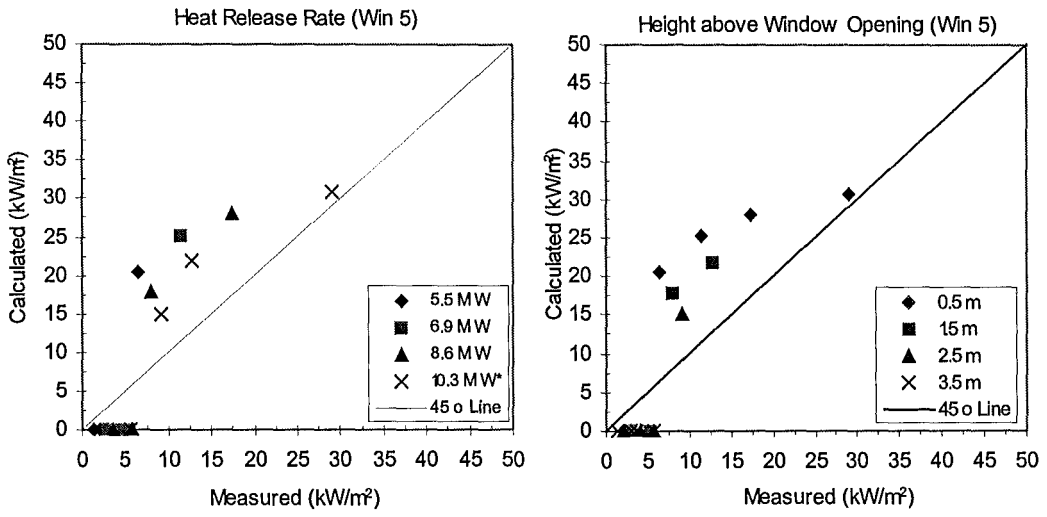

"*": Burning of excess fuel outside the fire compartment

Figure 4.13: Calculated and measured total heat flux density for all windows

The convective heat transfer coefficient given by Oleszkiewicz is not dependent on vertical height above window. Therefore, the convective heat transfer coefficient builds to a maximum level and essentially remains constant for all heights above the window.

The calculated values of the total heat flux density from Oleszkiewicz's method at the higher position above the window opening ($\geq$ 1.5 m) were generally higher because he used and correlated his method against the same experimental data sets.

For Windows 1 and 2, the model overestimates the total heat flux for all positions above the windows except at 0.5 m above the windows in ventilation-controlled fires (8.6 MW and 10.3 MW).

The model gives lower heat flux density than the actual measurements for Window 3. The "hugging effect" is expected for this window geometry. The difference becomes larger as the compartment becomes ventilation controlled and emits some excess fuel to burn outside the compartment.

As for Windows 4 and 5, the model gives conservative results for heat flux density. The model may slightly overestimate the heat flux near the top of the window, but not to a very great extent. There is no calculated heat flux at a certain height above the window, as the flame height does not reach this level. As mentioned earlier, the actual heat flux at this position is less than 10 kW/m^2, and therefore it can be disregarded.

4.6 Summary

The equations for describing the behaviour of the flame issuing through a window opening follows closely to Law's correlation. Law had looked at the flame behaviour projecting through a widow opening in a thorough fashion. Hence a reasonable prediction of the generalised flame shape was anticipated.

This chapter has attempted to compare the methods for predicting incident heat flux to the exterior wall cladding. Table 4.2 illustrates the prediction of total heat flux by three different methods for different window geometries.

Table 4.2: Prediction of total heat flux density

Methods	Aspect Ratio of Window		
	Width ≤ 0.5 x Height (narrow and tall window)	**Width ≈ Height (Squat window)**	**Width ≥ 0.5 x Height (Wide and low window)**
1. First principle methods	↑	↑	↓
2. Law	↓	↓	↓
3. Oleszkiewicz	↑	↑	↓

↑: Overestimate the total heat flux density
↓: Under estimate the total heat flux density

It was found that the First Principle's method gives conservative heat flux values except for wide and low windows. This method, being satisfactory, was incorporated into the *BRANZFIRE* model (described in the next chapter) for predicting heat flux exposure to exterior wall cladding.

None of the available methods work well for wide and low window due to the "hugging effect". A safety factor is recommended for calculating the heat flux density for this particular window geometry.

CHAPTER 5

5 HEAT TRANSFER AND FLAME SPREAD MODELS

5.1 Introduction

Wade [27] has developed a computer fire model (*BRANZFIRE*) to model the fire hazard associated with combustible room lining materials and building contents, and for quantifying their contribution to the rate of fire development within and between rooms. It incorporates a multi-room zone model integrated with flame spread and fire growth models applicable to room fire scenarios. The flame spread and fire growth model builds on previous work by Quintiere [28] for room-corner fire scenarios, with a number of improvements and modifications made by Wade to the original Quintiere model. The *BRANZFIRE* model predicts ignition, flame spread and the resultant heat release rate of the wall and ceiling material.

It is postulated that this model can be adapted to determine the rate and extent of flame spread on some exterior wall claddings due to exposure to a window fire plume. The assessment of the performance of an exterior wall cladding by the flame spread model must include a characterisation of the heat fluxes provided by the flame issuing from a window opening. The flame spread model is intended to simulate the physical processes that occur during the initiation and spread of fire over the exterior cladding system. This refers to how materials respond to the flame projecting from a window opening, from ignition through to the vertical flame spread on the exterior cladding systems.

The *BRANZFIRE* flame spread model consists of both upward and lateral flame spread but only upward flame spread is considered in this study, as it is the more important component of spread.

5.2 Description of the Heat Transfer Model

The following assumptions were made based on Law's procedure in order to represent the fire scenario as a result of a window fire plume. The resultant flame heat flux, due to the burning in the fire compartment, is assumed to prescribe over a region of the opening width and the flame height on the exposing wall. In general, the window fire plume heat flux depends on the size of the vent, the flame height and energy heat release rate, and the size of the fire.

5.2.1 Characterising the Flame Issuing from a Vent

To characterise the flame issuing through a window opening and exposing a facade above the window, the *BRANZFIRE* model treats it as a flame projecting through a vent connecting the fire compartment and an adjacent room. In this specific case, the emerging flame through a vent is assumed to expose the wall containing the cladding material.

The adjacent space is treated as a rectangular room. This rectangular room is assumed to be large enough and well ventilated in order to reduce the effect of an upper gas layer. Otherwise, the convective and radiative heat transfer terms to the boundary surfaces of the hot layer would be significant and not appropriate for simulating external conditions.

In order to simulate the impingement of a flame emerging from a vent on a cladding material, one side of the wall is treated as a wall containing exterior cladding materials. The wall opposite the wall cladding is fully vented to provide enough air into the compartment and minimise the development of the hot gas layer.

The trajectory of the flame is based on correlations by Law [16] for wood crib fires. The idealised trajectory of flame can be seen in Figure 5.1.

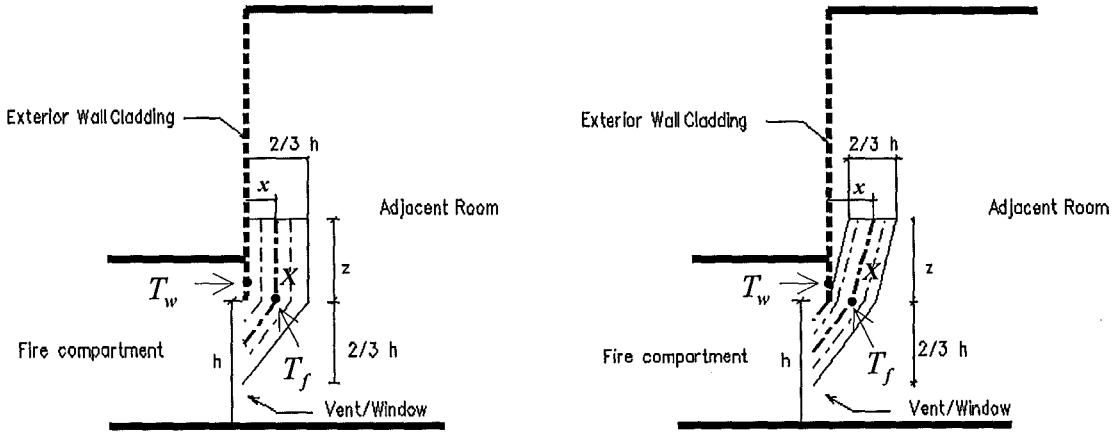

(a) h<1.25w (b) h>1.25w

Figure 5.1: Idealised trajectory of flame

Flame height is usually considered as a characteristic length for the heat transfer from the flame to the adjacent wall surface, since the scale of the luminous chemical reaction zone of the flame dominates convection and radiation heat transfer. The flame height can be worked out from the equation proposed by Law (Eq. 3.10). *BRANZFIRE* model calculates the fuel pyrolysis rate, $\dot{m}_f$, from the heat release rate and effective heat of combustion for the case of a user-defined fire. This burning rate is used in Eq. (5.1).

In order to calculate the incident heat flux from the flame, which is composed of a convective and a radiative portion, it is necessary to determine the flame temperature. The following equation proposed by Law is used to estimate the flame temperature at the vent soffit, T_o:

$$T_o = T_\infty + \frac{813 - T_\infty}{1 - 0.027\left(\frac{Xw}{\dot{m}_f}\right)} \quad \text{... (5.1)}$$

where 813 corresponds to the assumed flame temperature (K) at the tip, $\dot{m}$ is the pyrolysis rate of fuel (kg/s), X is the centre line distance of the flame tip from the window (m) and it can be estimated from Eqs. (3.18 or 3.19), w is the width of the vent and T_∞ is the surrounding temperature of the adjacent space.

The flame temperature at the vent soffit is applied in Eq. (5.2) to estimate the impinging heat flux on the wall. However, since the *BRANZFIRE* model treats the flame as being issued through a vent into the adjacent room, the surrounding temperature, T_∞, in Eq. (5.1) is assumed to be equal to the lower layer temperature of the adjacent room (roughly equal to the outside ambient temperature).

It is expected that the calculated value of flame temperature at the vent soffit will exceed the temperature in the fire compartment and the flame temperature above the window, due to the combustion of unburnt gas taking place at the vicinity of the vent.

5.2.2 Heat Flux to Wall Cladding

Eq. (5.2) gives the net heat flux to the wall cladding, $\dot{q}''_{net}$. The net heat flux to the wall is defined as the sum of the incident heat flux from the flame ($\dot{q}''_f$), the incident heat flux due to the heated gas layers and other room surfaces ($\dot{q}''_{\text{int}}$), and includes the reradiation from the wall surface.

$$\dot{q}''_{net} = \dot{q}''_f + \dot{q}''_{\text{int}} - \varepsilon_w \sigma T_w^4 \qquad \text{for } T_w \le T_{ig} \qquad \text{... (5.2)}$$

where ε_w is the emissivity of the wall cladding, σ is the Stefan-Boltzmann constant ($5.67x10^{-11}$ kW/m^2.K^4) and T_w is the temperature of the wall cladding (K).

The heating effect from the heated gas layers and other room surfaces, $\dot{q}''_{int}$, is expected to be minimal as the size of the room adjacent to the fire compartment is assumed to be large enough and well ventilated.

In order to determine the maximum incident heat flux to the wall cladding, the convective and radiative heat transfer from the flame must be calculated and combined into the following expression:

$$\dot{q}''_f = \alpha(T_F - T_w) + \varepsilon_f \sigma T_F^4 \quad \ldots (5.3)$$

where ε_f is the emissivity of the flame, T_F is the temperature of the flame and α is the convective heat transfer coefficient between the flame and the wall.

The flame temperature, T_F, is taken as the flame temperature at the vent soffit (Eq. 5.1). The emissivity of the flame can be estimated from Eq. (4.19) by taking the flame thickness as two-thirds of the vent height, which is recommended by Law.

In order to determine the convective heat flux, an appropriate convective heat transfer coefficient, α, must be determined for the wall being heated by the adjacent flame. The flame is treated as an applied flow across the surface of the wall; therefore, the wall will undergo forced convection, and temperature-dependent expressions for convective heat transfer coefficient are used. From the analysis of Chapter 4, it was decided to use the convective heat transfer coefficient developed from the first principle methods. This is because this method gives conservative values for the convective heat transfer coefficient except for wide and low vents.

The following equation is used to calculate the convective heat transfer coefficient:

$$\alpha = \frac{Nu.k}{d} \quad \ldots (5.4)$$

where Nu is the Nusselt Number, k is the thermal conductivity of the hot gases/flame (W/mK) and d is the characteristic dimension (m), which is taken as the height of the flame (Eq. 3.10).

The Nusselt Number, Nu, can be estimated from Eq. 4.16 or 4.17, depending on the nature of flow (i.e. turbulent or laminar flow). The required inputs into these equations are the Prandtl number, P_r, which is equal to 0.72 and the Reynolds number, which is given by:

$$\mathrm{Re} = \frac{\dot{m}_o d}{A_v \rho \upsilon} \qquad \ldots (5.5)$$

where $\dot{m}_o$ is the mass flow rate of hot gases out through the vent (kg/s), A_v is the upper area of the vent (m^2), ρ is the density of the outflowing gases (kg/m^3), υ is the kinematic viscosity of gases (m^2/s), and d is the characteristic dimension (m), which is equal to the height of the flame (Eq. 3.10). The height of the upper area of the vent is taken as the height of the upper layer interface in the fire compartment to the vent soffit, not the original assumed height above the neutral plane (i.e. 2h/3). This assumption will be reasonable for this analysis.

The kinematic viscosity, υ, of the hot gases is calculated by [29]:

$$\upsilon = 7.18x10^{-10}\left(\frac{T_o + T_w}{2}\right)^{7/4} \qquad \ldots (5.6)$$

The thermal conductivity, k, of the hot gases is calculated by [29]:

$$k = 2.72x10^{-4}\left(\frac{T_o + T_w}{2}\right)^{4/5} \qquad \ldots (5.7)$$

5.3 Description of the Flame Spread Model

The following modifications/assumptions were made to the existing flame spread model implemented in the *BRANZFIRE* model with minimum number of changes needed within the program coding, so that it could assess the rate and extent of upward flame spread on the wall cladding.

5.3.1 Ignition of Wall

The emerging flame is assumed to initially prescribe a uniform heat flux to the wall over a region defined by the flame height and the width of the vent. There will be some heating effect from the fire compartment to the unexposed side of the wall cladding. The model assumes the unexposed side of the exterior wall cladding to be equal to the upper wall surface temperature in the fire compartment.

Wade [27] modelled the surface temperature of the wall lining adjacent to the exposing flame on an implicit finite difference method [30], with the net heat flux to wall cladding ($\dot{q}_{net}$) from Eq. (5.2) as a boundary condition. Once the surface temperature of the wall lining reaches or exceeds the ignition temperature of the lining material, the wall will ignite and this is taken as the time to ignition. At this time, the material starts to contribute energy and the flame spread process begins.

5.3.2 Pyrolysis Area

According to the Quintiere model [28] in which the pyrolysis front has not yet reached the ceiling, determination of the pyrolysis area requires calculation of both the pyrolysis and burn-out fronts. The *BRANZFIRE* model incorporates time-dependent heat release rate data measured in cone calorimeter tests to eliminate the need to solve separately for the upward and lateral burnout fronts.

Figure 5.2 illustrates the configuration of the pyrolysis area. Initially, the pyrolysis region adjacent to the emerging flame is represented by $y_{p,o}$, which is defined by the estimated flame height at ignition and $x_{p,o}$ is the width of the window opening.

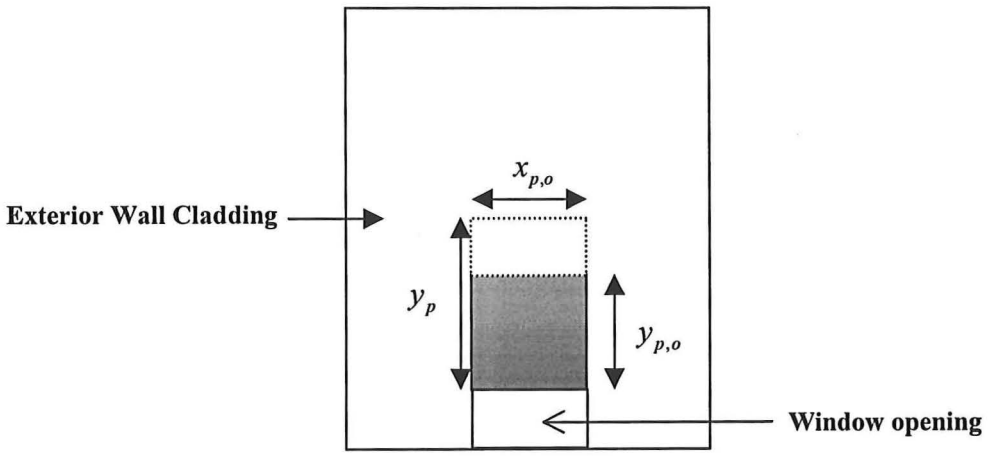

Figure 5.2: Pyrolysis regions when wall ignited

The pyrolysis area is given by:

$$A_p = y_p x_{p,o} \qquad \text{... (5.8)}$$

The current *BRANZFIRE* model does not consider lateral flame spread for spread into an adjacent space. Therefore the pyrolysis area given by Eq. (5.8) does not include the pyrolysis area in a lateral direction.

5.3.3 Heat Release Rate of Wall Cladding Material

The model enables all the heat release rate data from the cone calorimeter to be used in working out the suitable heat release rate of the burning lining material per unit area. The energy release rate per unit area, $\dot{Q}''(t)$, is considered as a function of time (from ignition), and it is influenced by the net heat flux, which is determined by the model (Eq. 5.2).

The appropriate heat release rate at each time-step is solved using a third-order curve or a cubic spline interpolation [31] applied to subsets of the input heat release rate curves obtained from cone calorimeter testing at various external heat fluxes. However the desirable heat release rate of burning material at a given time is bounded to the input heat release curves at different irradiance levels. For example, if the input heat release rate curves are in the range of 75 kW/m^2 to 35 kW/m^2 irradiance levels and the impinging heat flux on wall is calculated to be 90 kW/m^2, the model will take the heat release rate at the maximum irradiance level of 75 kW/m^2.

The model considers different pyrolysis regions outside the initial emerging flame region from that impinged on by the emerging flame. Figure 5.3 represents the pyrolysis region adjacent to the emerging flame, the pyrolysis region beyond emerging flame and the preheated region ahead of the flame front. The net flame heat flux over the pyrolysis region is taken as being 35 kW/m^2. This represents the heat flux to the material surface over the height of the emerging flame and the heat flux from the flames over the burning region of the material. The external wall flame heat flux to the unburned material above the pyrolysis region is assumed to have a constant value of 30 kW/m^2.

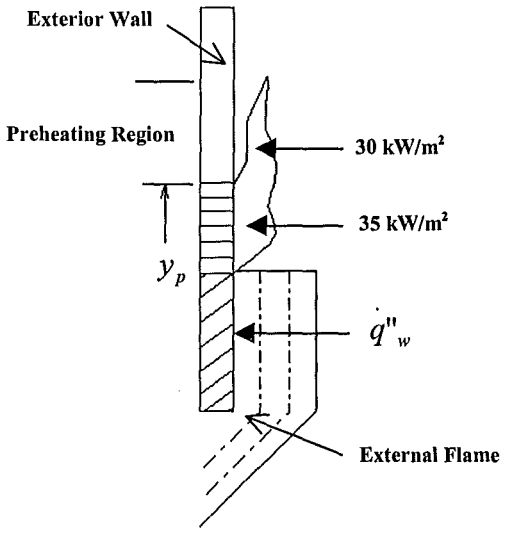

Figure 5.3: Pyrolysis regions used in *BRANZFIRE* model

The total energy release for the cladding, $\dot{Q}(t)$, is given by:

$$\dot{Q}(t) = \Sigma(\dot{Q}''(t)\Delta A_p(t)) \quad \ldots (5.9)$$

where $\dot{Q}''(t)$ is the heat release rate per unit area from the cladding material at time t (measured from ignition), and $\Delta A_p(t)$ is the incremental change in pyrolysis area.

The energy heat release for the burning area is obtained by multiplying the incremental pyrolysis area by the time-dependent heat release rate from cone calorimeter tests. It is assumed that each incremental area on the surface goes through the same burning history as in the cone calorimeter test results.

5.3.4 Material Property Data

5.3.4.1 Grenier and Janssens' Method

Cone calorimeter tests were conducted to obtain suitable the material properties of each cladding material, so that they can be used as input into the flame spread model. The *BRANZFIRE* model will correlate the ignition data from cone calorimeter as follows to determine the surface ignition temperature (T_{ig}) and the effective thermal inertia ($k\rho c$). The peak heat release rate is correlated to estimate the heat of gasification. The procedure used in the *BRANZFIRE* model for determining ignition temperature and effective thermal inertia is based on the work by Grenier [32] and Janssens [32, 33 & 34].

Ignition Temperature (T_{ig})

When correlating ignition times, $(1/t_{ig})^n$ is plotted against the externally applied heat flux ($\dot{q}''_e$).The value of n that gives the highest correlation coefficient (R^2) is to be determined. The range of n is between 0.547 and 1. When the "best fit" line intersects

the X-axis, the time of ignition goes to infinity. The X-intercept is taken as the critical heat flux, $\dot{q}''_{crit}$.

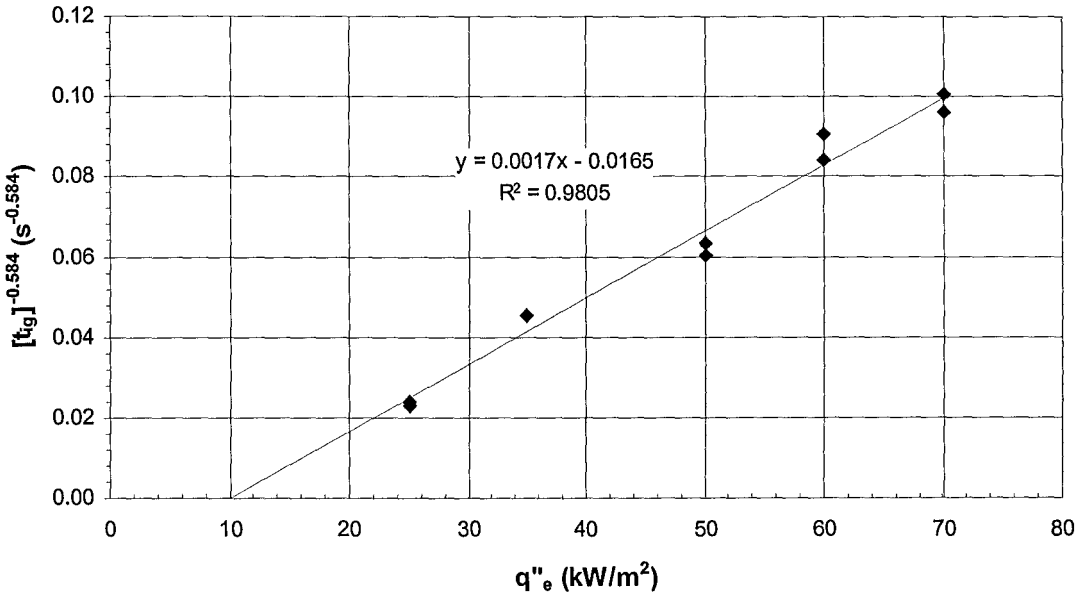

Figure 5.4: Plot of $(1/t_{ig})^n$ versus $\dot{q}''_e$ for 10 mm hardboard (Grenier & Janssens's method)

Eq. (5.10) is iterated to solve for the surface temperature for ignition (T_{ig}). The convective heat transfer coefficient (α) is taken as 0.0135 kW/m^{2}K for horizontal exposure in a cone calorimeter, and the surface emmisivity at ignition, ε, as appropriate for the tested material or approximately 0.9 in the absence of better information.

$$\varepsilon \dot{q}''_{crit} = \alpha\left(T_{ig} - T_\infty\right) + \varepsilon\sigma\left(T_{ig}^4 - T_\infty^4\right) \qquad \ldots (5.10)$$

where σ is the Stefan-Boltzmann constant ($5.67x10^{-11}$kW/m^2.K^4) and T_∞ is the ambient temperature.

Thermal Inertia ($k\rho c$)

T_{ig} is substituted into the following equation to work out the total heat transfer coefficient for the surface at ignition (h_{ig}). The total heat transfer coefficient at ignition (h_{ig}) incorporates both the radiative and convective components.

$$h_{ig} = \frac{\varepsilon \dot{q}''_{crit}}{(T_{ig} - T_{\infty})} \quad \text{... (5.11)}$$

Grenier & Janssens' correlation plots the data again as $(t_{ig})^{0.547}$ versus $\dot{q}''_e$. n is taken as 0.547 for thermally thick material. For simplicity, the "best fit" line is taken as a straight line drawn through two points. These points are taken as $\dot{q}''_{crit}$ and the data point for the highest heat flux. The slope of this "best fit" line is substituted into Eq. (5.12) to estimate the thermal inertia, $k\rho c$.

$$k\rho c = h_{ig}^2 \left[\frac{1}{0.73 slope\, \dot{q}''_{crit}} \right]^{1.83} \quad \text{... (5.12)}$$

The thermal inertia and ignition temperature obtained from the Grenier & Janssens method are substituted into Eq. (5.20) to work out the time to ignition. However, the Grenier & Janssens method is more applicable to timber products that exhibit thermal thick behaviour, and does not work well for fire retardant treated plywood as well as materials other than wood products. Therefore, a more appropriate method by Silcock and Shields [35] has been implemented into the *BRANZFIRE* model as an alternative method to predict the time to ignition for combustible materials (including polymeric materials).

5.3.4.2 Silcock and Shields' Method

Silcock and Shield recommended the Flux Time Product (FTP) to predict the time to ignition from data generated by the cone calorimeter. The FTP can be assumed to be the excess absorbed energy up to the point of ignition of a combustible material. They assumed a power law expression based on physically consistent dimensionless groups relevant to piloted ignition process and formulated the following expression:

$$(\dot{q}''_e - \dot{q}''_{crit})^n t_{ig} = FTP_n \quad \text{for} \quad n \geq 1 \qquad \ldots (5.13)$$

where FTP_n is the flux time product and n is the flux time product index. By rearranging Eq. (5.13), the incident heat flux, $\dot{q}''_e$, is given by:

$$\dot{q}''_e = \dot{q}''_{crit} + \frac{FTP_n^{1/n}}{t_{ig}^{1/n}} \qquad \ldots (5.14)$$

Eq. (5.14) resembles a straight line and by plotting the data obtained from a series of cone calorimeter tests (Figure 5.5), a best-fit straight linear regression line can be achieved with an appropriate n value (typically $1 \leq n \leq 2$). The best-fit line is extrapolated to obtain the critical heat flux, $\dot{q}''_{crit}$. The slope of the best-fit linear regression line is equivalent to the value of $FTP_n^{1/n}$. Thus, the Flux Time Product, FTP_n, can be expressed as:

$$FTP_n = (slope)^n \qquad \ldots (5.15)$$

If the incident heat flux is constant, Eq. (5.13) can be rewritten as follows to give the time to ignition, t_{ig} :

$$t_{ig} = \frac{(FTP_n)}{(\dot{q}''_e - \dot{q}''_{crit})^n} \qquad \ldots (5.16)$$

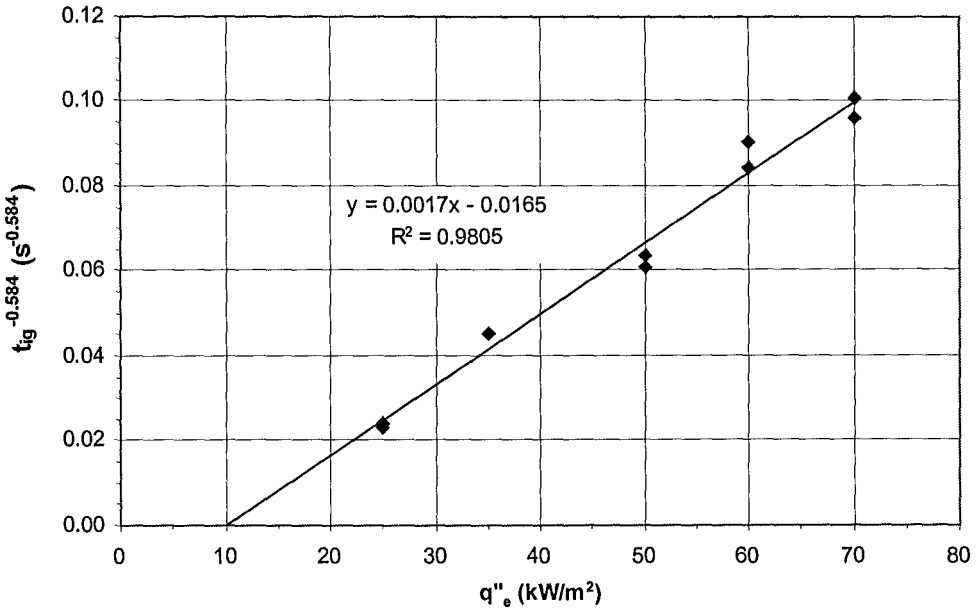

Figure 5.5: Plot of $(1/t_{ig})^n$ versus $\dot{q}''_e$ for 10 mm hardboard (Silcock & Shields' method)

5.3.5 Upward Flame Spread

Upward flame spread occurs as a result of heating the unignited portion of the fuel to a temperature at which the vigorous pyrolysis begins. In general, the pyrolysis front is assumed to reach a point, y_p, exactly when the surface temperature at that height reaches the ignition temperature of the wall material, T_{ig}. The governing equation for upward flame spread is based on a constant flame spread heat flux applied over the flame extension region beyond y_p whose initial temperature is T_s, and this is given by:

$$\frac{dy_p}{dt} = \frac{y_f - y_p}{t_{ig}} \qquad \text{... (5.17)}$$

y_p is applied to upward spread along the wall, and y_f is the flame length in upward direction and this is given by :

$$y_f = K\left(\dot{Q}'_f + \dot{Q}''_p y_p\right)^n \quad \text{... (5.18)}$$

$\dot{Q}''_p$ is the peak heat release rate for the cladding materials measured in cone calorimeter tests. The appropriate peak heat release rate is found by using a similar method for solving $\dot{Q}''(t)$. The cubic spline interpolation is applied to subsets of the measured peak heat release rate in the cone calorimeter testing at various external heat fluxes.

The emerging flame effect is included in Eq. (5.18), where $\dot{Q}'_f$ is the energy release rate for the emerging flame equivalent to a line source such that the emerging flame length is equal to $K\dot{Q}''^n_f$ and it is given by:

$$\dot{Q}'_f = \left(\frac{z}{K}\right)^{1/n} \quad \text{... (5.19)}$$

The flame length for wall flames is given such that K is the flame area constant (0.067) and the flame length power, n is $2/3$.

The ignition temperature and effective thermal inertia can be found from the Grenier & Janssens method (Section 5.3.4.1) using the ignition data from cone calorimeter tests. The time to ignition, t_{ig} is given by:

$$t_{ig} = \frac{\pi}{4} k\rho c \left[\frac{T_{ig} - T_s}{\dot{q}''_f}\right]^2 \quad \text{... (5.20)}$$

The heat flux of the preheated region ahead of the flame front, $\dot{q}''_f$, is assumed to be 30 kW/m^2.

Alternatively, the time to ignition can be worked out from the recommended method by Silcock and Shields.

CHAPTER 6

6 BENCH-SCALE AND FULL-SCALE EXPERIMENTS

This chapter provides a brief description of the cone calorimeter tests and full-scale tests. A sensitivity analysis was performed on the time to ignition obtained from the cone calorimeter at various heat fluxes for one of the cladding materials in order to observe their effect on the material properties ($k\rho c$ and T_{ig}). Material properties obtained from the ignition correlations for all the tested cladding materials are included. A summary of experimental observations regarding the full-scale tests is also provided.

6.1 Bench-Scale Cone Calorimeter Testing

In order to determine the material properties of each cladding material required as input to the flame spread model, a range of exterior cladding materials and products with different generic behaviours using the cone calorimeter method of ISO 5660 [36] was tested. Four cladding materials were selected for analysis:

- Cellulose fibre-cement sheet (7.5 mm thick)
- Extruded foamed uPVC weatherboard with co-extruded UV protection uPVC exterior layer, rusticated profile (7 mm)
- Plywood[+], 5-ply radiata pine, rough sawn face containing a vertical grooved profile (12 mm thick)

[+] This is a "LOSP"-treated plywood. LOSP is a light organic solvent preservative containing a fungucide (TBTN) for rot protection, a mouldicide for short term mould resistance prior to coating, an insecticide and a wax water repellent to stabilise the surface fibres for painting.

- Reconstituted timber weatherboard (i.e. not a solid timber) manufactured from selected Australian hardwood; wood residues are incorporated into boards without synthetic resins (10 mm)

Both cellulose fibre-cement sheet and plywood had been tested previously at BRANZ. Therefore, it was necessary to test only the foamed uPVC weatherboard and hardboard.

The samples were conditioned in a climate-controlled environment at a temperature of 23 °C and a relative humidity of 50% prior to testing. Each sample was cut to 100 mm by 100 mm in size and was then tested in the cone calorimeter for at least 15 minutes, under irradiances ranging from 75 kW/m^2 to 25 kW/m^2. At least two replicates were tested for each irradiance level, and data was averaged for the time to ignition, total heat release and the peak heat release rate.

6.2 Sensitivity Analysis of Ignition Data

Sensitivity analysis was undertaken on the parameters derived from cone calorimeter tests so that the influence of each parameter on the ignition temperature, critical heat flux and thermal inertia of the cladding materials could be determined. 12 mm plywood was chosen for the sensitivity analysis.

Table 6.1 shows the average time to ignition at each irradiance level as recorded by the cone calorimeter operator.

Table 6.1: Time to ignition and peak heat release rate for plywood

Irradiance Level (kW/m^2)	Ignition Time (secs)	Peak HRR (kW)
35	34.7	229.1
50	17.5	234.5
60	8.2	273.9
75	4.5	290.8

It can be expected that there will be some error associated with the direct observation of the time to ignition by the operator. To minimise the error associated with the direct observation of the time to ignition, an alternative approach was to take the time of ignition as the time for the heat release rate to reach 30kW/m^2. The observed time to ignition usually varies within 1 to 2 seconds with the ignition time at 30 kW/m^2. It is expected that the ignition time was recorded after the ignition had occurred, which was the visual observation made when the material ignited. Therefore, 2 seconds was subtracted from the nominal values at 75 kW/m^2 only and at all the irradiance levels to see the effect it has on $k\rho c$ and T_{ig}. A variation of ± 5-10% was also assigned to each nominal value of $k\rho c$ and T_{ig}. The sensitivity of these parameters with respect to the variation in their nominal values is presented in Table 6.2.

Table 6.2:Variations of T_{ig} and $k\rho c$ with time to ignition

Irradiance Level (kW/m^2)	Variation to t_{ig}						
	Nominal (secs)	-10%	-5%	5%	10%	- 2 secs for t_{ig} at 75 kW/m^2	- 2 secs for t_{ig} at all irradiance levels
35	34.7	31.2	33.0	36.4	38.2	34.7	32.7
50	17.5	15.8	16.6	18.4	19.3	17.5	15.5
60	8.2	7.4	7.8	8.6	9.0	8.2	6.2
75	4.5	4.1	4.3	4.7	5.0	2.5	2.5
kρc (kW/m^{2}K)^{2}s	0.104	0.096	0.100	0.108	0.117	0.031	0.033
T_{ig} (°C)	416.5	413.9	415.2	417.6	414.6	500.9	490.2
	Percentage of Variation from the Nominal Value (%)						
kρc (kW/m^{2}K)^{2}s	-	-7.7	-3.8	3.8	12.5	-70.2	-68.3
T_{ig} (°C)	-	-0.6	-0.3	0.3	-0.5	20.3	17.7

In the analysis shown here, both T_{ig} and $k\rho c$ are relatively insensitive to the small variation in time to ignition (± 5-10%). However, $k\rho c$ is profoundly affected by the small changes in time to ignition data at the highest irradiance level (75 kW/m^2), as the time to ignition at this irradiance level is the shortest at the higher heat fluxes. For

example, a change of two seconds on the time to ignition at 75 kW/m^2 resulted in a drop of 70.2% in the nominal value of $k\rho c$.

The inclusion of time to ignition at the high irradiance level (75 kW/m^2) has the effect of increasing the slope of the line of best fit and the critical heat flux value calculated from the chart. This can lead to unrealistic material properties. The error associated with ignition times, which can be very short, for example at 75 kW/m^2 (i.e. 2.5 seconds), is too large, and it should not be included in the ignition correlation.

6.3 Cladding Material Properties

The ignition times of the cladding materials tested at various heat fluxes in the cone calorimeter tests are used by the *BRANZFIRE* model to calculate the ignition temperature, T_{ig}, and the thermal inertia, $k\rho c$, using the method proposed by Grenier and Janssens. The material property data will then be used to work out the time to ignition at a certain incident heat flux (Eq. 5.20). An alternative way to obtain the time to ignition is by using the method proposed by Silcock and Shields (Section 5.3.4.2). Gernier and Janssens' method is only applicable for wood products, whereas Silcock and Shields' method may be more applicable to other combustible materials such as polymeric material. These two methods were ultilised to obtain the time to ignition for wood-based samples. The time to ignition for foamed uPVC weatherboard and cellulose fibre-cement sheet was found by using the Silcock and Shields' method only.

To obtain the ignition temperature by the Silcock and Shields' method, similar methodology to Janssens was used. The "n" value is allow to vary in the range of 0.5 to 1 (equivalent to n flux time product index of $1 \leq n \leq 2$ in Silcock and Shields' method).

The cladding material properties associated with each of the tested cladding materials are given in Table 6.3. The respective plots of the correlated ignition data are shown in Appendix A.

Table 6.3: Material properties

Cladding Materials	Grenier & Janssens				Silcock & Shields			
	$\dot{q}''_{cr}$ (kW/m^2)	T_{ig} (°C)	$k\rho c$ (kW^2 s/m^4.K^2)	n*	$\dot{q}''_{cr}$ (kW/m^2)	T_{ig} (°C)	FTP (kW s/m)	n**
1. Plywood	10.4	307	0.226	0.547	8.2	266	23489	2.0
2. Hardboard	9.9	300	2.4	0.584	9.9	299	57662	1.7
3. Foamed uPVC	-	-	-	-	9.0	281	125400	2.0
4. Fibre-cement	-	-	-	-	9.8	341	71948	1.8

*Grenier & Janssens method: (thermally thick) $0.547 \leq n \leq 1$ (thermally thin)
**Silcock & Shields method: (thermally thin) $1 \leq n \leq 2$ (thermally thick)

There was no ignition for 7 mm foamed uPVC tested at 25 kW/m^2. The samples melted and shrank during the 15 minutes exposure to this heat flux. It is interesting to see that two ignitions occurred in some of the cone calorimeter tests. The first flame, resulting from the first ignition, only lasted for a few seconds before it went out. The second ignition did not occur straight after the first ignition. The observed time to ignition was taken as the time to ignition at the second flaming.

To prevent the foamed PVC samples tested in the cone calorimeter tests from bubbling and expanding, a retaining grid was placed on top of each tested samples. It is possible that the retaining grid may have delayed the ignition process and thus the time to ignition. However the significance of this effect is unclear at this stage.

It is recommended to use Silcock and Shields' method when correlating the ignition data from cone calorimeter tests. Grenier & Janssens' method assumed that the material behaves as a thermally thick solid and it may not be appropriate for some materials which exhibit thermal thin or thermally intermediate behaviour. Grenier & Janssens' method should be used only for wood products. Further research is required on the application of this method to other materials.

6.4 Full-Scale Experiments

A series of full-scale experiments on fire spread on exterior cladding systems had been conducted at the Building Research Association of New Zealand (BRANZ) prior to this research. The tests were carried out to determine the comparative flame spread characteristics of exterior wall cladding systems by looking at the flame spread over the external facade and the mechanical response, such as damage and collapse associated with each cladding material.

Figure 6.1 illustrates the BRANZ full-scale test facility. The vertical wall of the test facility has an overall height of 6 m and a width of 3.6 m. The main test face extended at least 5 m over the top of the opening (6.0 ± 0.1 m height by 2.1 ± 0.1 m width). The same cladding materials tested in the cone calorimeter (fibre-cement, foamed uPVC, hardboard and plywood) were used for the full–scale experiments.

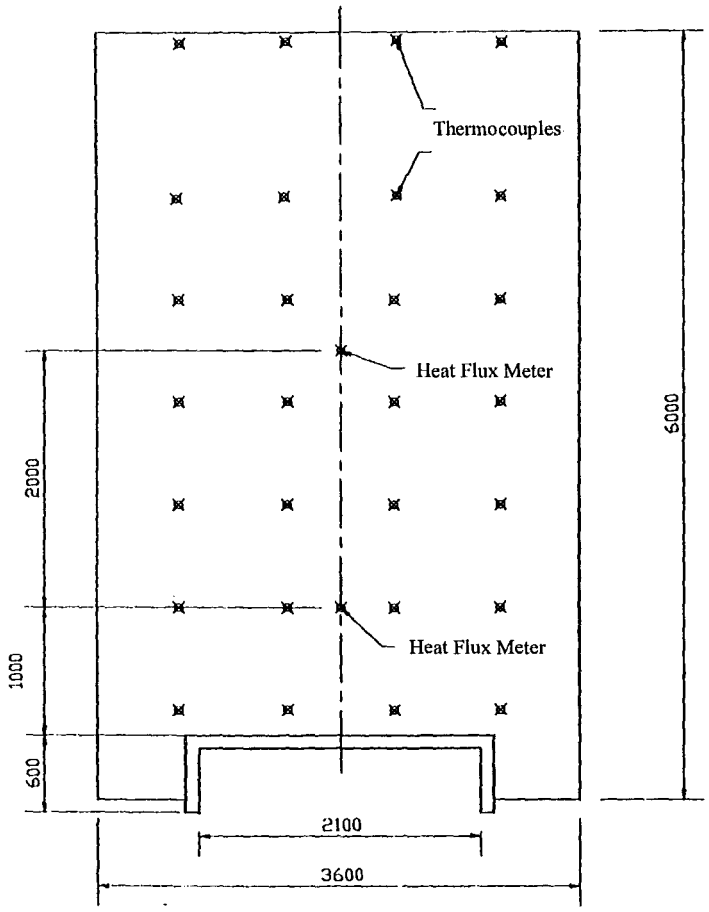

Figure 6.1: Front view of the full-scale test rig [14]

The fire scenario was represented by a flame venting through a window opening (opening of the combustion chamber in this experiment) as a result of a fully developed fire in a room typical of a small-scale commercial or residential building. The venting flame was expected to expose the external facade.

The tests were begun with the ignition of a two fuel trays (1.0 m length by 0.25 m width and 0.1 m depth) containing liquid fuel (Pegasol AA by Mobil) at the base of the test sample. The liquid fuel has a heat of combustion of greater than 42 MJ/kg and contains a high proportion of hexane. The heat source was intended to provide a total heat output of 1500 MJ over 20 minutes at a peak rate of 1.0 ± 0.2 MW.

6.4.1 Instrumentation

Two heat flux meters were placed at 1.0 m and 3 m above the top of the opening. The heat flux meters are aligned on the centre line of the opening and on the plane of the cladding system. The incident heat flux at a location of 1.0 ± 0.1 m above the opening was 70 ± 20 kW/m^2 over the period from 5 minutes to 15 minutes. The average value of total heat flux at the same location was maintained at 70 ± 5 kW/m^2 over the period from 5 minutes to 10 minutes.

External temperatures on the facade were monitored by twenty eight thermocouples as shown in Figure 6.1.

A videographic record and photographic records were ultilised during the duration of the tests in order to show the condition of the external appearance of the full height of the main test face.

6.4.2 Observations

A summary of observations made from the full-scale test is included in Table 6.4. The photographs showing the size of the emerging fire, flame spread along the wall and localised damage for all cladding materials are given in Figures B.2 to B.5.

Table 6.4: Summary of experimental observation

Cladding Materials	Observations	Figures (in Appendix B)
1. Cellulose fibre-cement sheet (7.5 mm thick)	♦ Debris fell from the damaged region ♦ Flame did not spread to the top of the wall ♦ Damage was confined to the region directly exposed to the flame	B.2
2. Plywood (12 mm thick)	♦ Flame spread to the top of the wall	B.3
3. Timber reconstituted weatherboard (10 mm)	♦ Substantial flaming occurred during the flame spread along the wall ♦ Flame spread to the top of the wall ♦ Flame damaged approximately 85% of the total wall area	B.4
4. Extruded formed uPVC weatherboard (7 mm)	♦ Self-sustained wall flame ♦ High smoke production ♦ Rapid flame spread to the top of the wall ♦ Extensive melting and severe damage to the wall	B.5

CHAPTER 7

7 MODELLING AND COMPARISON OF RESULTS

7.1 Introduction

The modelling using the *BRANZFIRE* model is divided into two parts, namely the incident heat flux to the exterior wall cladding as a result of flame issuing through a vent, and the flame spread on the exterior wall cladding. The predicted incident heat flux was compared with the experimental data available from the literature, whereas the predicted results from the fame spread model were compared with the full-scale tests previously conducted at BRANZ.

7.2 Predicting the Incident Heat Flux to the Exterior Wall Claddings

7.2.1 Model Simulation

The comparison of the heat transfer model was to be made with the existing experimental data obtained from full-scale tests [23]. The heat transfer model was set up to describe the flame issuing through a vent which connected the fire compartment to the adjacent space. The following inputs were specified in the model, which include:

- Dimensions of the fire compartment - It was specified in accordance with the inside dimensions of the two burn facilities used in the full-scale experiments (a smaller burn facility with a 2.4 m wide, 3.6 m deep and 2.4 m high burn room, and a three-storey burn facility with a 5.95 m wide, 4.4 m deep and 2.75 m high burn room)

- Dimensions of the adjacent space – This was specified to be 30 m wide, 30 deep and 10 m high
- Wall, ceiling and floor lining materials – For large burn room, the walls and ceiling were covered on the layer exposed to the interior of the room with 25 mm thick ceramic fibre insulation, and concrete as the substrate underneath the ceramic fibre insulation. The floor was covered with 57 mm thick fired clay paving stones in the full-scale tests. The floor was assumed to be made of concrete in the simulation. As for the small burn room, the exposed wall was concrete blocks covered with 13 mm thick non-combustible board
- Vents – The vent connecting between the fire compartment and the adjacent space is similar to the size of the window opening used in the full-scale tests. It is assumed that the vent sill height is 1 m. The dimensions of the vent connecting the adjacent space to the outside was 30 m wide by 10 high
- Specifying the fire – A 25 kg/m^2 fire load comprising six wood cribs was used as the experimental fire. The input heat release rate data for this type of fire is given in Appendix C
- Simulation time – Each simulation was run over a period of 20 minutes

The variable outputs from the model are the height of the flame issuing through the vent connecting the fire compartment and the adjacent space, the flame temperature at the vent soffit, and the incident heat flux to the wall.

7.2.2 Comparisons with Full-Scale Tests

The experimental data obtained from wood crib fires was used for comparison with the model, as the correlations used in the model for predicting the height and temperature of the flame were derived from the experiments which used the cellulosic fuels as the experimental fire load.

Two experiments were conducted using smaller burn facilities. There were three experiments conducted using the three-storey burn facility. However, only one set of heat flow data collected in one of the experiments tests was given in the literature for the 2.6 m by 1.37 m high window.

7.2.2.1 Small Burn Facility

The measured and calculated total heat flux density impinging on the exposed wall are shown in Figures 7.1 and 7.2.

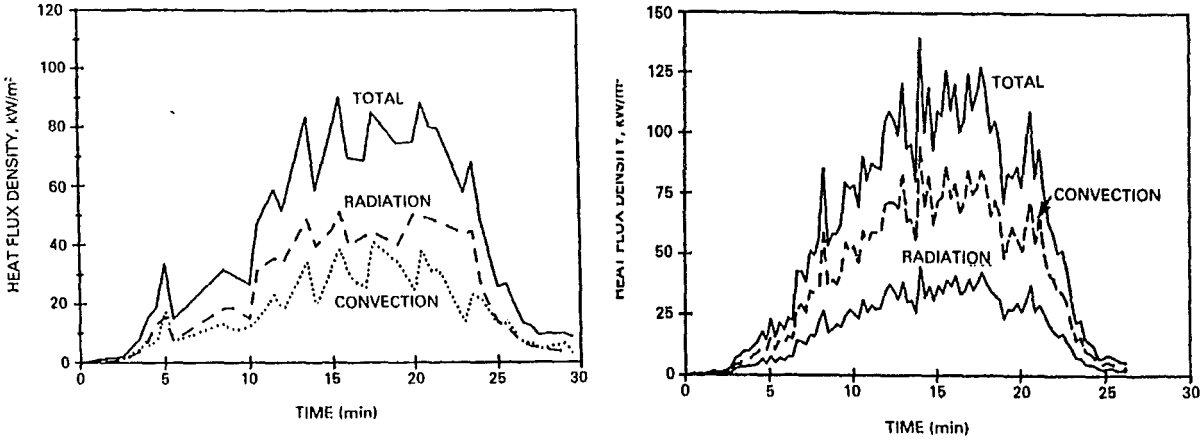

a) 1.13 m square window **b) 0.69 m wide by 1.5 m high window**

Figure 7.1: Measured total heat flux density received by the exposing wall [23]

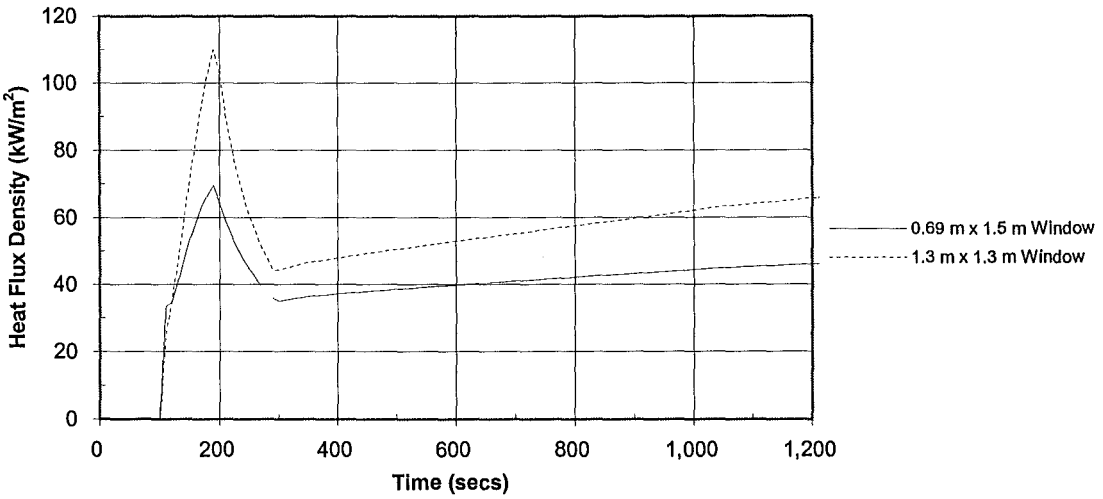

Figure 7.2: Calculated total heat flux density received by the exposing wall

For the small burn facility, the model's prediction of a peak heat flux of 110 kW/m^2 was reached three minutes after the ignition for a 1.3 m square window. When the burn room reached the steady state fire, the heat flux impinging on the wall stabilised to a range of 50 to 70 kW/m^2 till the end of the simulation (15 minutes after the peak heat

flux). It can be seen from Figure 7.1 that the calculated heat flux density for this particular window varies from 50 to 90 kW/m^2. Good prediction was made by the heat transfer model for this particular burn room and window.

Another simulation was run for the 0.69 m wide by 1.5 m high window in the small burn room with the same fire load. The predicted and measured heat flux impinging on the wall is also shown in Figures 7.1 and 7.2 respectively. The predicted heat flux by the model reached a stable value of 40 to 50 kW/m^2 over a period of 15 minutes.

It is expected that the predicted heat flux with this type of window is lower than the predicted heat flux for a squat window (1.3 m square window), as the narrow and tall window tends to project the flame further away from the exposing wall. The reversed condition was observed in the full-scale tests where the measured heat flux, at 0.25 m above the top of the window, exceeded 100 kW/m^2 for a substantial period of the experiment (Figure 7.1 b). Thus, the model underestimates the heat flux density for this type of window. Only one test was conducted in this facility for this type of window; thus, a firm conclusion regarding the accuracy of the model can not be made.

7.2.2.2 Large Burn Facility

The predicted heat flux was also compared with the experimental data obtained from the large burn facility for a 2.7 m wide by 1.37 high window. The results from the model prediction and the experiments are shown in Figures 7.3 and 7.4 respectively.

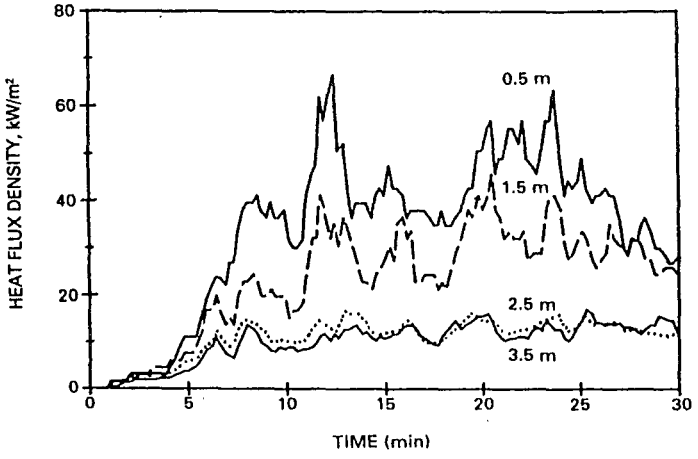

Figure 7.3: Measured total heat flux density received by the exposing wall [23]

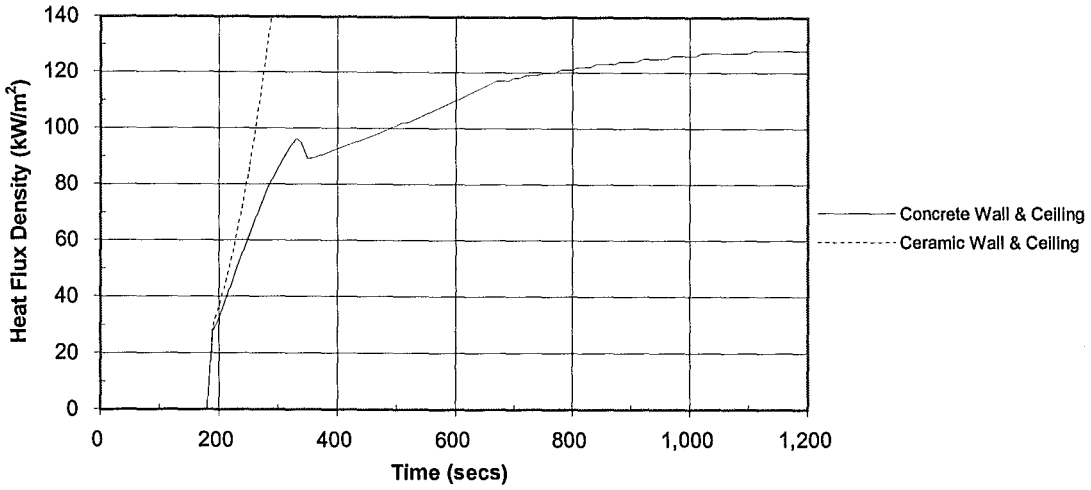

Figure 7.4: Calculated total heat flux density received by the exposing wall

It can be seen from Figure 7.4 that the model failed to predict the heat flux impinging on the exposed wall. The model was experiencing a convergence problem with ceramic fibre insulation on the wall and ceiling of the burn room. (As the correlations used in predicting the height and temperature of the emerging flame are derived from experiments which were conducted in the concrete burn room, it may not be suitable for this type of covering.) Another simulation was run by using the concrete wall and ceiling and a better prediction was obtained. The predicted total heat flux density rose steadily to a maximum of approximately 120 kW/m^2. A comparison of the model's output with the measured heat flux density showed that the model gives conservative results for this type of window and room size.

7.3 Modelling the Flame Spread on Exterior Wall Claddings

7.3.1 Model Simulation

For the purpose of comparing the extent of flame spread along the wall cladding with the full-scale tests conducted at BRANZ, it is desirable to specify the expected average heat flux to the wall and the flame height in the full-scale tests in order to give the most representative and comparable results. In the full-scale tests, the incident heat flux on the test specimen at a location one metre above the opening on the centre line of the opening and in the plane of the facade was specified to be 70 ± 20 kW/m^2 over the period from 5 minutes to 15 minutes. Actual flame heights were also estimated visually from the videographic records of the full-scale tests, and they were found to vary between 0.8 m to 1.2 m over the period from 10 minutes to 15 minutes. Therefore, 1 m flame height and heat flux density of 90 kW/m^2 were chosen as inputs into the flame spread model. The burner is assumed to expose an area of 0.67 m$^+$ high by 2 m^{++} wide on the wall to a maximum heat flux of 90 kW/m^2. The 90 kW/m^2 heat flux, however, appears to be a conservative value for a one metre high flame. Alternatively, the input heat flux into the flame spread model can be estimated by taking the average heat flux emitted by the liquid fuel burner or by the heat flux measurement in the vicinity of the opening.

The model also requires input data regarding the following:

- Room geometry
- Opening dimensions
- Width of the vent
- Selection of wall, ceiling and floor materials
- Initial surface temperature of the wall cladding
- Ignition data from the cone calorimeter tests

$^+$ Two-thirds of the one metre flame height.
$^{++}$ Length of the tray containing liquid fuel.

The adjacent room dimensions were specified as 30 m by 30 m by 10 m high. One side of the room (30 m by 10 m high) was treated as an opening. The effect of the upper hot layer is minimised by allowing the adjacent space to be well ventilated and relatively large.

The wall, ceiling and floor materials are specified as concrete, except for the wall containing the exterior wall cladding.

The width of the vent is 2 m, which is consistent with the length of the fuel tray.

The cone calorimeter data, which include the heat release rate and ignition time of the exterior wall cladding material at various irradiance levels, can be fed into the *BRANZFIRE* model. The format of the input cone data file is given in Appendix D.

Other material properties such as the density, thermal conductivity, specific heat, emmisivity and heat of combustion (from cone calorimeter tests) will have to be specified for each cladding material for the purposes of heat transfer calculations.

It is important to note that the above assumptions made for the input variables in the flame spread model are not a prediction but a validation of the model by experiment in the sense that the maximum heat flux to the wall and the flame height were estimated from the full-scale tests.

7.3.2 Comparison with Full-Scale Tests

The prediction of upward spread by the model was compared with the results from the full-scale tests to demonstrate the effectiveness of the model to predict flame spread on a wall cladding in full-scale tests. It will be more appropriate to look at the temperature history of each thermocouple on the surface of the sample during testing, along with the calculated time to ignition, to allow the determination of the speed of the flame front along the sample surface. Due to time constraints, data reduction of the measurements made in the full-scale tests was not carried out for this study. Instead, a

qualitative comparison between the model simulation results and full-scale experiments was made.

The determination of the time for the flame to reach the top of the wall was made by visual observations through the videographic records. The measure of the pyrolysis front (y) was based on visual flame propagation during the tests (in relation to the location of heat flux metres) and darkening or damage of the cladding materials.

The flame spread model was applied to predict the rate of heat release of the cladding materials and the upward flame spread in terms of the upward pyrolysis front (m) and the flame spread velocity (m/s). A copy of the model input for the flame spread model is given in Appendix E for one of the cladding materials (12 mm plywood).

The model predictions of the upward flame spread for each of the four exterior wall cladding materials and comparison with the full-scale tests are considered separately as follows. The predicted variations of the upward flame spread velocity and the heat release rates of the cladding materials with time are included in Appendix F.

7.3.2.1 Plywood

Figure 7.5 shows the extent of upward flame spread for plywood from the model prediction and full-scale tests.

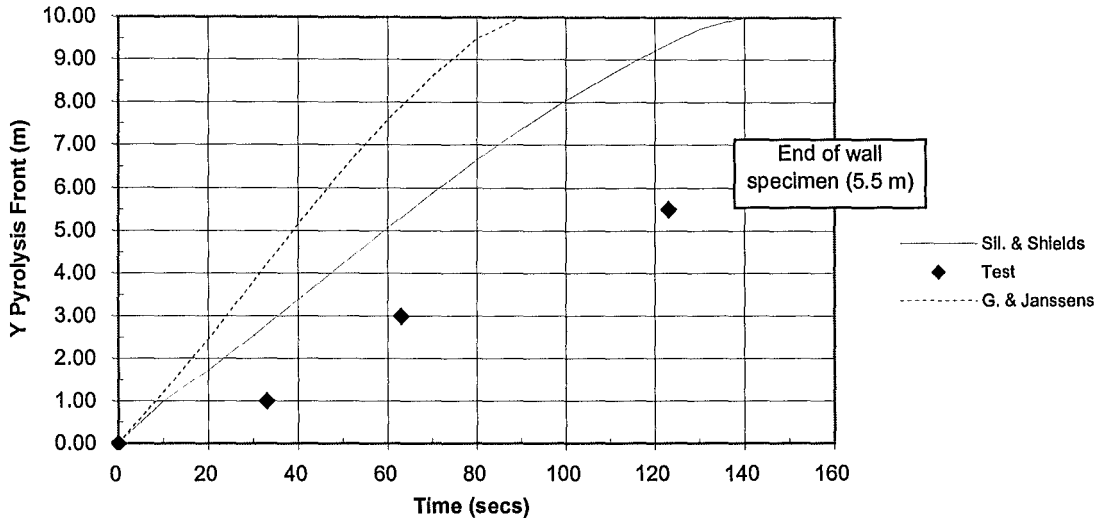

Figure 7.5: Location of pyrolysis front as a function of time for 12 mm plywood

Figure 7.5 shows that for the plywood the model predicts a rapid rise in the upward flame spread. The model gives the fastest rate of upward flame spread when the ignition data was correlated using Grenier & Janssens' method. Part of the reason for this may have been the appropriateness of Grenier & Janssens' method in deriving the material property data for the "LOSP"-treated plywood. It has been reported that Janssens' method does not adequately model the fire retardant treated plywood [37], and therefore it is suspected that this method may not be appropriate for the treated plywood as well. Computer simulations using property data derived from Silcock and Shields' method seemed to give better agreement than did those derived using Janssens' method.

In the full-scale experiment, the flame reached the top of the wall specimen (5.5 m above the combustion chamber) in approximately 123 seconds, whereas the predicted

times to reach the top of the wall specimen flame are 45 seconds and 70 seconds for Janssens' method and Silcock and Shields' method respectively.

The flame spread model, although giving a faster rate of flame spread than the actual tests, is able to predict the flame spread on plywood with reasonable accuracy.

7.3.2.2 Hardboard

Figure 7.6 shows the extent of upward flame spread for hardboard from the model prediction and full-scale tests.

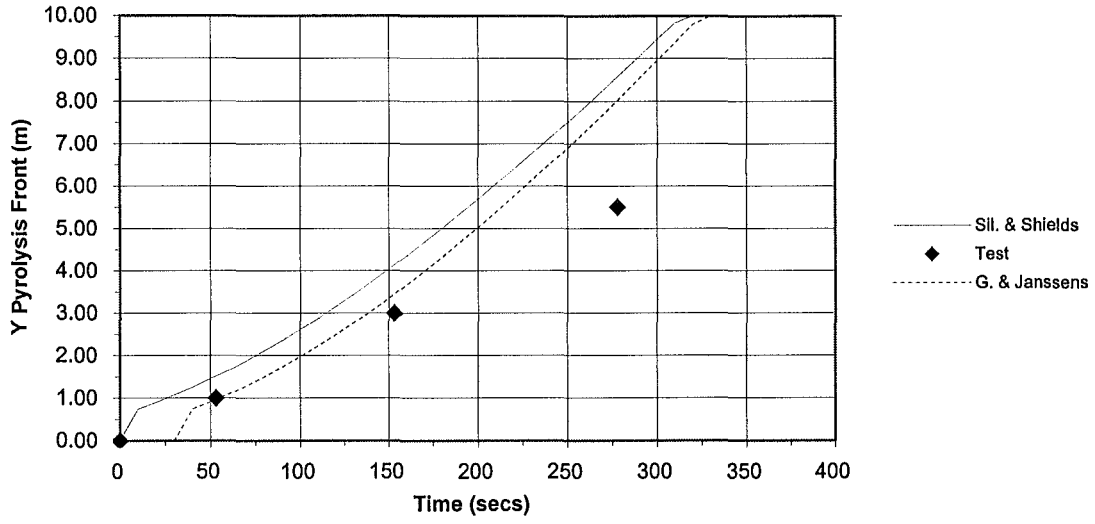

Figure 7.6: Location of pyrolysis front as a function of time for 10 mm hardboard

It can be seen from Figure 7.6 that the rate of upward flame spread predicted by the model is again faster than the actual flame spread rate in the full-scale tests. The shape of the rate of upward flame spread curves for both Grenier & Janssens' and Silcock & Shields' methods is similar. The predicted rate of flame spread for the Grenier & Janssens' method produces results in better agreement with the full-scale experimental data.

7.3.2.3 Foamed uPVC Weatherboard

Figure 7.7 shows the extent of upward flame spread for foamed PVC from the model prediction and full-scale tests.

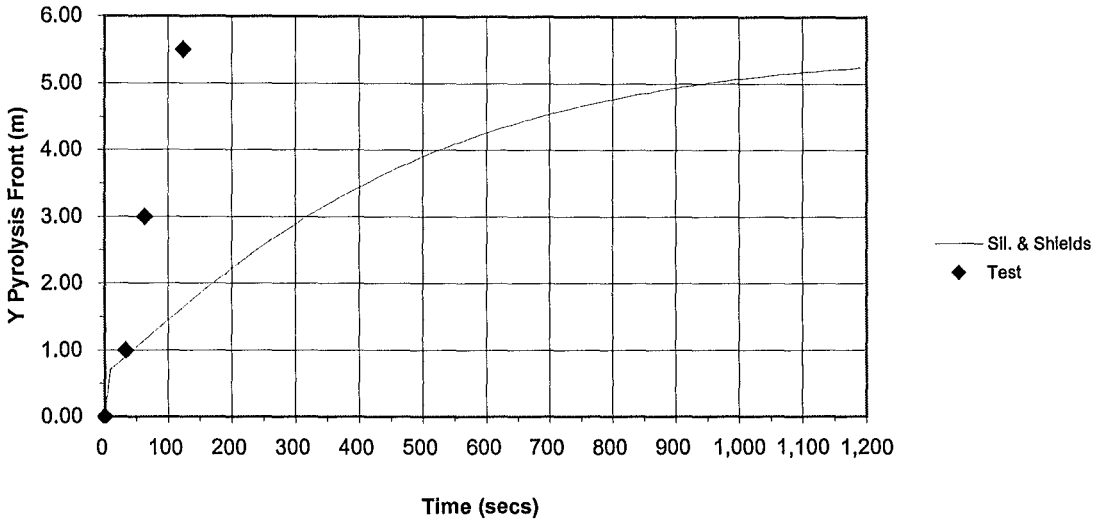

Figure 7.7: Location of pyrolysis front as a function of time for 7 mm foamed uPVC weatherboard

It can be seen from Figure 7.7 that the model under-predicts the rate of flame spread for foamed uPVC weatherboard. Rapid upward flame spread to the top of the wall in approximately two minutes was observed in the full-scale tests. Flame spread to the top of the wall is not predicted by the model. The predicted flame front reaches only 5.5 m along the wall specimen after 20 minutes.

A large effective surface area with many fine projections is typically found in PVC materials [38]. Thus, this fine microstructure probably contributes significantly to the ease of ignition and consequently the rapid flame propagation over the surface of foamed PVC.

7.3.2.4 Cellulose Fibre-Cement Sheet

Figure 7.8 shows the extent of upward flame spread for cellulose fibre-cement sheet from the model prediction and full-scale tests. The locations of the pyrolysis front in the full-scale tests were not given in Figure 7.8 because there was no flame spread recorded in the full-scale tests. Damage was due to the exposure of heat from the flame but not necessarily to the flame spread along the cladding material.

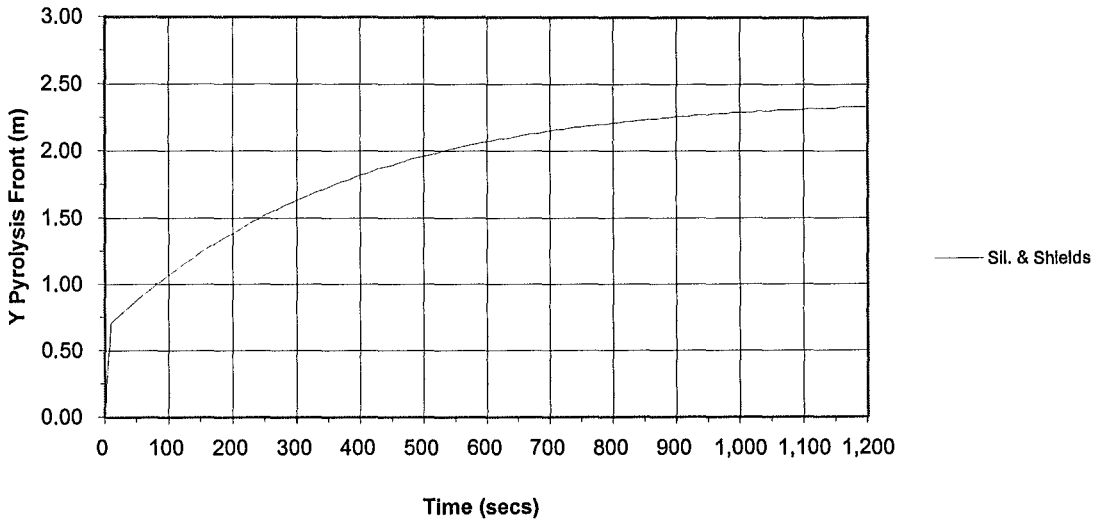

Figure 7.8: Location of pyrolysis front as a function of time for 7.5 mm cellulose fibre-cement sheet

The model prediction shows that flame does not spread to the top of the wall specimen. This was consistent with the full-scale tests in that there was no flame spread to the top of the wall. The model predicts that the flame spread reaches only 2.3 m above the combustion chamber after 17 minutes.

The full-scale tests show that the damage was confined to the region directly exposed to the flame. The damage may be caused by the heat from the flame, rather than the direct contribution of flame spread.

Clearly, the full-scale tests and the model prediction show that cellulose fibre-cement sheet, although combustible, does not contribute to flame spread.

CHAPTER 8

8 CONCLUSIONS AND RECOMMENDATIONS

8.1 Structure of the Models

The primary objective of this study was to modify an existing flame spread model to predict upward flame propagation on exterior wall cladding systems, as a result of flame issuing though a vent or window. A heat transfer model was also set up to predict the heat flux exposure on the exposed wall. Generally the structure of the heat flux and flame spread models presented in this study can be summarised in the following flow chart.

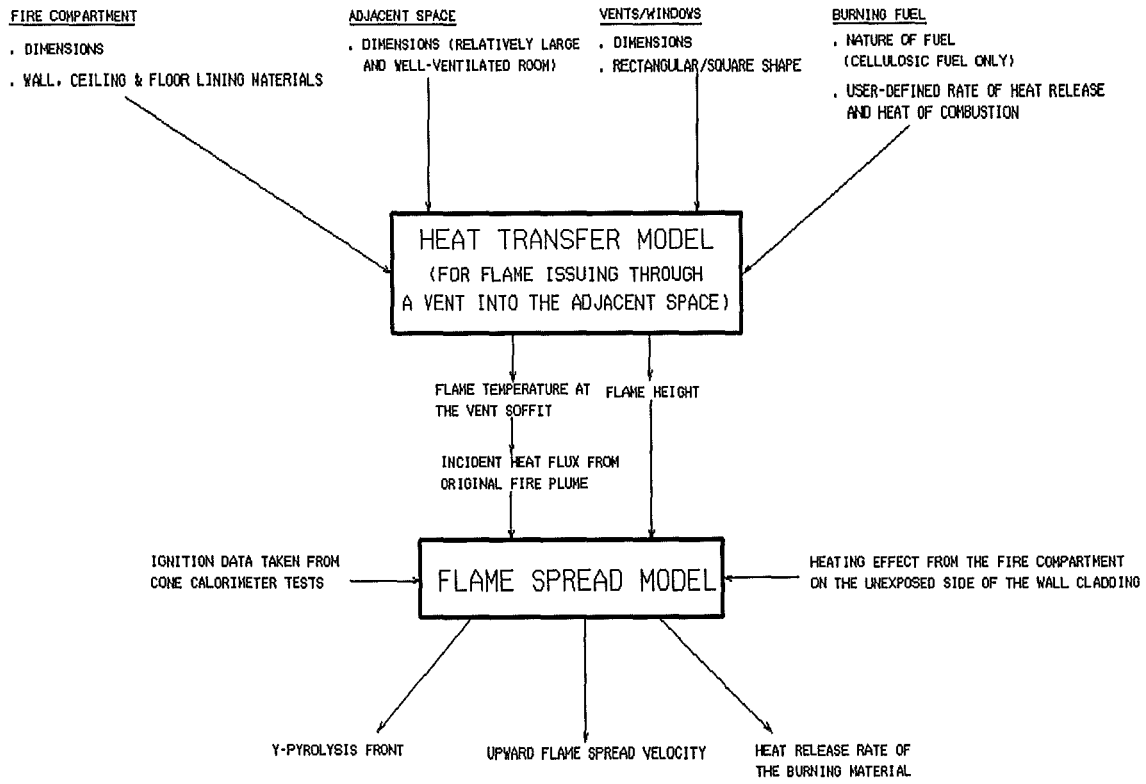

Figure 8.1: Structure of the models

The flammability properties of the cladding materials used in the model are derived from data taken from cone calorimeter tests. Sensitivity analysis of the ignition data from cone calorimeter tests for plywood shows that small variations in time to ignition can lead to large differences in the material property data. The significant variation arises when the time to ignition is very short. Therefore they should not be included in the ignition correlations.

8.2 Predictions Made by the Models

Full-scale tests were previously conducted at BRANZ with four types of cladding material, including "LOSP"-treated plywood, reconstituted hardboard, foamed uPVC weatherboard, and cellulose fibre-cement sheet. Flame propagation was observed for all the materials with the exception of the cellulose fibre-cement sheet.

A qualitative comparison was made between the predicted rate of upward flame spread with the full-scale experiments. The model predictions are able to differentiate between the relative performances of the four different cladding materials, that is, the contribution of the cladding material to the extent of flame spread. The flame spread model appears to be adequate and somewhat conservative for the limited comparison to experimental data for four different cladding materials except for the foamed uPVC weatherboard where flame spread was underpredicted. Furthermore, flame spread to the top of the foamed uPVC wall specimen was not predicted by the model.

In addition, the inclusion of the heat flux prediction method, based on a number of simplifying assumptions, makes the *BRAZNFIRE* model capable of estimating the height and centerline temperature of flame issuing through a window opening and the total heat flux density impinging on the exterior wall cladding. These parameters vary with the sizes of the fire compartment and window and the rate of heat release of the fire compartment.

The heat transfer model is conservative in predicting the total heat flux to the exterior wall although the overall trend was to overestimate the total heat flux to the exterior wall and underestimate the total heat flux for wide and low windows. The

underprediction of the model for this type of window may be due to the simplistic assumed flame shape, which may not have fully accounted for the hugging effect.

8.3 Limitations

The major limitations associated with each of the model are outlined in the following sections:

8.3.1 Heat Transfer Model

1. The heat transfer model is limited to flame projecting through a window opening and in natural draft conditions (i.e. still air condition).

2. The symmetrical fire is more suitable as the fuel burns evenly in the idealised environment. An analysis of exterior flame is complex and the heat transfer models which have been developed are based on a number of simplifying assumptions.

3. The empirical correlations used for predicting the geometry and temperature of the flame issuing through a window opening are suitable for compartment fires that involve mostly cellulosic fuels, such as wood furniture and other relatively thick objects made of charring materials. The higher burning rate of non-cellulosic materials such as plastics can possibly change the behaviour of the flame issuing through a window opening.

4. The empirical correlations used for predicting the geometry and temperature of the flame issuing through a window opening were derived from experiments conducted in a concrete burn room with cellulosic fuels. The correlations should begin to fail when the fire compartment is not a concrete shell.

The comparison made with the experimental data [23] for validating the heat transfer model may not be very accurate. The transducers used in the experiments were not very suitable for the experiment when they were used as convective or total heat flux

transducers because they tended to underestimate the convective or total heat flux density. It is desirable to compare the calculated results from the heat transfer model with more experimental data in order to validate the model.

8.3.2 Flame Spread Model

1. The flame spread model considered only the surface flame spread of the mechanically stable cladding materials. Other modes of flame spread, such as the breaking of the surface layer and thus the exposing of more combustible materials beneath, were not considered.

2. The flame spread model focuses on upward spread of flame on the surface of a cladding material because it typically represents the fastest mode of fire growth. No lateral flame spread is considered in adjacent room case. This mode of flame spread could contribute additional heat, such as on foamed uPVC weatherboard, which has extensive lateral spread.

Another limitation associated with this study is the qualitative comparison with the full-scale tests. Estimations of the upward pyrolysis front on the wall were made by visual observation of the flame propagation and damage of the wall. For cladding materials like foamed uPVC weatherboard, it is very difficult to see exactly the extent of flame spread because the wall specimen produced a lot of black smoke. Furthermore, although flaming was observed at a distance above the combustion chamber (2 m) for the cellulose fibre-cement sheet, this flaming was thin and intermittent. This type of flaming may have been contributed to by the emerging flame, rather than the burning of the cladding. Also, the surface darkening of the cladding material may be caused by the heat from the flame, but not the direct contribution of the flame spread. A more accurate comparison making use of the thermocouple records is recommended.

8.4 Recommendations

The heat transfer model and flame spread model described in this study potentially provide good engineering design procedures for fire engineers to evaluate the flame spread associated with an external wall cladding system, based on scientific and engineering principles taking into account the fire size in the compartment, the window geometry and the material flammability properties. The usefulness and capability of the heat transfer model and the flame spread model could be enhanced by carrying out the following tasks.

8.4.1 Heat Transfer Model

1. More work is needed in modifying the model to represent more realistically fires that involve non-cellulosic fuel. The successful modelling of this type of fire would represent a significant step in representing a more realistic window fire plume involving the burning of non-cellulosic fuel.

2. The full-scale results indicate that the heat flux resulting from flame issuing through a wide and low window opening is substantially higher than the model suggests, and further analysis will have to be conducted to improve the prediction of the heat flux exposure under this type of window geometry and the burning of the excess fuel outside the fire compartment.

3. The heat transfer model could be extended for a room that involves forced draft conditions. For example, extra air is supplied from the openings on the opposite side of the fire compartment.

4. The incident heat flux from the window fire plume is approximated in the model. In order to better understand the actual heat exposure conditions, full-scale heat flux measurements can be carried out to obtain the detailed heat flux profiles. The wide range of heat fluxes reported for different window geometries makes it critical to establish more definitive predictive methods.

8.4.2 Flame Spread Model

1. The flame spread model can be extended to predict the upward flame spread on composite cladding materials.

2. More meaningful comparison of the upward pyrolysis front can be made based on the actual temperature history of the wall surface during full-scale tests.

3. More full-scale tests could be carried out for other exterior cladding materials. The results are to be compared with the flame spread model outputs in order to assess the overall effectiveness of the model.

4. Incident heat flux from the emerging flame has been included in calculating the net heat flux to the exposing wall. The radiation from flames from the burning of the combustible cladding material could be included in the flame spread model, as this radiation would contribute to the total radiation received by the cladding material.

5. Lateral spread can be integrated into the flame spread model for the adjacent room. The required material dependent properties such as minimum surface temperature of spread ($T_{s,\min}$) and flame spread parameter (ϕ) are derived from the LIFT test.

6. The inclusion of more time to ignition data from cone calorimeter tests should improve the certainty of the estimation of the critical heat flux and critical temperature.

7. Ultimately, the heat transfer model could be integrated with the flame spread model to provide a more general model (Figure 8.1) that requires a minimum of input data to characterise flame spread accurately along the exterior wall cladding subject to a window fire plume, and to help the engineers to better design the height of spandrel panels on the exterior of buildings, based on the predicted heat flux exposure.

REFERENCE

[1] New Zealand Building Code. Published as the First Schedule of the Building Regulations under the authority of the New Zealand Government. 1992.

[2] Building Industry Authority. Approved Documents. Published by Standards New Zealand, Wellington. 1992.

[3] Simultaneous Determination of Ignitability, Flame Propagation, Heat Release and Smoke Release. AS 1530: Part 3. Standards Association of Australia. 1989.

[4] Combustibility Test for Materials. AS 1530: Part 1. Standards Association of Australia. 1989.

[5] C. Wade. Fire Performance of External Wall Claddings Under a Performance-based Building Code. *Fire and Materials*, Vol. 19, pp. 127-132, 1995.

[7] G.S. Cowles and E. Soja. Flame Spread Classification Method for Exterior Wall Claddings. In *Proceedings of the Eighth Interflam Conference*, 1999.

[8] A.H. Buchanan (Editor). *Fire Engineering Design Guide*, Center For Advanced Engineering, University of Canterbury, 1994.

[9] D. Yung and I. Oleszkiewicz. Fire Spread via Exterior Walls of Buildings. In *Proceedings of the Fourth Conference on Building Science and Technology*, Toronto, Ontario, 1988.

[10] I. Oleszkiewicz. Vertical Separation of Windows Using Spandrel Walls and Horizontal Projections. *Fire Technology*, Vol. 25(4), pp. 334-340, 1991.

[11] C.A. Wade and J. Clampett. Fire Performance of External Claddings – A Review. BRANZ Study Report (Draft), Wellington, New Zealand, 1999.

[12] J. Morris. The First Interstate Bank Fire – what went wrong? *Fire Prevention No. 226*, pp. 20-26, January/February 1990.

[13] A.E. Willey. High-Rise Building Fire. *Fire Journal*, Vol. 66(5), 1972.

[14] C.A. Wade and J. Clampett. Performance of External Claddings in Selected Fire Test Methods. BRANZ Study Report (Draft), Wellington, New Zealand, 1999.

[15] I. Oleszkiewicz. Fire Exposure to Exterior Walls and Flame Spread in Combustible Cladding. *Fire Technology*, Vol. 25(4), pp. 357-375, 1990.

[16] M. Law. Fire Safety of External Building Elements – The Design Approach. *AISC Engineering Journal*, Second Quarter, pp. 59-74, 1978.

[17] Dougal Drysdale. Mechanism of Flashover: An Overview. In *Proceedings of the Interflam Conference*, pp. 155-57, 1996.

[18] A.J.M. Heselden and P.J. Thomas. Fully Developed Fires in Single Compartments CIB Report No.20, Fire Research Note 923. Joint Fire research Organisation, Borehamwood, 1972.

[19] S. Yokoi. Study on the Prevention of Fire-Spread Caused by Hot Upward Current. Report of the Building Research Institute, 1960.

[20] L.G. Seigel. The Projection of Flames from Burning Buildings. *Fire Technology*, Vol. 5(1), 1969.

[21] P.H. Thomas and M. Law. The Projection of Flames from Buildings on Fire. *Fire Prevention Science and Technology*, Vol. 10, pp. 19-26, 1974.

[22] S. Klopovic and O.F. Turan. Flames Venting Externally During Full-scale Flashover Fires: Two Sample Ventilation Cases. *Fire Safety Journal*, Vol. 31, pp. 117-142, 1998.

[23] Igor Oleszkiewicz. Heat Transfer from a Window Fire Plume to a Building Facade. *Proceedings of the Winter Annual Meeting of the America Society of Mechanical Engineers*, San Francisco, HDT – Vol. 123, pp. 163-170, 1989.

[24] Howard W. Emmons. *SFPE Handbook of Fire Engineering*, chapter 2 Section 5 Vent Flows. National Fire Protection Association, 2nd edition, 1995.

[25] Arvind Atreya. *SFPE Handbook of Fire Engineering*, chapter 1 Section 3 Convection Heat Transfer. National Fire Protection Association, 2nd edition, 1995.

[26] D.G. Lilley. Dynamics of Fire Behaviour. *30th Proceeding Intersociety Energy Conservation Eng Conference*, pp. 485-90, 1995.

[27] C. Wade. *BRANZFIRE* Technical Reference Guide. Building Research Association of New Zealand, Porirua City, New Zealand, June 1999.

[28] James G. Quintiere. A Simulation Model for Fire Growth on Materials Subject to a Room-Corner Test. *Fire Safety Journal*, Vol. 20, pp. 313-339, 1993.

[29] Richard D. Peacock, Glenn Forney, Paul A. Reneke, Rebecca Portier, and Walter W. Jones. CFAST, the Consolidated Model of Fire and Smoke Transport. NIST Technical Note 1299, National Institute of Standards and Technology, February 1993.

[30] Frank P. Incropera. and David P. De Witt. Fundamentals of Heat and Mass Transfer. John Wiley and Sons, 1990.

[31] Jr C. David Eagle. BNALib A Basic Numerical Analysis Library for Personal Computers. Technical Report, 1997.

[32] A.T. Grenier and M.L. Janssens. An Improved Method for Analyzing Ignition Data of Composites. *In Proceedings of the International Conference on Fire Safety Vol 23*, 1997.

[33] Marc Janssens. Piloted Ignition of Wood: A Review. *Fire and Materials*, Vol 15, pp. 151-67, 1991.

[34] Marc Janssens. *Heat Release in Fires*, chapter 9 Determining Flame Spread Properties from Cone Calorimeter Measurements. Elsevier Applied Science, 1992.

[35] G.W.H. Silcock and T.J. Shields. A Protocol for Analysis of Time-to-Ignition Data from Bench Scale Tests. *Fire Safety Journal*, Vol. 24, pp. 75-95, 1995.

[36] ISO 5660 Fire Tests – Fire Tests – Reaction to Fire – Part 1 Rate of Heat Release from Building Products (Cone Calorimeter method). International Organization for Standardization, Geneva, 1993.

[37] C.M. Fleischmann. Piloted Ignition of Solid Materials Under Radiant Exposure. University of Canterbury, New Zealand, 1999.

[38] N.A. Dembsey and R.B. Williamson. Evaluation of a Fire Spread Model's Prediction of Critical Ignition Source Strength. In *Proceedings of the Interflam Conference*, 1996.

APPENDIX A

Piloted Ignition Correlations

A.1 12 mm "LOSP"-treated Plywood

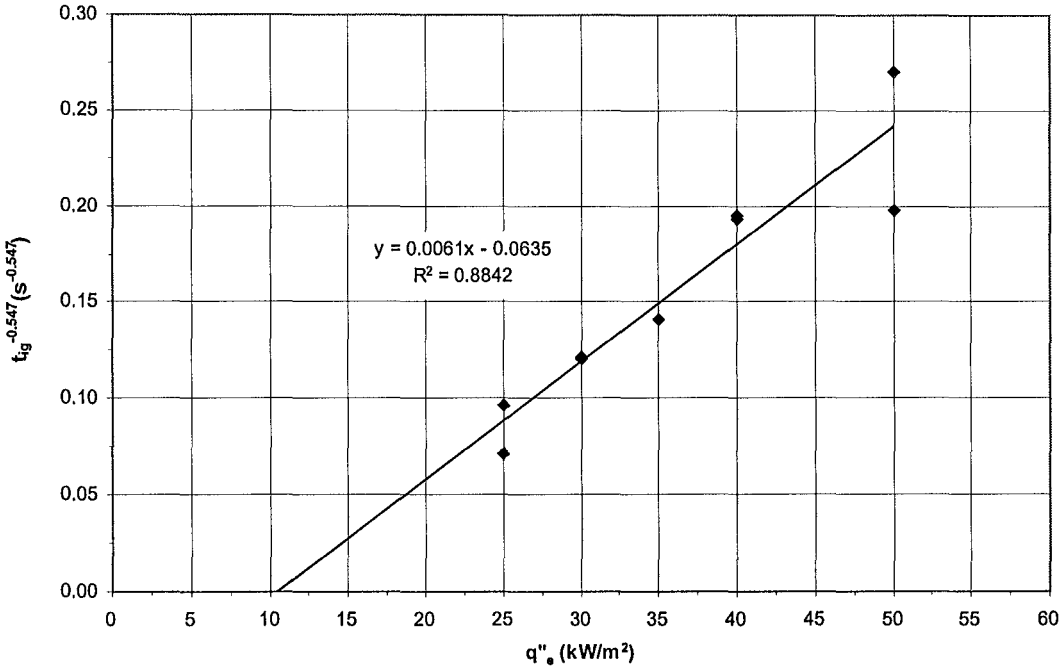

Figure A.1: Grenier & Janssens' method

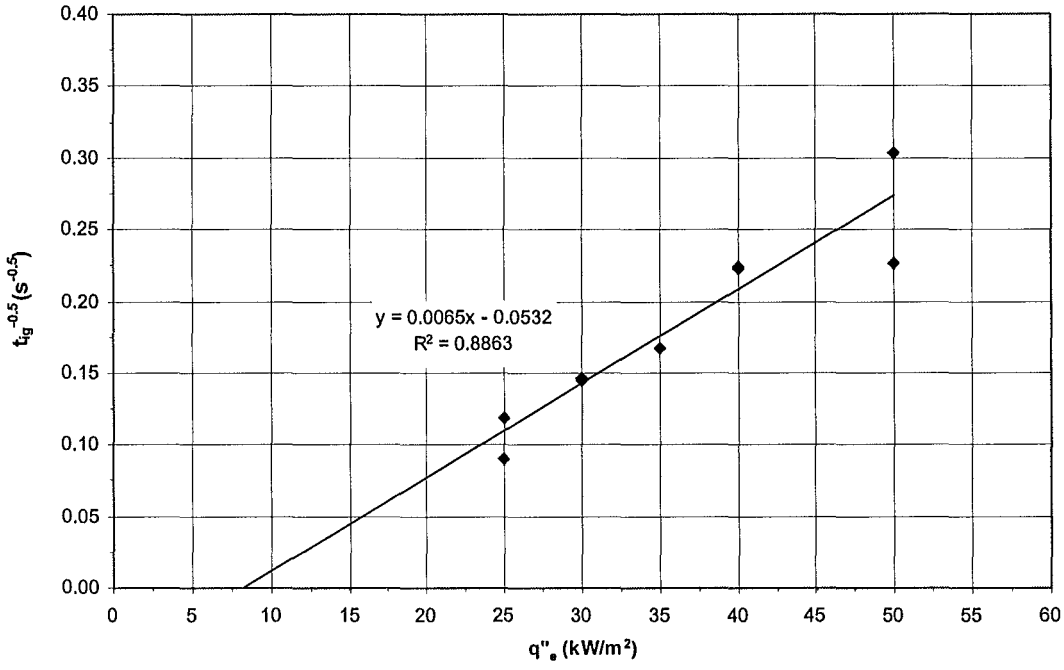

Figure A.2: Silcock & Shields' method

A.2 10 mm Hardboard

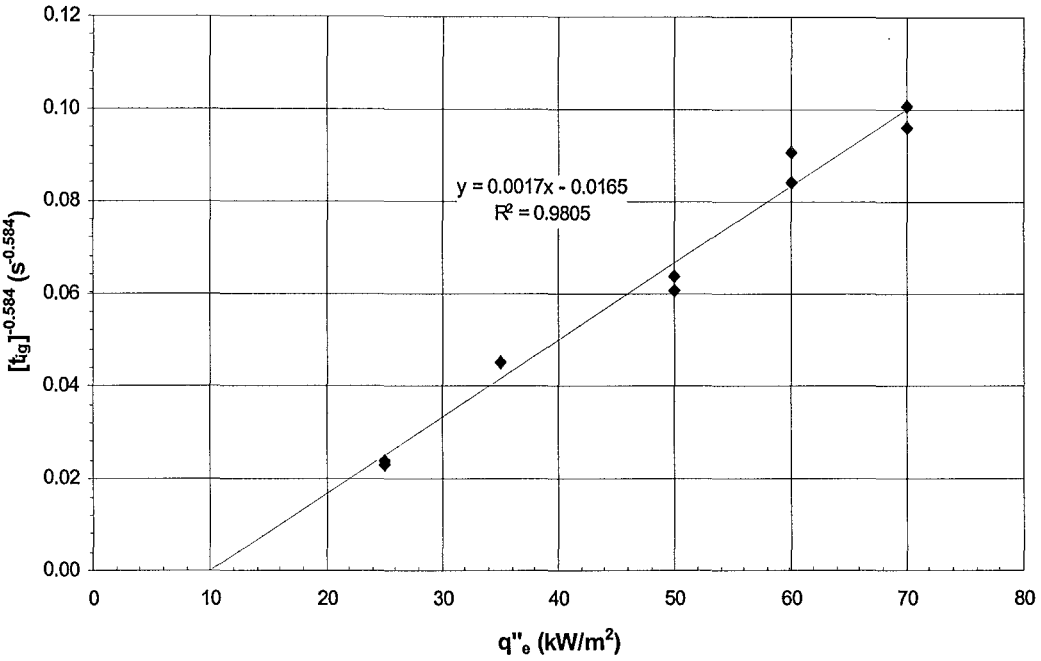

Figure A.3: Grenier & Janssens' method

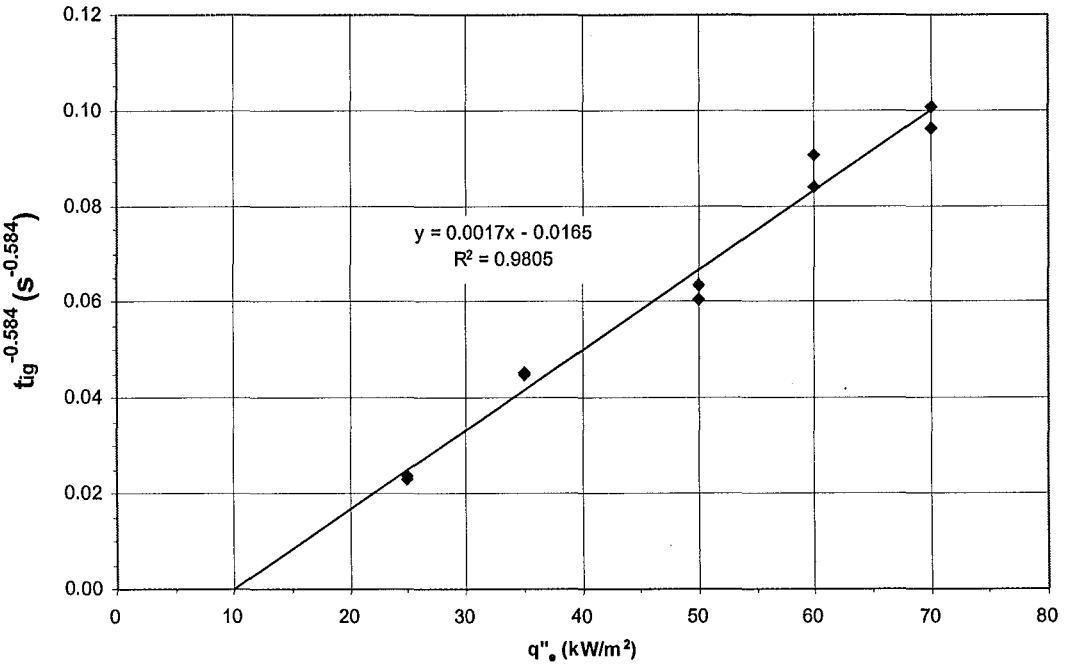

Figure A.4: Silcock & Shields' method

A.3 7.5 mm Cellulose Fibre-Cement Sheet

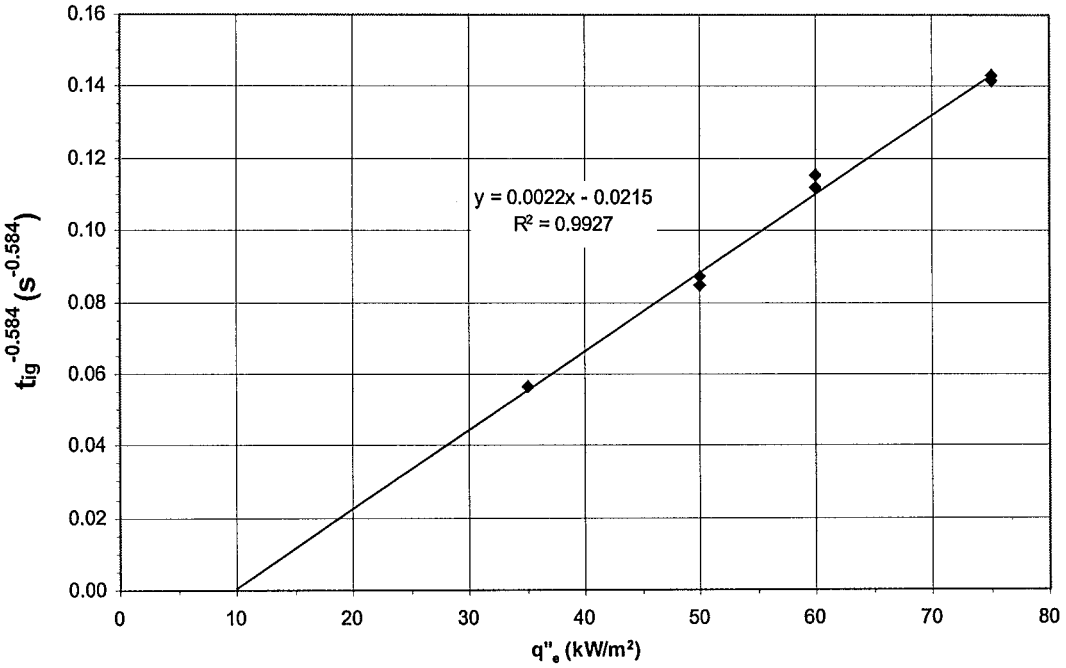

Figure A.5: Silcock & Shields' method

A.4 7 mm Extruded Foamed uPVC Weatherboard

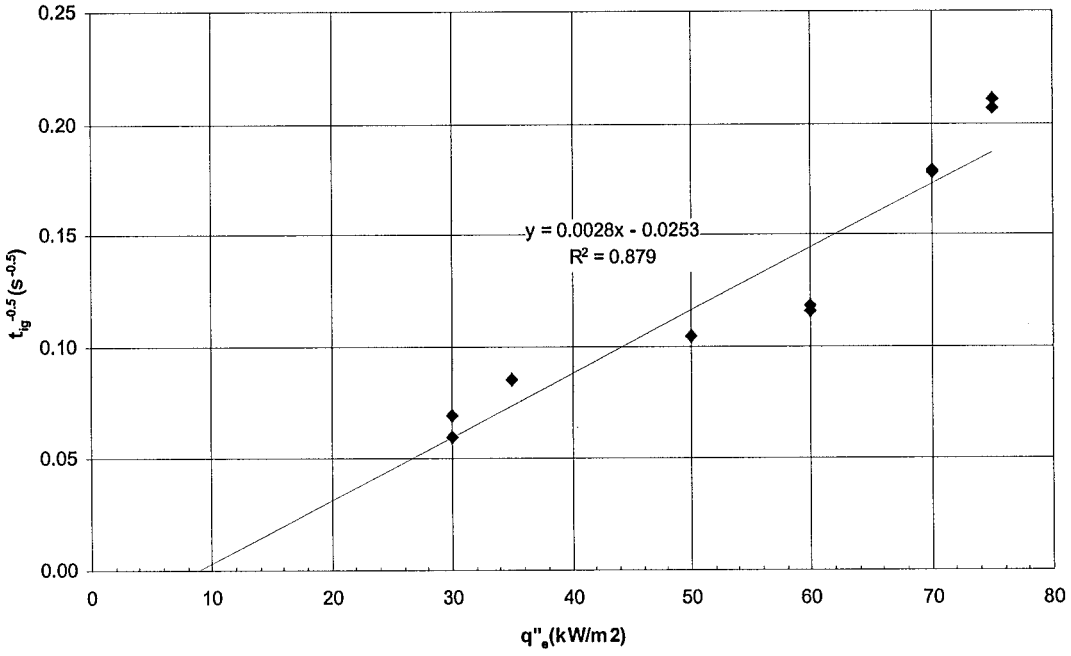

Figure A.6: Silcock & Shields' method

APPENDIX B

Full-Scale Testing of Exterior Wall Claddings at BRANZ

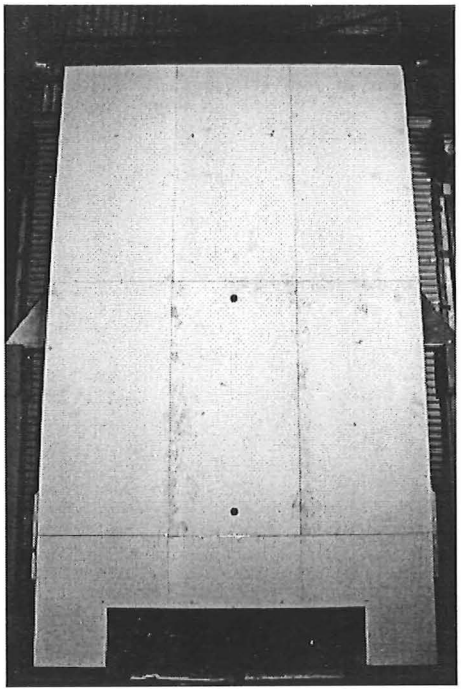

Figure B.1: Front view of the full-scale test rig

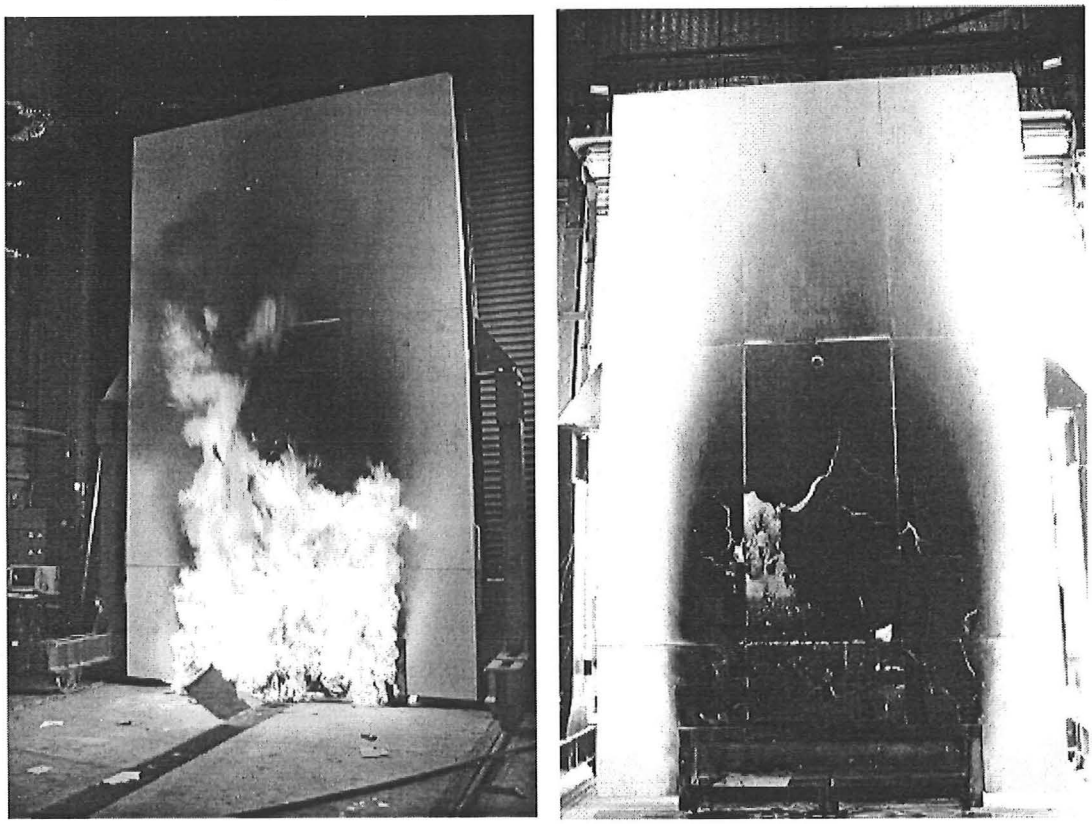

Figure B.2: Cellulose fibre cement sheet (7.5 mm)

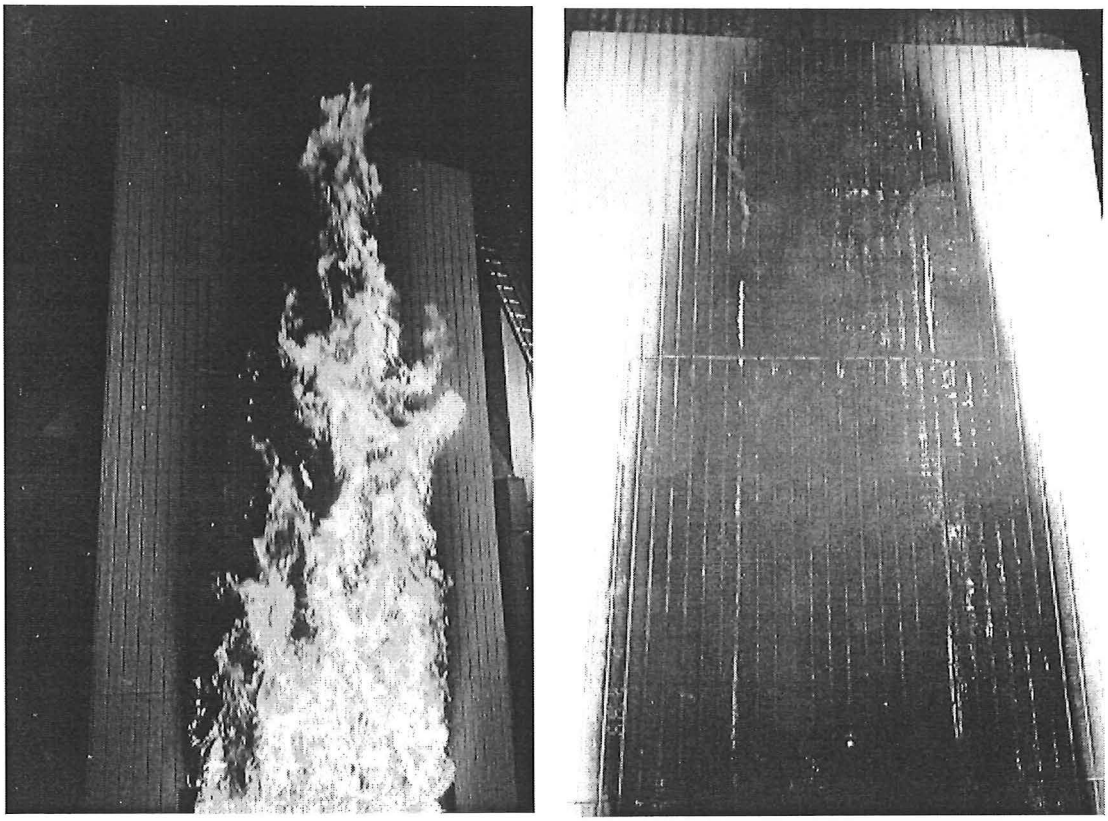

Figure B.3: LOSP-treated plywood (12 mm)

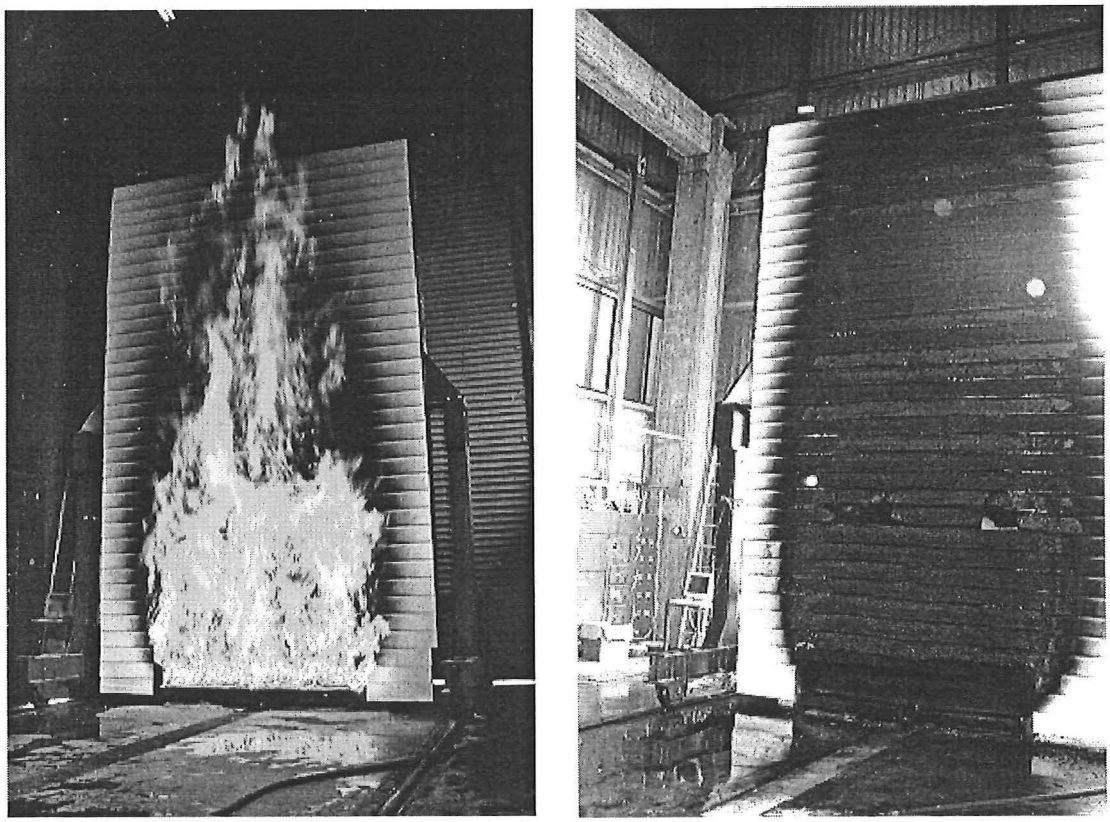

Figure B.4: Reconstituted timber weatherboard (10 mm)

Figure B.5: Extruded foamed uPVC weatherboard (7 mm)

APPENDIX C

Calculation of Heat Release Rate in the Burn Facilities

C.1 SMALLER BURN FACILITY

1. Dimensions of burn room: 2.4 m wide x 3.6 m deep x 2.4 m high
2. Fuel type: 6 wood cribs made of 41 mm x 41 mm pine studs distributed uniformly in the burn room
3. Fire load per unit area: 25kg/m^2
4. Fire growth rate: Fast
5. Growth constant, k = 150 s/MW$^{0.5}$

The fire is assumed to be have an increased heat output according to the t^2 fire curve. The peak heat release rate is achieved when the fire reaches maximum burning rate. The numerical expression of the maximum burning rate[+] is as follows:

$$\dot{m} = \frac{4}{D} m_o \upsilon_p \left(1 - \frac{2\upsilon_p t}{D}\right) \qquad \text{(for fuel surface control)}$$

where D is the stick thickness (41 mm)

m_o is the crib initial mass (216 kg)

υ_p is the fuel surface regression velocity (2.2 x 10^{-6}D$^{-0.6}$ for wood)

t is the time since ignition (t = 0)

Therefore, the maximum burning rate is found to be **0.32** kg/s.

Once the burning rate is computed, the heat release rate can be obtained as:

$$\dot{q} = \Delta h_c \dot{m}$$

where Δh_c is the heat of combustion taken as 12 x 10^3 kJ/kg for wood

Therefore, the peak heat release rate achieved in the small burn facility is **3.8** MW.

[+] Vytenis Babrauskas. *SFPE Handbook of Fire Engineering*, chapter 1 Section 3 Burning Rates. National Fire Protection Association, 2nd edition, 1995.

C.2 Large Burn Facility

1. Dimensions of burn room: 5.95 m wide x 4.4 m deep x 2.75 m high
2. Fuel type: 6 wood cribs made of 41 mm x 89 mm pine studs distributed uniformly in the burn room
3. Fire load per unit area: 25kg/m^2
4. Fire growth rate: Fast
5. Growth constant, k = 150 s/MW$^{0.5}$

The fire is assumed to be have an increased heat output according to the t^2 fire curve. The peak heat release rate is achieved when the fire reaches maximum burning rate. The numerical expression of the maximum burning rate is as follows:

$$\dot{m} = \frac{4}{D} m_o \upsilon_p \left(1 - \frac{2\upsilon_p t}{D}\right) \qquad \text{(for fuel surface control)}$$

where D is the stick thickness (taken as average thickness of 65 mm)

m_o is the crib initial mass (655 kg)

υ_p is the fuel surface regression velocity ($2.2 \times 10^{-6} D^{-0.6}$ for wood)

t is the time since ignition (t = 0)

Therefore, the maximum burning rate is found to be **0.46** kg/s.

Once the burning rate is computed, the heat release rate can be obtained as:

$$\dot{q} = \Delta h_c \dot{m}$$

where Δh_c is the heat of combustion taken as 12×10^3 kJ/kg for wood

Therefore, the peak heat release rate achieved in the large burn facility is **5.5** MW.

C.3 Input Heat Release Rate Curves

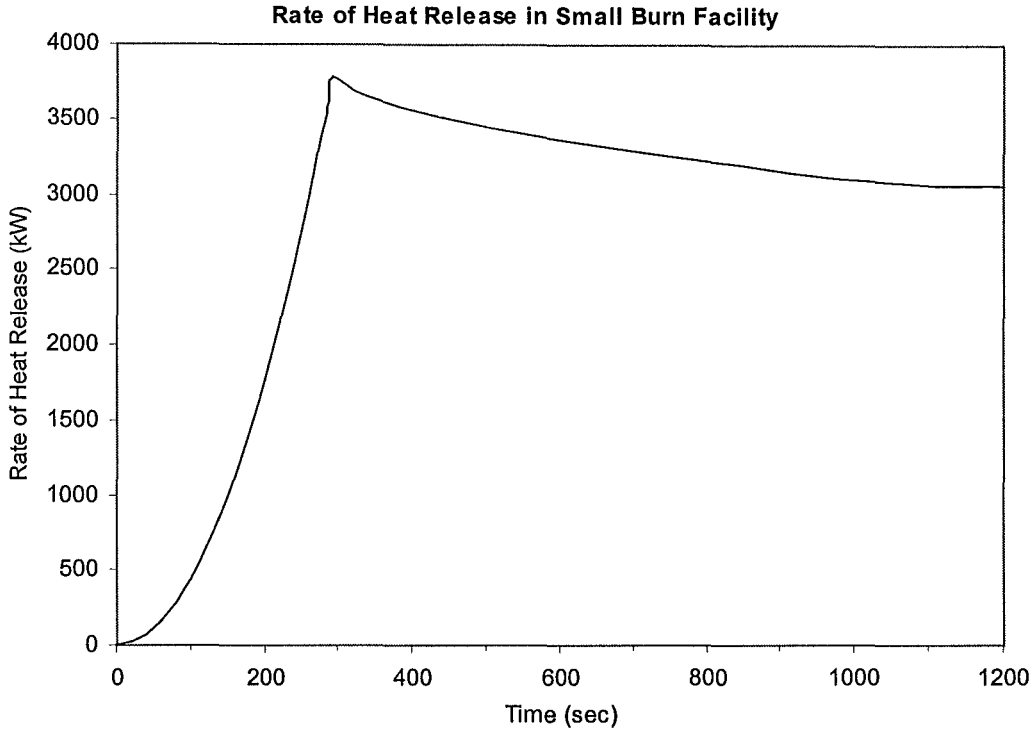

Figure C.1: Rate of heat release in small burn facility

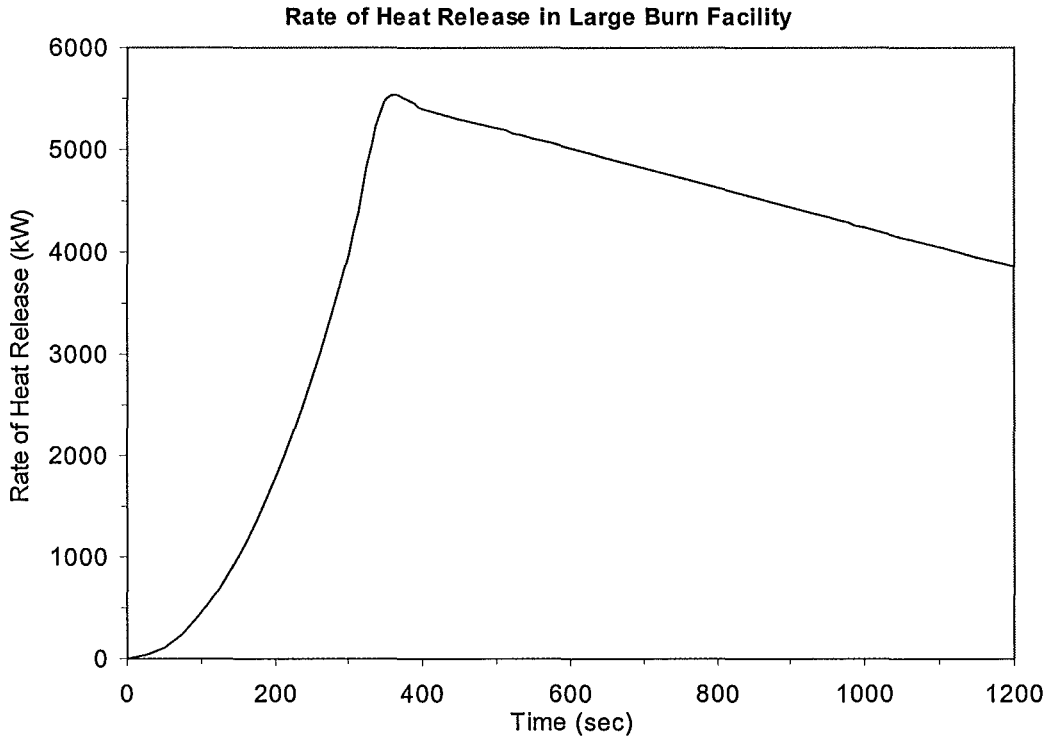

Figure C.2: Rate of heat release in large burn facility

APPENDIX D

Format of Cone Data File

An example of a ".txt" file for including the material cone calorimeter data is presented here.

"Material Description"
"Number of HRR Curves",4
"Heat Flux",35
"Number of HRR Data Pairs",404
"sec,kw/m2"
0,64.1
1.9,65.5
3.6,61.4
.
.
804.4,0
806.3,0
"Heat Flux",50
"Number of HRR Data Pairs",324
"sec,kw/m2"
0,62.3
4.5,56.2
9.2,37
.
.
1287.7,0
1292.4,0
"Heat Flux",60
"Number of HRR Data Pairs",359
"sec,kw/m2"
0,84.8
1.6,91.3
3.7,90.7
5.7,80.8
.
.
715.5,0
"Heat Flux",75
"Number of HRR Data Pairs",225
"sec,kw/m2"
0,70.9
3.5,88.1
.
.
895.4,0
"Ignition Data"
"Number of Pairs",4
"flux kw/m2,ignition time sec, peak hrr kw/m2"
35,187.5,65.5
50,86,56.6
60,52.5,89.3
75,33.5,80.5
"Flame Spread Parameter",0
"Min Surface Temp For Spread",0
"Effective Heat of Combustion",4.9

Four input heat release rate curves for cladding material tested at 35, 50, 60 and 75 kW/m^2.

The model will correlate the ignition data to estimate T_{ig} and $k\rho c$.

APPENDIX E

Input for Flame Spread Model Simulation

12 mm Plywood as Exterior Wall Cladding Material

```
Monday,February 14,2000,10:48 AM
Input Filename : C:\Program Files\BRANZFIRE\data\Shadowclad.mod

BRANZFIRE Room Fire Model (Ver 2000.030)

Shadowclad

======================================================================
Description of Rooms
======================================================================
Room  1  :
         Room Length (m) =                                  30.00
         Room Width (m) =                                   30.00
         Maximum Room Height (m) =                          10.00
         Minimum Room Height (m) =                          10.00
         Floor Elevation (m) =                              0.000
         Room  1  has a flat ceiling.

         Wall Surface is Plywood, Shadowclad
         Wall Density (kg/m3) =                             583.0
         Wall Conductivity (W/m.K) =                        0.120
         Wall Emissivity =                                  0.88
         Wall Thickness (mm) =                              12.0

         Wall Substrate is plasterboard
         Wall Substrate Density (kg/m3) =                   760.0
         Wall Substrate Conductivity (W/m.K) =              0.160
         Wall Substrate Thickness (mm) =                    16.0

         Ceiling Surface is Plasterboard
         Ceiling Density (kg/m3) =                          760.0
         Ceiling Conductivity (W/m.K) =                     0.160
         Ceiling Emissivity =                               0.88
         Ceiling Thickness (mm) =                           16.0

         Floor Surface is plasterboard
         Floor Density (kg/m3) =                            760.0
         Floor Conductivity (W/m.K) =                       0.160
         Floor Emissivity =                                 0.88
         Floor Thickness = (mm)                             16.0


======================================================================
Description of Wall Vents
======================================================================
From room  1  to outside, Vent No 1
                  Vent Width (m) =                          30.000
                  Vent Height (m) =                         10.000
                  Vent Sill Height (m) =                    0.000
                  Vent Soffit Height (m) =                  10.000
                  Opening Time (sec) =                      0
                  Closing Time (sec) =                      0


======================================================================
Description of Ceiling/Floor Vents
======================================================================
======================================================================
Ambient Conditions
======================================================================
Interior Temp (C) =                                         20.0
Exterior Temp (C) =                                         22.0
Relative Humidity (%) =                                     52
```

```
======================================================================
Tenability Parameters
======================================================================
Monitoring Height for Visibility and FED (m) =              1.50
Occupant Activity Level =                                   Light
Visibility calculations assume:                             reflective signs
FED Start Time (sec)                                        0
FED End Time (sec)                                          1200


======================================================================
Sprinkler / Detector Parameters
======================================================================
No thermal detector or sprinkler installed.

======================================================================
Mechanical Ventilation (to/from outside)
======================================================================
Mechanical Ventilation not installed in Room 1


======================================================================
Description of the Fire
======================================================================
Radiant Loss Fraction =                                     0.30
Smoke Emission Coefficent (1/m) =                           0.80
Characteristic Mass Loss per Unit Area (kg/s.m2) =          0.011
Air Entrainment in Plume uses McCaffrey (recommended)

Burning Object No 1

               Located in Room                              1
               Energy Yield (kJ/g) =                        12.0
               CO2 Yield (kg/kg fuel) =                     0.000
               Soot Yield (kg/kg fuel) =                    0.000
               H2O Yield (kg/kg fuel) =                     0.000
               Fire Height (m) =                            0.000
               Fire Location (m) =                          Wall

               Time (sec)              Heat Release (kW)
                0                      0
                100                    0

This simulation includes flame spread on linings.
Ignition data is correlated using the method of Grenier and Janssens.
Quintiere's Room Corner Model is used.
Flame length power =                                        0.667
Burner flame heat flux (kW/m2) =                            90.0
Heat flux ahead of flame (kW/m2) =                          30.0
Flame area constant =                                       0.067
Burner Width (m) =                                          2.000

Room 1
Wall heat of gasification (kJ/g) =                          10.8
Wall heat of combustion (kJ/g) =                            12.1
Wall min surface temp for spread (C) =                      120.0
Wall flame spread parameter =                               12.9
Wall Total Energy Available (kJ/m2) =                       85396
Ignition temperature of wall lining (C) =                   307.4
Thermal inertia of wall lining =                            0.226
Wall cone HRR data file used =                              shadowclad.txt
```

APPENDIX F

Rate of Heat Release and Upward Flame Spread Velocity

F.1 12 mm "LOSP"-treated Plywood

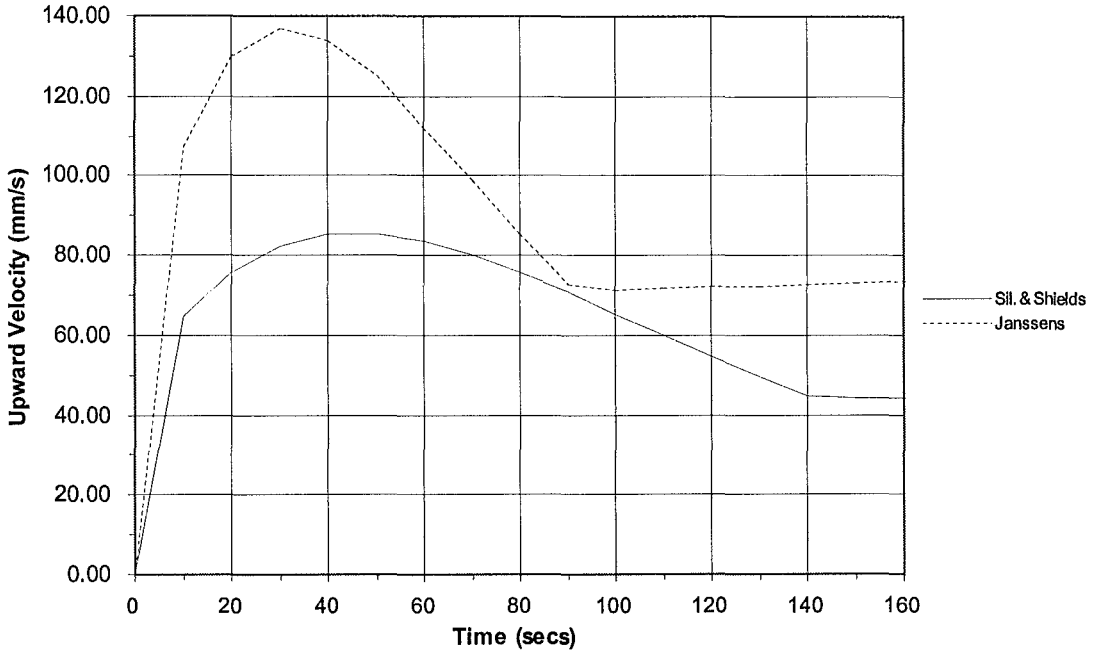

Figure F.1: Upward flame spread velocity

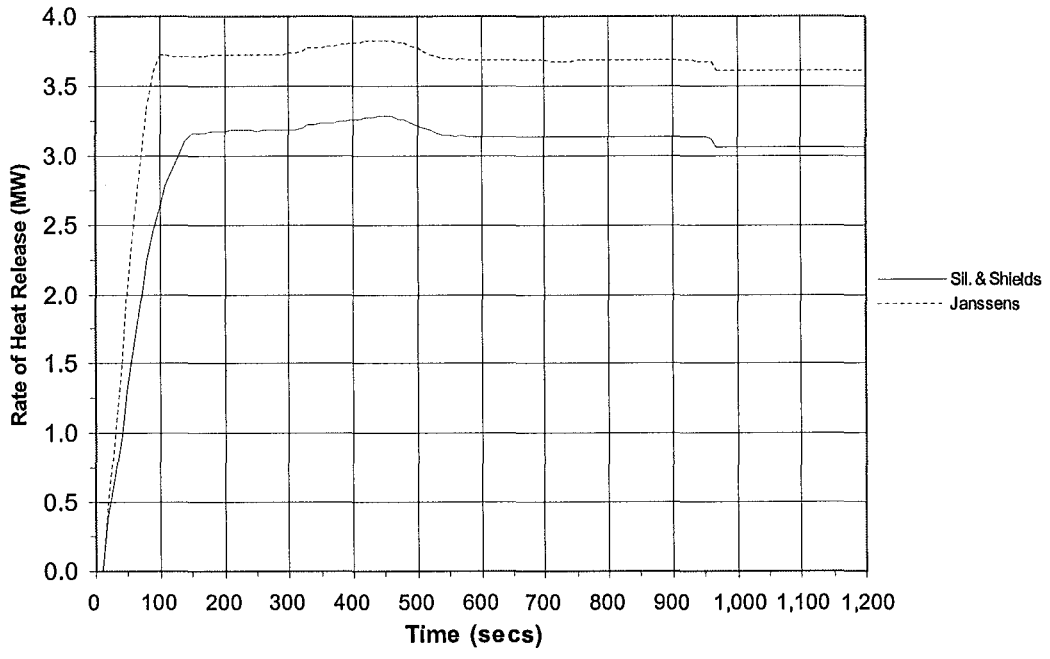

Figure F.2: Heat release rate

F.2 7 mm Extruded Foamed uPVC Weatherboard

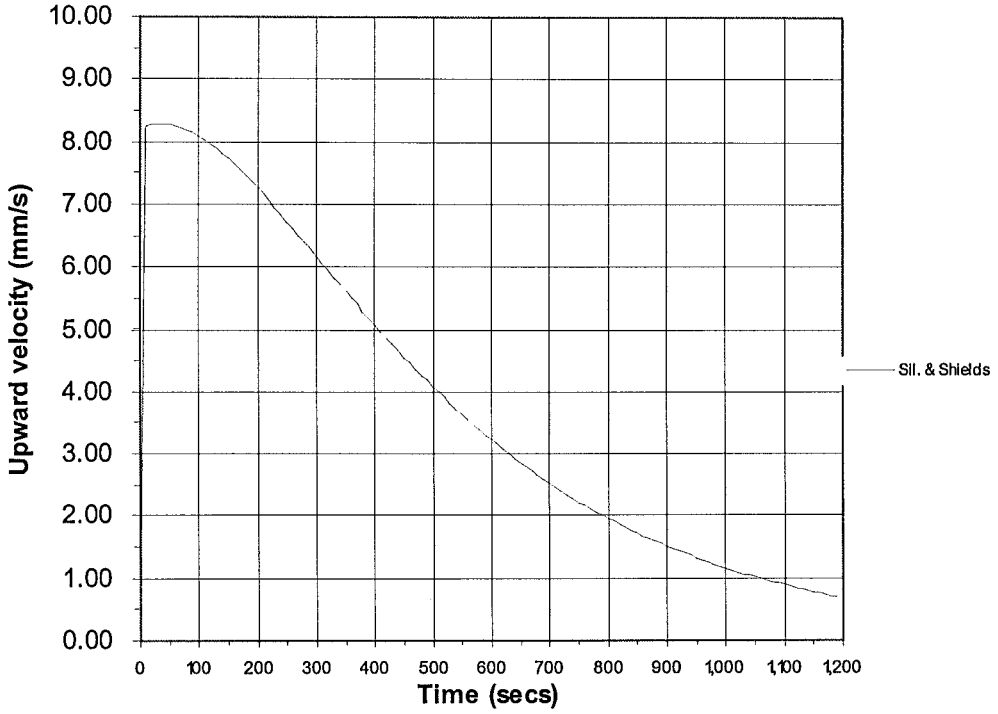

Figure F.3: Upward flame spread velocity

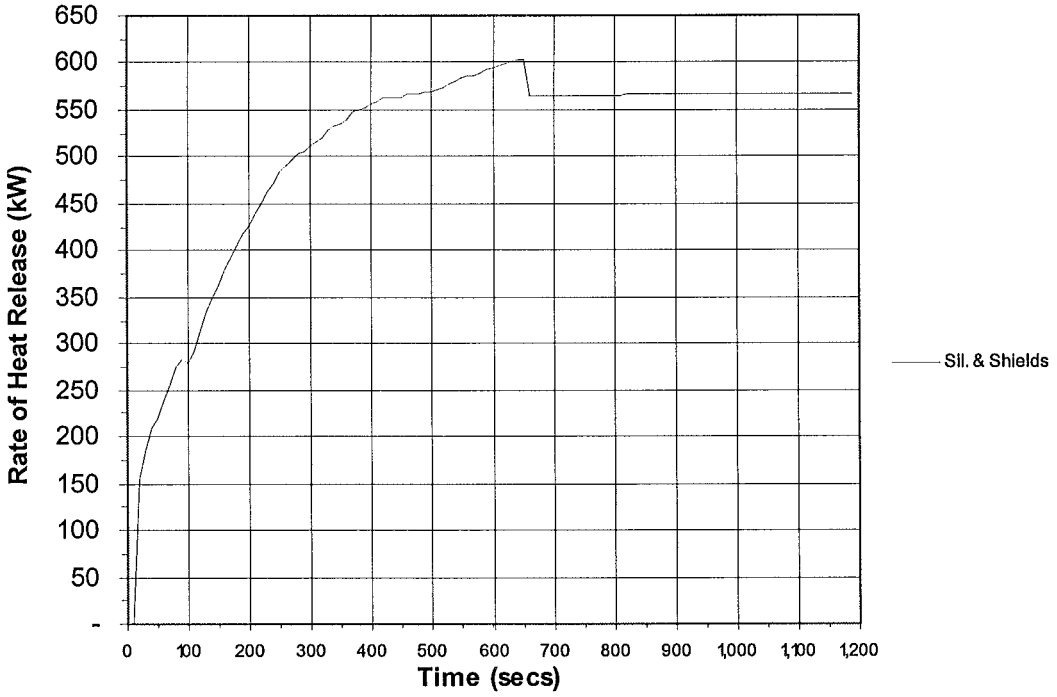

Figure F.4: Heat release rate

F.3 10 mm Hardboard

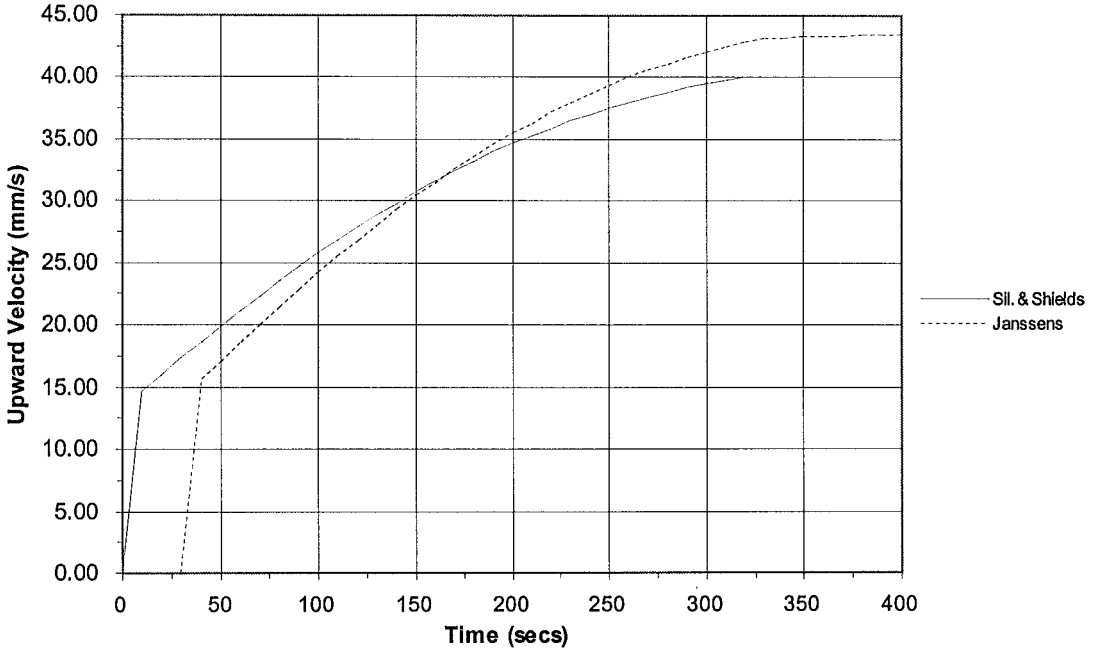

Figure F.5: Upward flame spread velocity

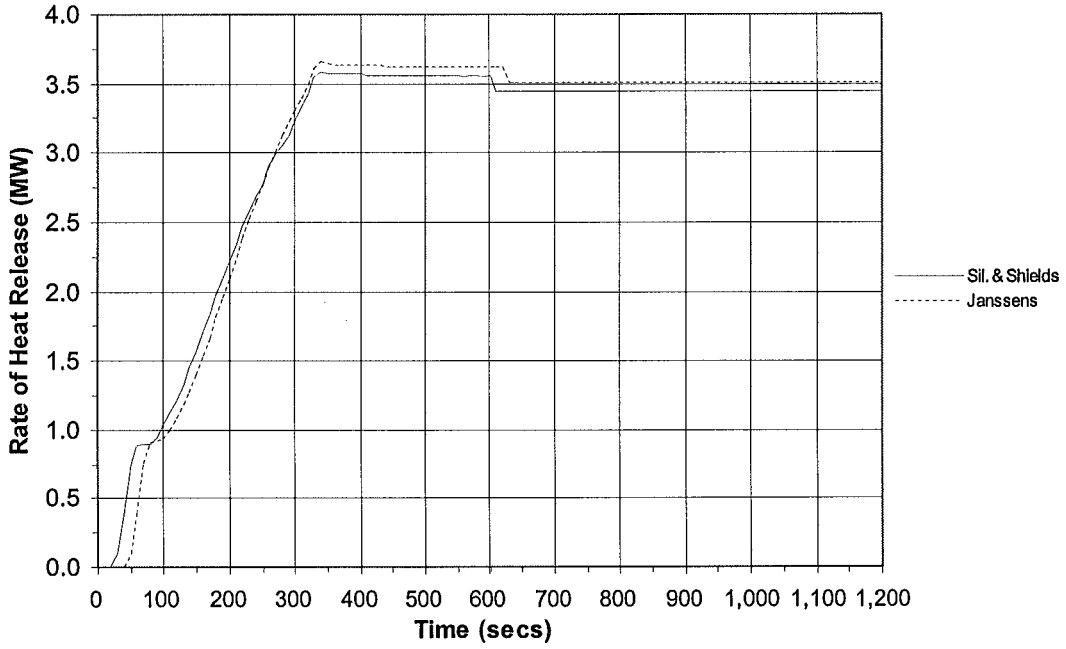

Figure F.6: Heat release rate

F.4 7.5 mm Cellulose Fibre-Cement Sheet

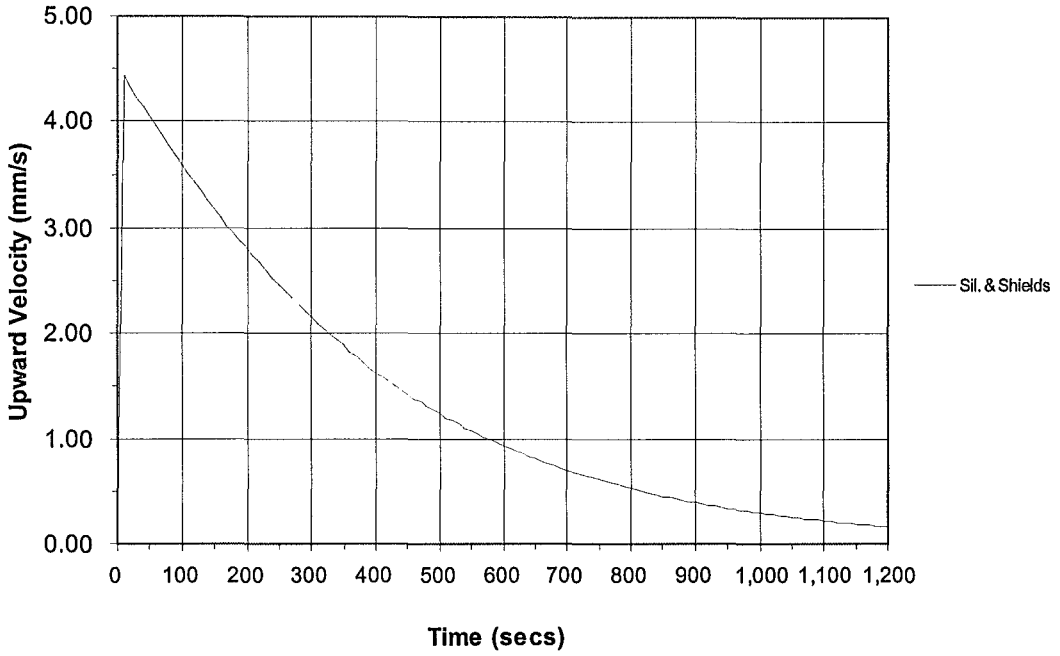

Figure F.7: Upward flame spread velocity

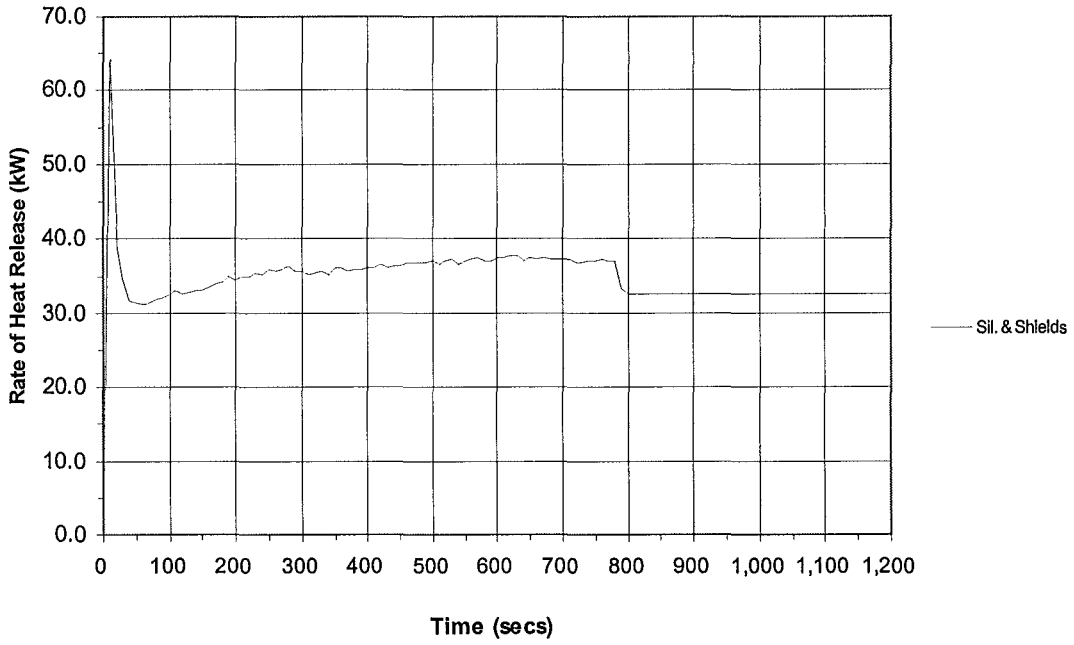

Figure F.8: Heat release rate